

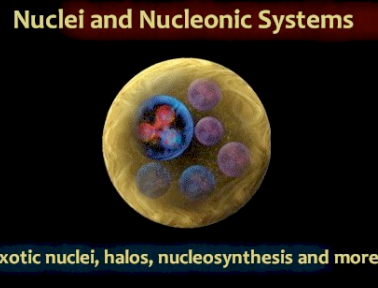
# Effective field theory and the renormalization group for nuclear systems

Achim Schwenk



CANADA'S NATIONAL LABORATORY FOR PARTICLE AND NUCLEAR PHYSICS

*Owned and operated as a joint venture by a consortium of Canadian universities via a contribution through the National Research Council Canada*



20th Chris Engelbrecht Summer School  
Stellenbosch, ZA, Jan. 19-28, 2009

supported by



**NRC-CNR**

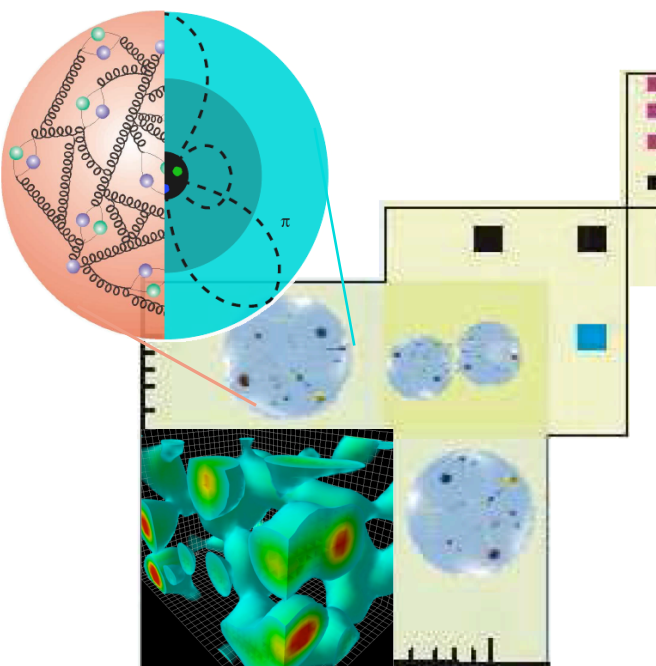
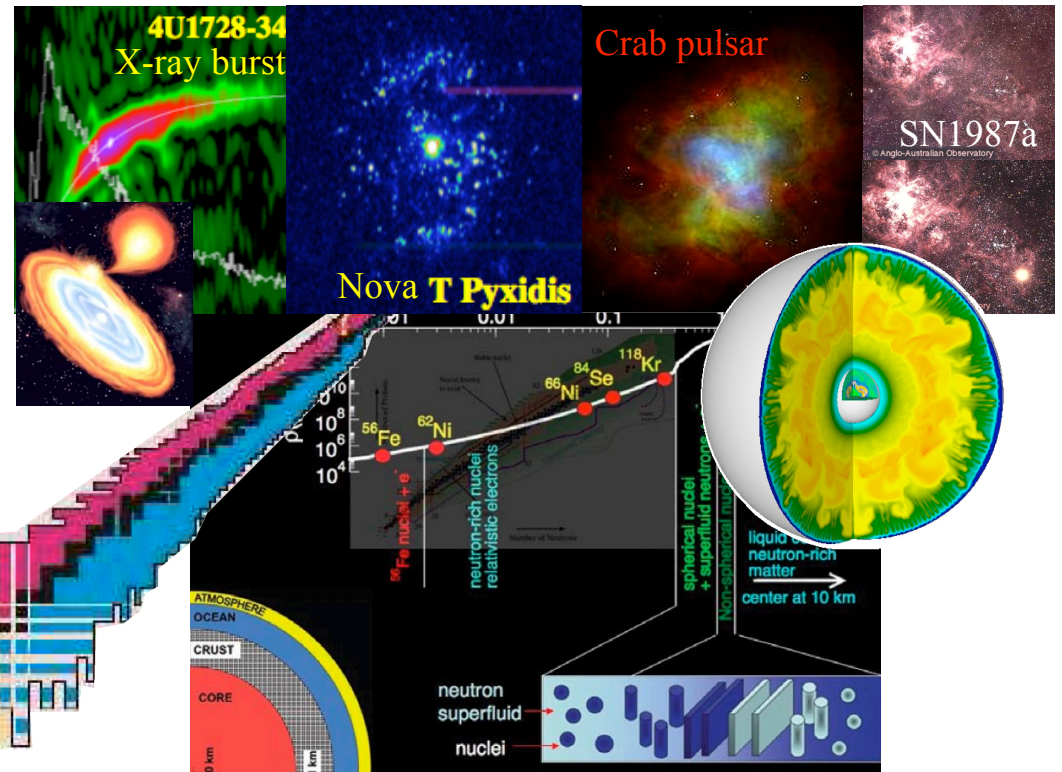
# Strong interaction physics in the lab and cosmos

Matter at the extremes:

density  $\rho \sim 10^{11} \dots 10^{15} \text{ g/cm}^3$

neutron-rich to proton-rich  
 $Z/N \sim 0.05 \dots 0.6$

temperatures  $T \sim \dots 30 \text{ MeV}$



Interaction challenges:

QCD  $\Rightarrow$  chiral EFT  $\Rightarrow$  RG evolved  
low-momentum interactions for all nuclei

Many-body challenges

Astrophysics challenges

# Frontiers in nuclear theory

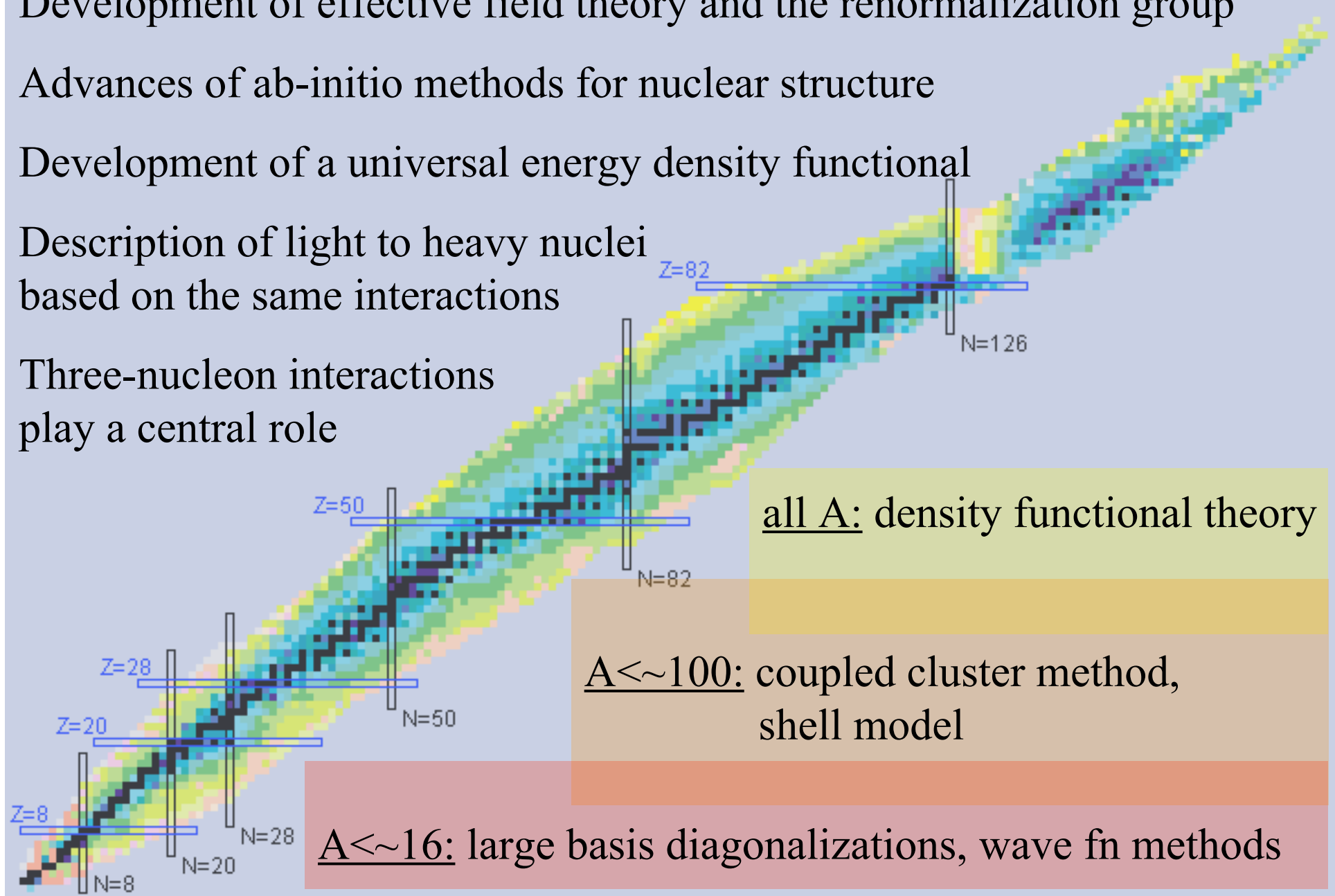
Development of effective field theory and the renormalization group

Advances of ab-initio methods for nuclear structure

Development of a universal energy density functional

Description of light to heavy nuclei  
based on the same interactions

Three-nucleon interactions  
play a central role



# Frontiers in nuclear theory

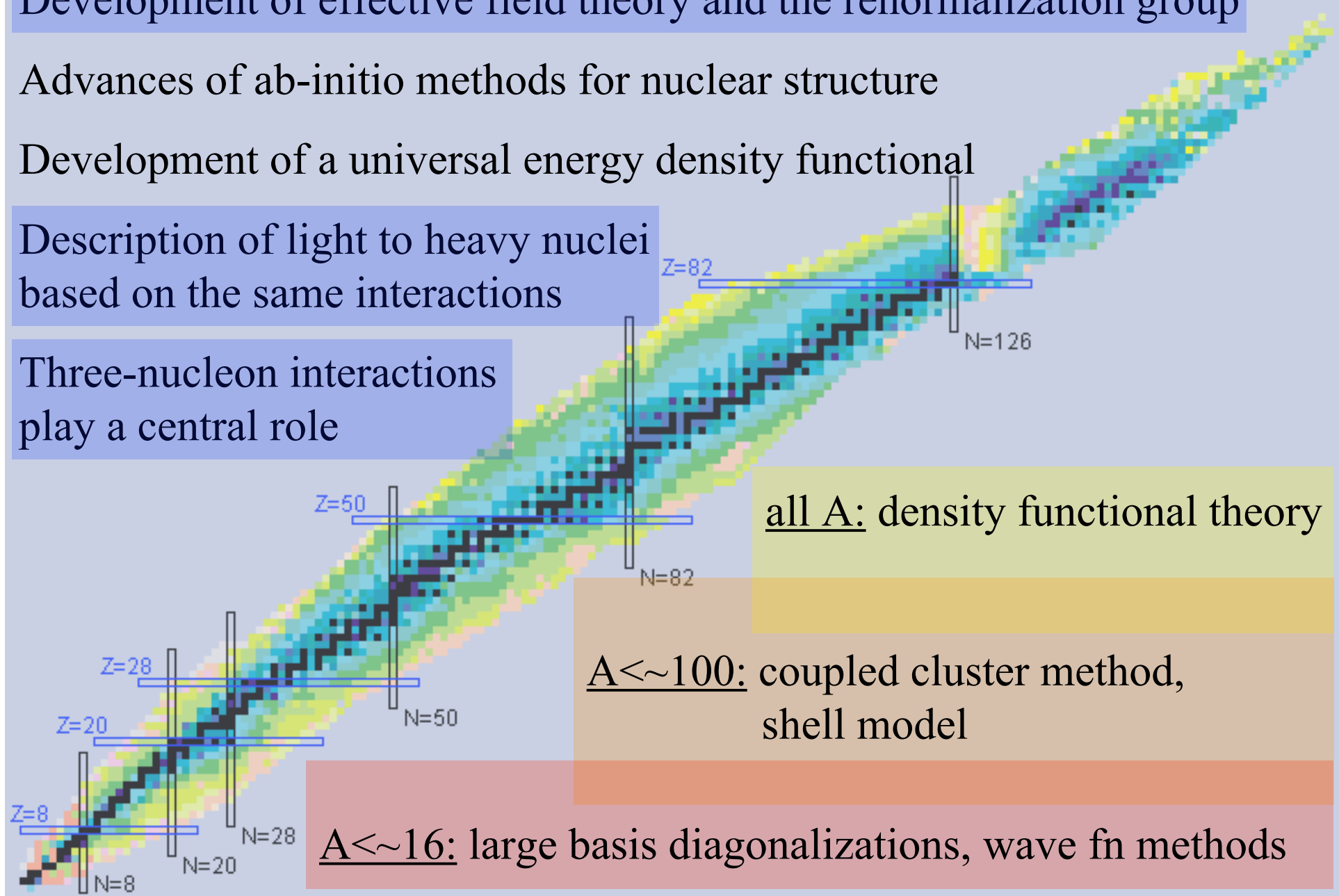
Development of effective field theory and the renormalization group

Advances of ab-initio methods for nuclear structure

Development of a universal energy density functional

Description of light to heavy nuclei  
based on the same interactions

Three-nucleon interactions  
play a central role

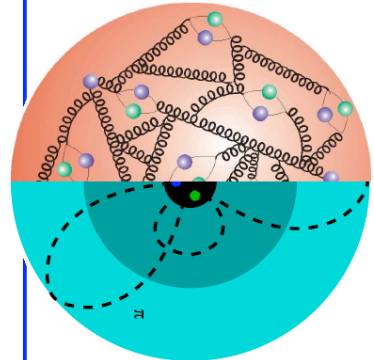


## Outline

1. Introduction to effective field theory and the renormalization group
2. Chiral effective field theory
3. Renormalization group for nuclear forces
4. EFT and RG for nuclear matter
5. Nuclear matter in astrophysics
6. Neutrino processes in supernovae from chiral EFT

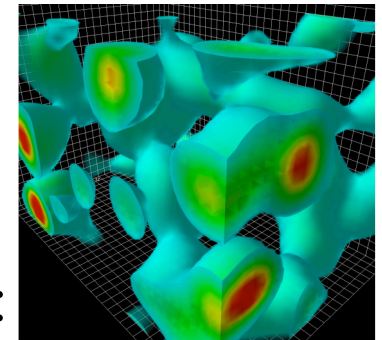
# $\Lambda$ / Resolution dependence of nuclear interactions

with high-energy probes:  
quarks+gluons



$\Lambda_{\text{chiral}}$   
momenta  $Q \sim \lambda^{-1} \sim m_\pi$

at low energies:  
complex QCD vacuum

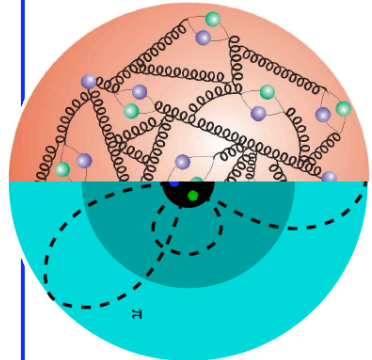


lowest energy excitations:  
pions, nearly massless,  $m_\pi = 140  
“phonons” of QCD vacuum$

$\Lambda_{\text{pionless}}$   
 $Q \ll m_\pi = 140$

# $\Lambda$ / Resolution dependence of nuclear interactions

with high-energy probes:  
quarks+gluons



Effective theory for NN, many-N interactions,  
operators depend on resolution scale  $\Lambda$

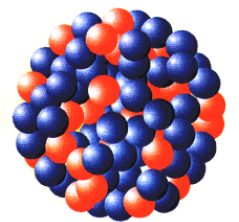
$$H(\Lambda) = T + V_{NN}(\Lambda) + V_{3N}(\Lambda) + V_{4N}(\Lambda) + \dots$$

$\Lambda_{\text{chiral}}$

momenta  $Q \sim \lambda^{-1} \sim m_\pi$ : chiral effective field theory

nucleons interacting via pion exchanges + contact interactions

typical Fermi momenta in nuclei  $\sim m_\pi$



$\Lambda_{\text{pionless}}$

$Q \ll m_\pi = 140 \text{ MeV}$ : pionless effective field theory

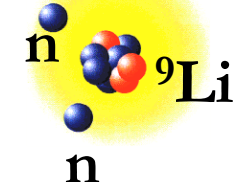
nucleons interacting via contact interactions only

large scattering lengths + corrections

applicable to loosely-bound, dilute systems, reactions at astro energies

halo nuclei

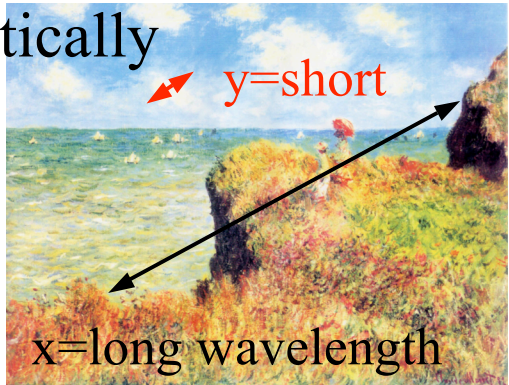
.....



## Idea of the renormalization group (RG)

integrate out high-momentum modes that are not resolved  
and incorporate their effects in couplings of effective theory

schematically

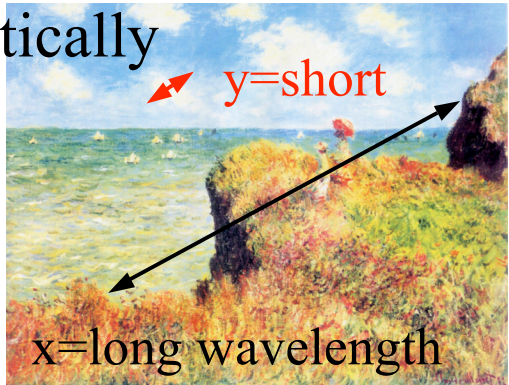


$$\begin{aligned} Z &= \int dx \int dy e^{-S(x,y)} = \int dx \int dy e^{-a(x^2+y^2)-b(x^2+y^2)^2} \\ &= \int dx e^{-S_{\text{eff}}(x)} = \int dx e^{-a'x^2-b'x^4-c'x^6+\dots} \end{aligned}$$

## Idea of the renormalization group (RG)

integrate out high-momentum modes that are not resolved  
and incorporate their effects in couplings of effective theory

schematically



$$\begin{aligned} Z &= \int dx \int dy e^{-S(x,y)} = \int dx \int dy e^{-a(x^2+y^2) - b(x^2+y^2)^2} \\ &= \int dx e^{-S_{\text{eff}}(x)} = \int dx e^{-a'x^2 - b'x^4 - c'x^6 + \dots} \end{aligned}$$

separate into slow and fast modes  $\phi(\omega, k) = \begin{cases} \phi_<(\omega, k) & \text{for } \omega, k < \Lambda \\ \phi_>(\omega, k) & \text{else} \end{cases}$   
and integrate out fast modes

$$\begin{aligned} Z &= \int \prod d\phi_<(\omega, k) e^{-S_{\text{free}}[\phi_<]} \int \prod d\phi_>(\omega, k) e^{-S_{\text{free}}[\phi_>] - S_{\text{int}}[\phi_<, \phi_>]} \\ &= \int \prod d\phi_<(\omega, k) e^{-S_{\text{eff}}[\phi_<]} \end{aligned}$$

when we integrate out momentum modes by  $\delta\Lambda$  the couplings evolve

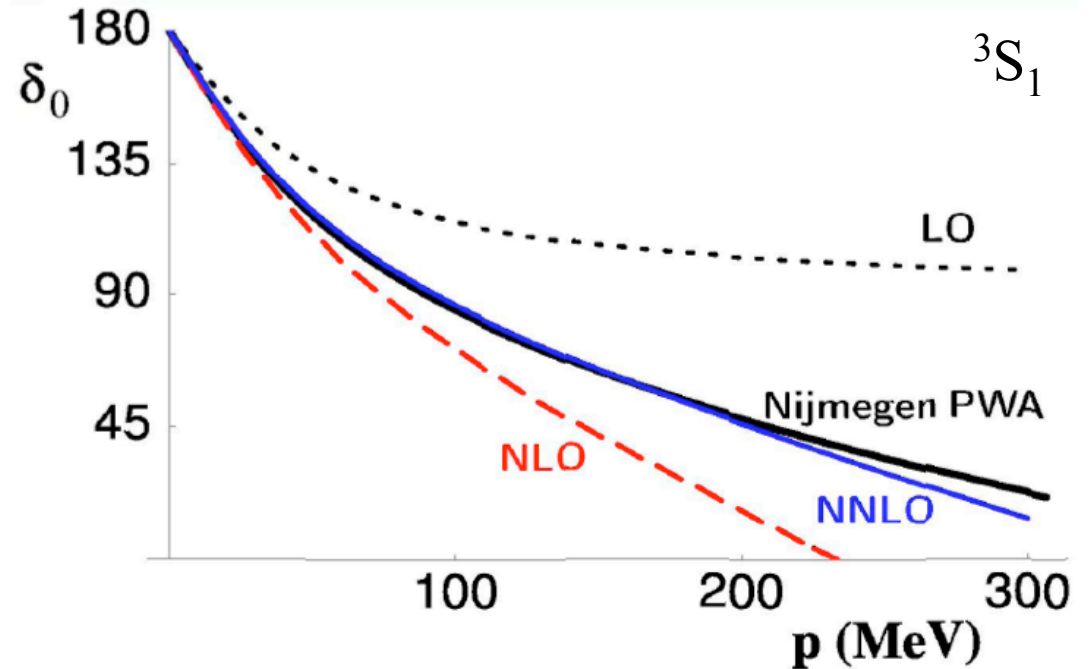
$$g_i(\Lambda - \delta\Lambda) = g_i(\Lambda) - \frac{\delta\Lambda}{\Lambda} \beta_i(\{g_j(\Lambda)\}, \Lambda)$$

resolution/ $\Lambda$ -dependent couplings and RG eqns  $\Lambda \frac{d}{d\Lambda} g_i(\Lambda) = \beta_i(\{g_j(\Lambda)\}, \Lambda)$

## Phase shifts in pionless EFT

converges to PWA  
(partial wave analysis  
of NN scattering data)

order-by-order improvement



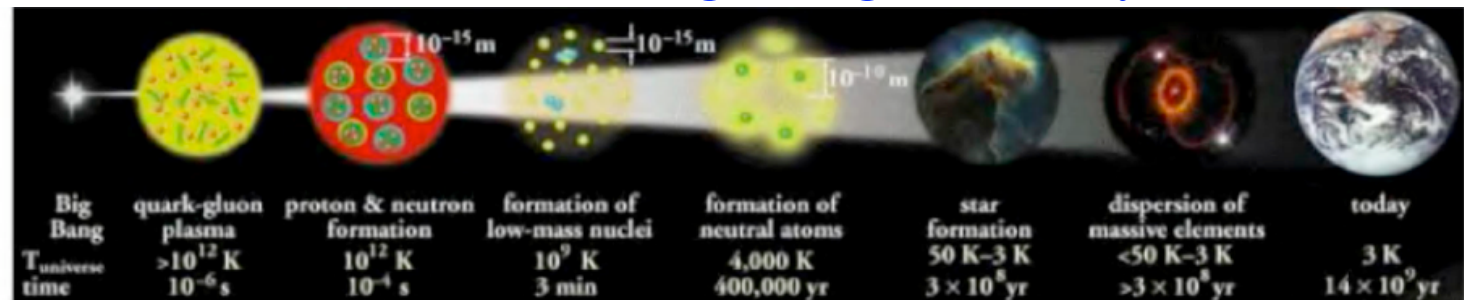
pionless EFT reproduces effective range expansion,  
but EFT advantages:

systematic electroweak currents

systematic few-body calculations

systematic finite temperature, finite density,...

# Pionless EFT and big-bang nucleosynthesis

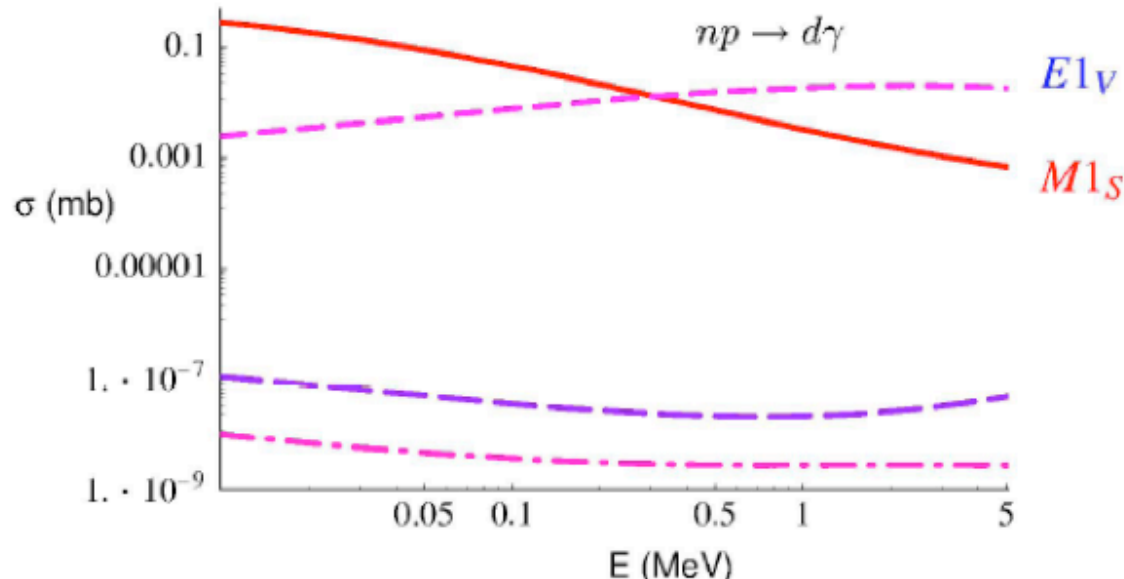


$E_{\text{typ}} \approx 0.02 - 0.2$  MeV, light-element abundances sensitive to **baryon density**.

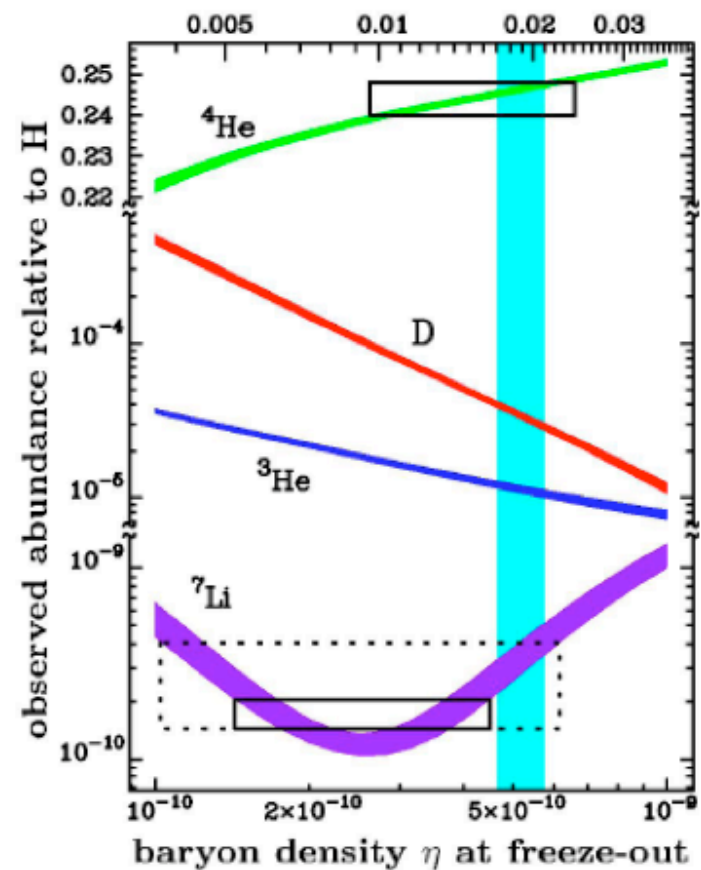
Accurate theoretical determination necessary: **error-estimate!**

$np \rightarrow d\gamma$  **biggest uncertainty**, but “impossible” to measure.

EFT( $\pi$ ) to N<sup>4</sup>LO in closed form: accuracy  $\lesssim 1\%$ . Rupak 1999



slide from Griesshammer; Chen, Savage (1999), Rupak (2000)



# Pionless EFT applied to few-body systems

Leading-order NN contact interactions  ${}^1\text{S}_0 + {}^3\text{S}_1$   $C_0(\Lambda)$  lead to divergence in triton channel, cutoff dependence generates Phillips line [Bedaque et al. \(1999\)](#)

and band around Tjon line in  $A=3,4$  system [Platter et al. \(2005\)](#)

promote 3N contact interaction  $D_0(\Lambda)$  to leading order, coupling fixed by triton energy, exhibits RG limit cycle

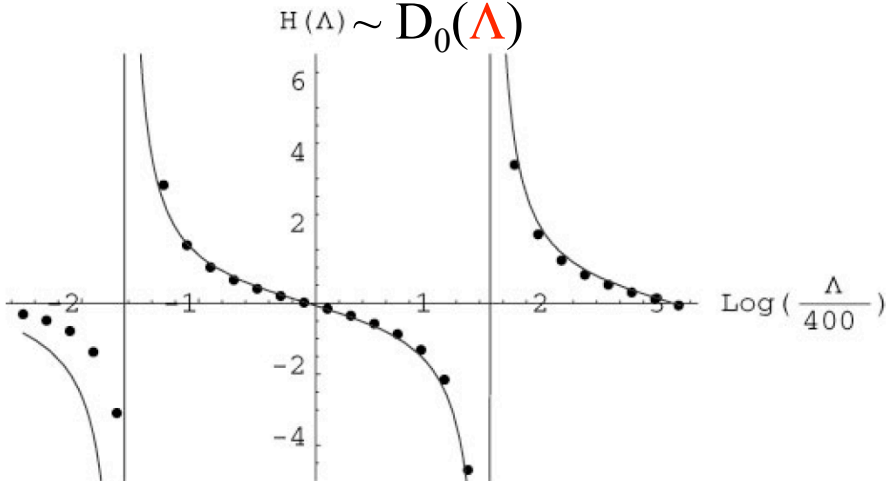


**Figure 7** Three-body force coefficient  $H(\Lambda)$  computed analytically (line) and numerically (points) as a function of  $\log(\Lambda/400 \text{ MeV})$ .

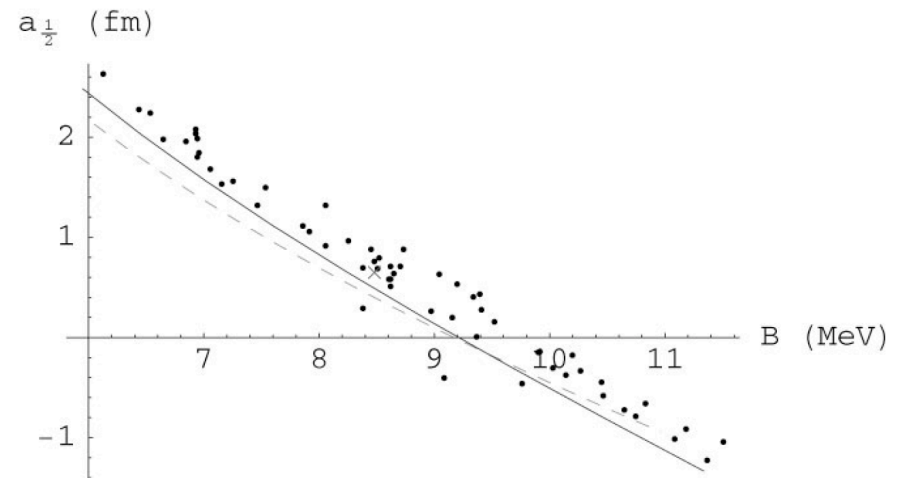
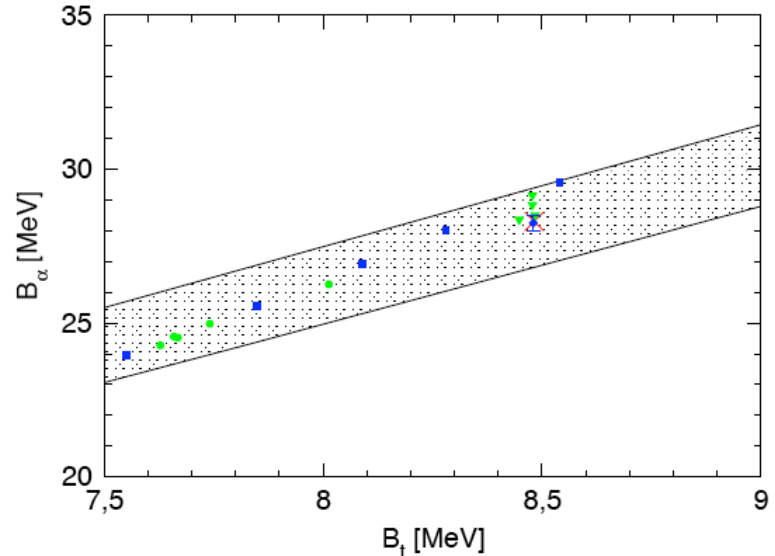


**Figure 9** Correlation between the doublet S-wave nucleon-deuteron scattering length and the triton binding energy (Phillips line): predictions of different models (points), EFT at LO (light dashed line) and NLO (dark solid line), and experimental value (cross).



# Strong interactions with cold atoms

Controlled strong interactions:  
large scattering lengths via  
Feshbach resonances

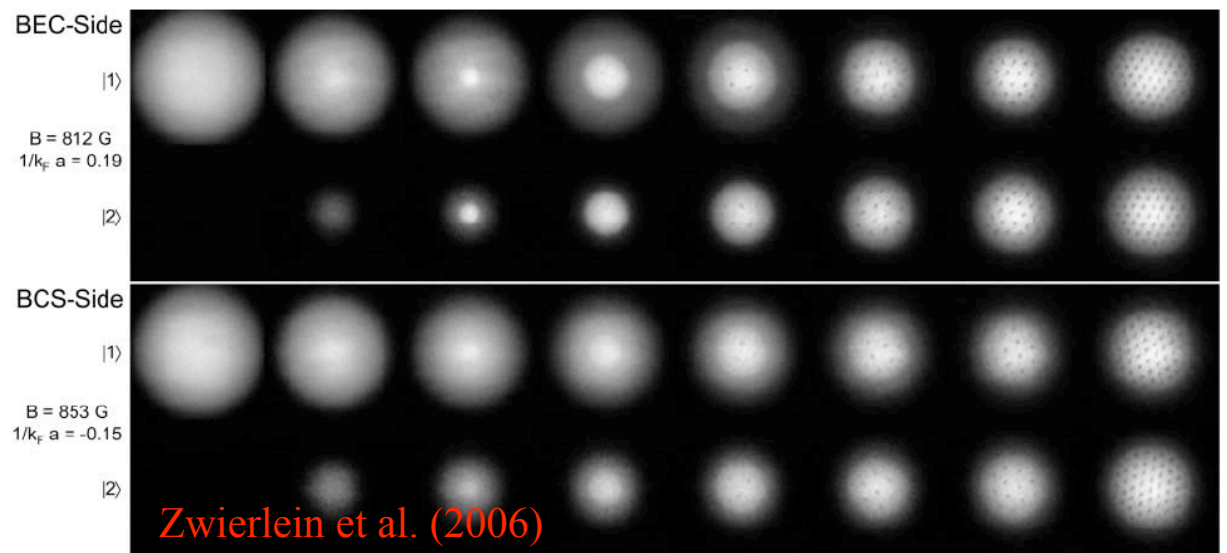
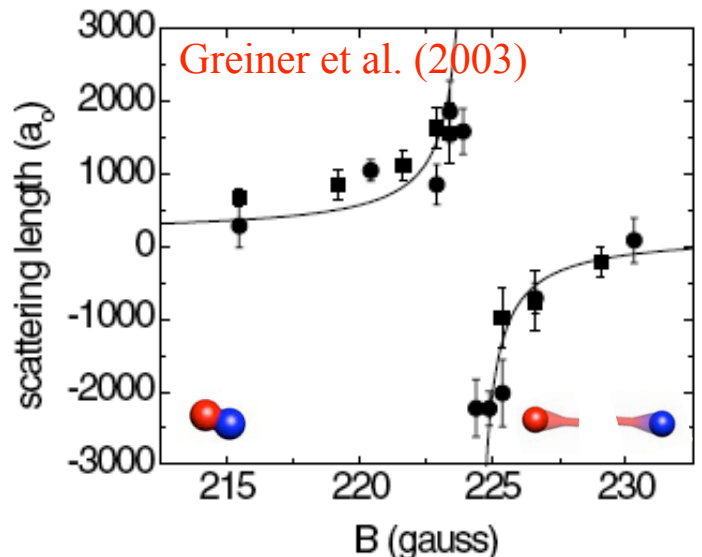
Many control knobs:  
wide/narrow, S-wave, P-wave,...

Variable composition:  
spin-polarization,  $m/M$ ,  
Bose-Fermi mixtures

Rotation

Optical lattices

.....

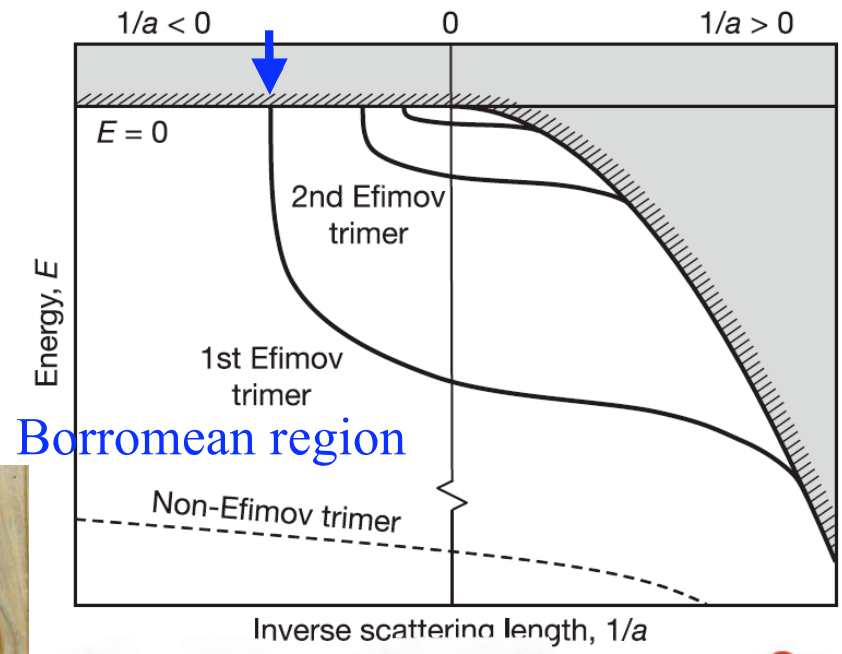


# Large scattering lengths lead to Efimov effect

leading-order two- and three-body contact interactions:

Efimov spectrum for 3 distinguishable particles or 3 bosons with identical pair-wise scattering lengths

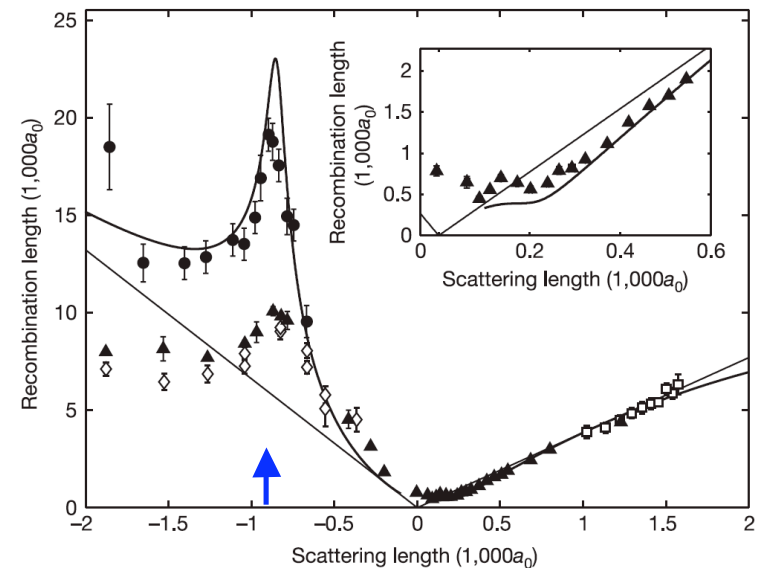
predicts Borromean states ~three rings quantum three-body bound states, all two-body subsystems unbound



Universal physics on resonance:  
infinite tower of bound excited states  
with universal scaling  $E_n/E_{n+1} = 515$

observed first Efimov resonance in  
3-body losses for Cs bosons

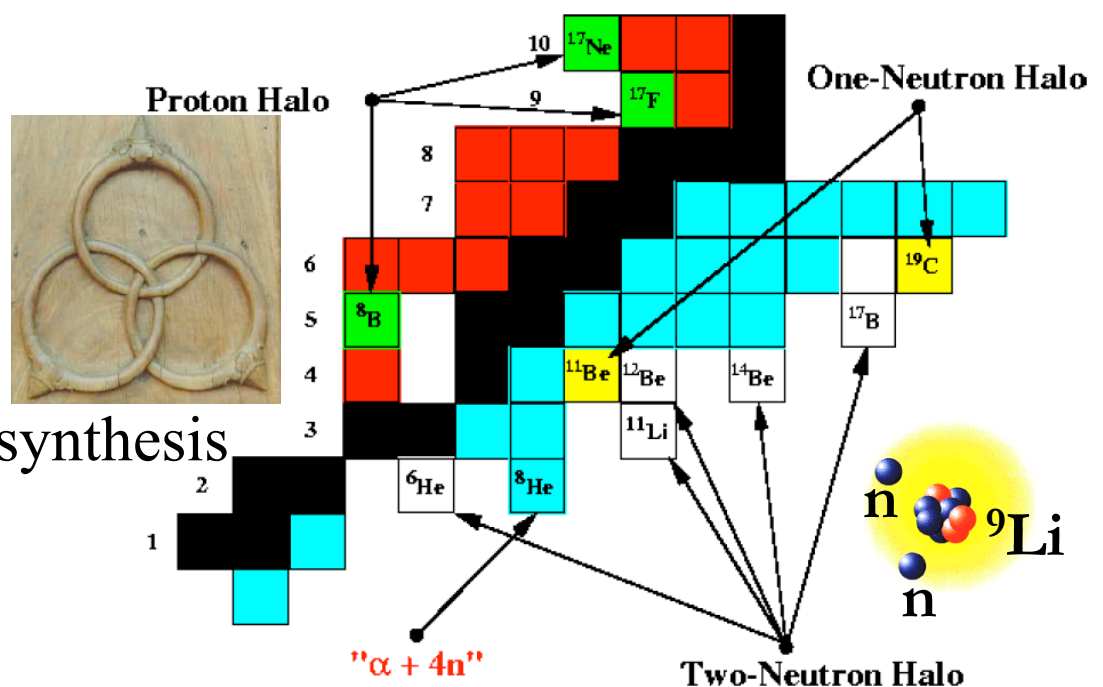
Kraemer et al. (2006)



# Borromean states in nuclei

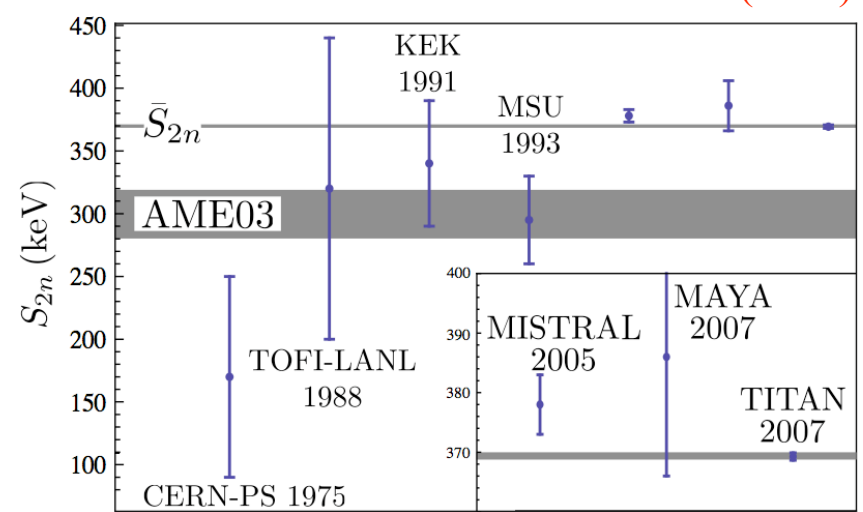
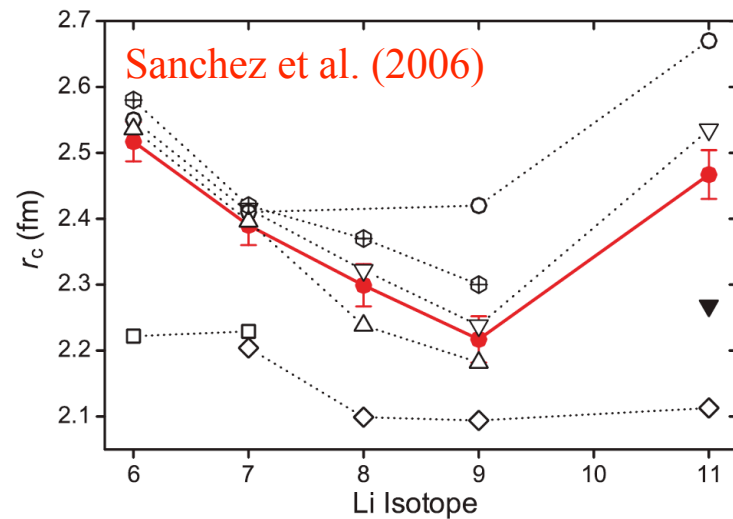
nn halos near neutron drip-line  
are the only known examples  
of Borromean states in nature

Partly responsible for  $A=5$   
mass gap, important for nucleosynthesis



Recent results for short-lived  ${}^{11}\text{Li}$ : charge radius and mass

Smith et al. (2008)



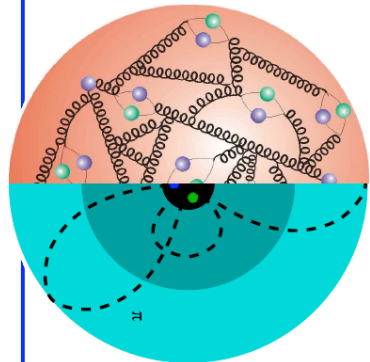
## Outline

1. Introduction to effective field theory and the renormalization group
2. Chiral effective field theory
3. Renormalization group for nuclear forces
4. EFT and RG for nuclear matter
5. Nuclear matter in astrophysics
6. Neutrino processes in supernovae from chiral EFT

# $\Lambda$ / Resolution dependence of nuclear interactions

with high-energy probes:  
quarks+gluons

cf. scale/scheme dependence  
of parton distribution functions



**Lattice QCD**

Effective theory for NN, many-N interactions,  
operators depend on resolution scale  $\Lambda$

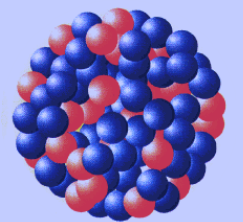
$$H(\Lambda) = T + V_{NN}(\Lambda) + V_{3N}(\Lambda) + V_{4N}(\Lambda) + \dots$$

$\Lambda_{\text{chiral}}$

momenta  $Q \sim \lambda^{-1} \sim m_\pi$ : chiral effective field theory

nucleons interacting via pion exchanges + contact interactions

typical Fermi momenta in nuclei  $\sim m_\pi$



$\Lambda_{\text{pionless}}$

$Q \ll m_\pi = 140 \text{ MeV}$ : pionless effective field theory

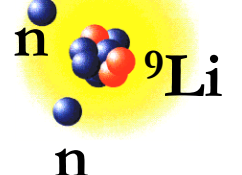
nucleons interacting via contact interactions only

large scattering lengths + corrections

applicable to loosely-bound, dilute systems, reactions at astro energies

halo nuclei

.....



# Lattice QCD and nuclear forces

Long-range couplings:

pion-NN coupling  $g_a$  from full QCD

Edwards et al. (2006)

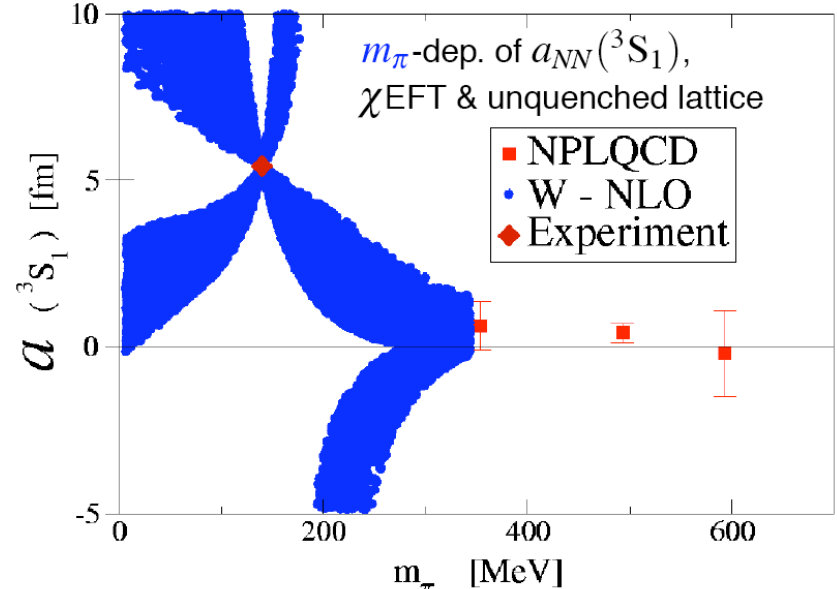
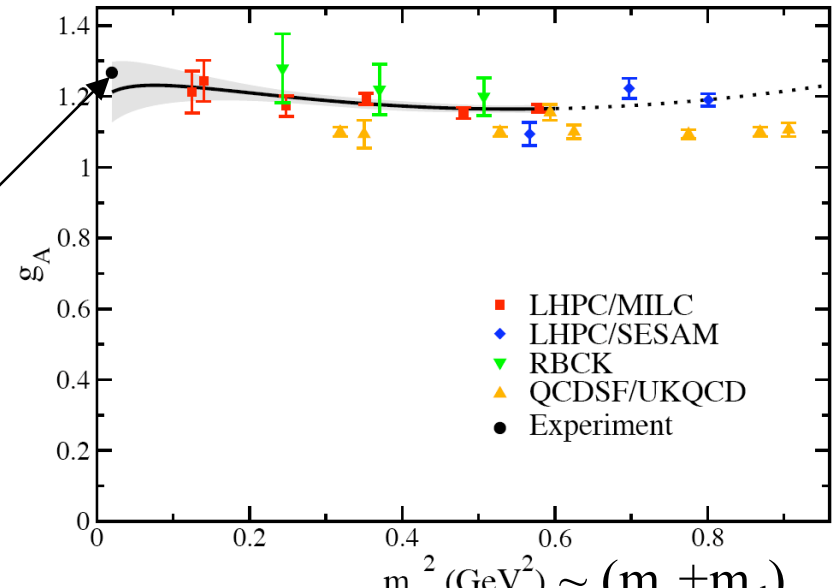
chiral EFT extrapolation to physical pion mass agrees with experiment

constrain higher-order long-range pion-, N-, ... couplings (scheme: chiral EFT)

Few-nucleon observables:

NN scattering lengths from full QCD, dependence on quark masses Beane et al. (2006)

Constrain experimentally difficult observables: 3-neutron properties  
first steps: 3 pions on a lattice Detmold et al. (2008)



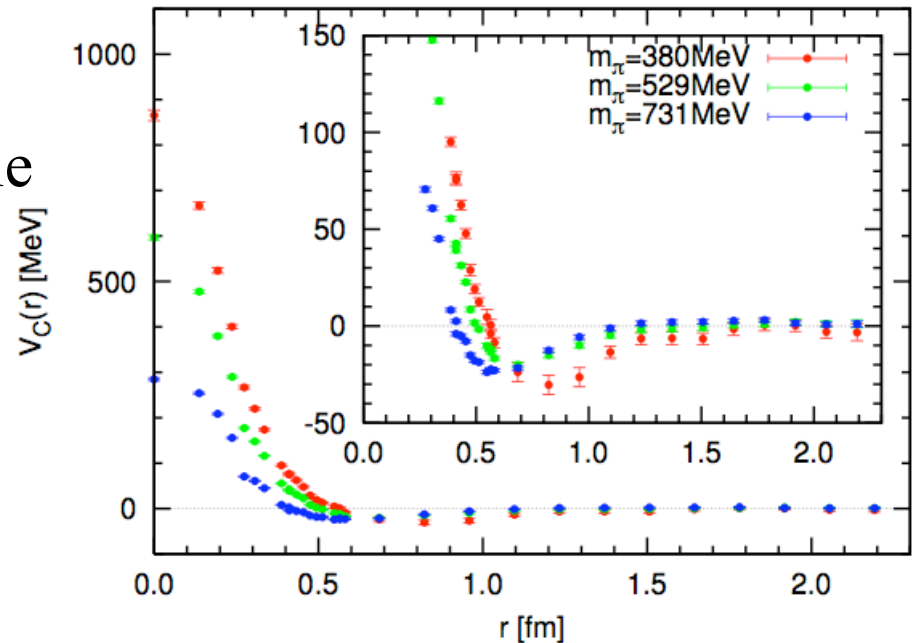
# Lattice QCD and nuclear forces

NN potential:

not unique, especially short-range  
properties depend on scheme and scale

Ishii, Aoki, Hatsuda (2007)

scheme: quasi-local potential,  
nucleon interpolating field,...  
(not chiral EFT)



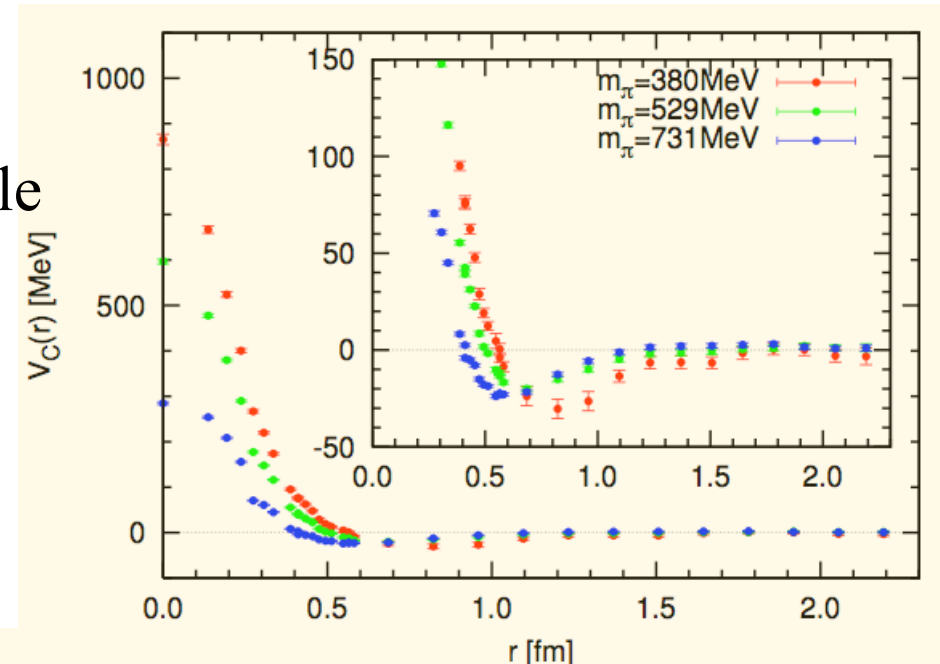
# Lattice QCD and nuclear forces

## NN potential:

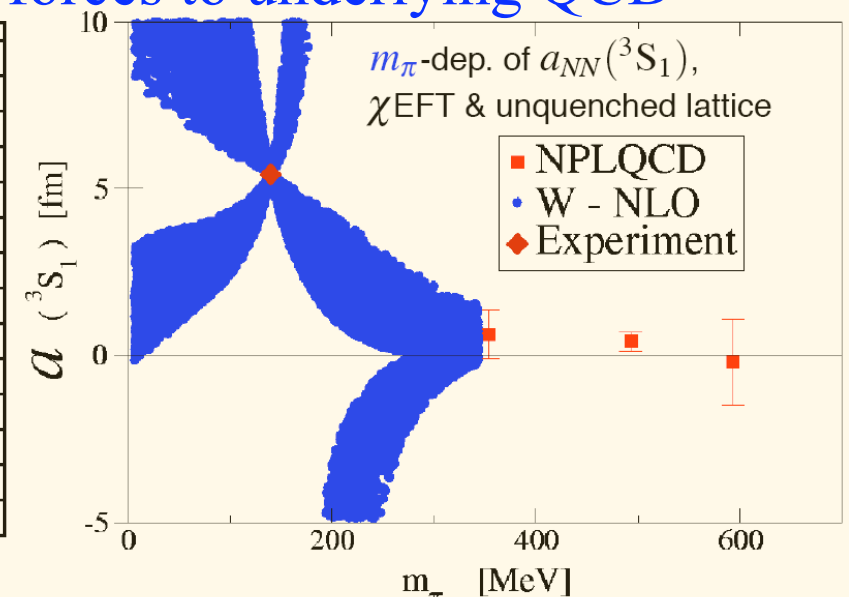
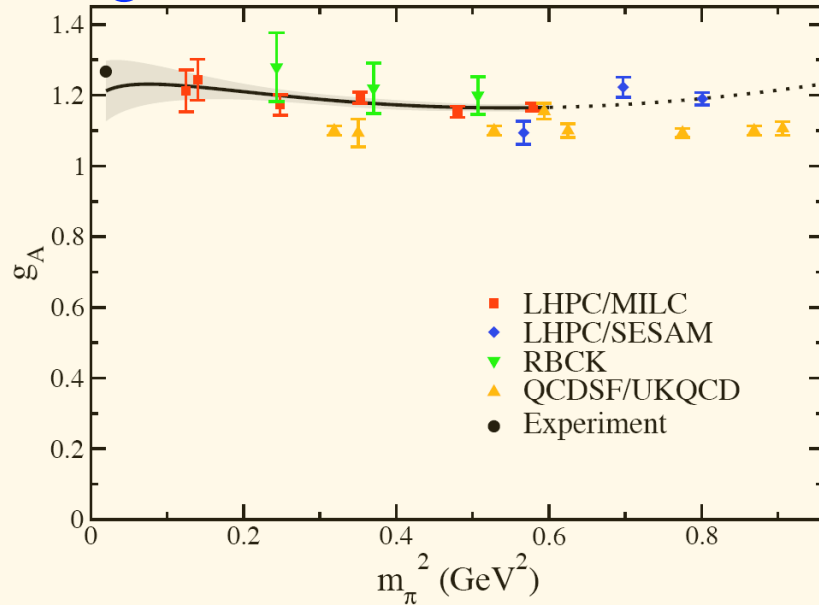
not unique, especially short-range  
properties depend on scheme and scale

Ishii, Aoki, Hatsuda (2007)

scheme: quasi-local potential,  
nucleon interpolating field,...  
(not chiral EFT)



First, exciting efforts to connect nuclear forces to underlying QCD



## References

P. Lepage, How to renormalize the Schroedinger equation, nucl-th/9706029.

P. Bedaque and B. van Kolck, EFT for few-nucleon systems, Ann. Rev. Nucl. Part. Sci. **52**, 339 (2002), nucl-th/0203055.

D. Phillips, Building light nuclei from neutrons, protons and pions, Czech J. Phys. **52**, B49 (2002), nucl-th/0203040.

D. Kaplan, Five lectures on EFT, nucl-th/0510023.

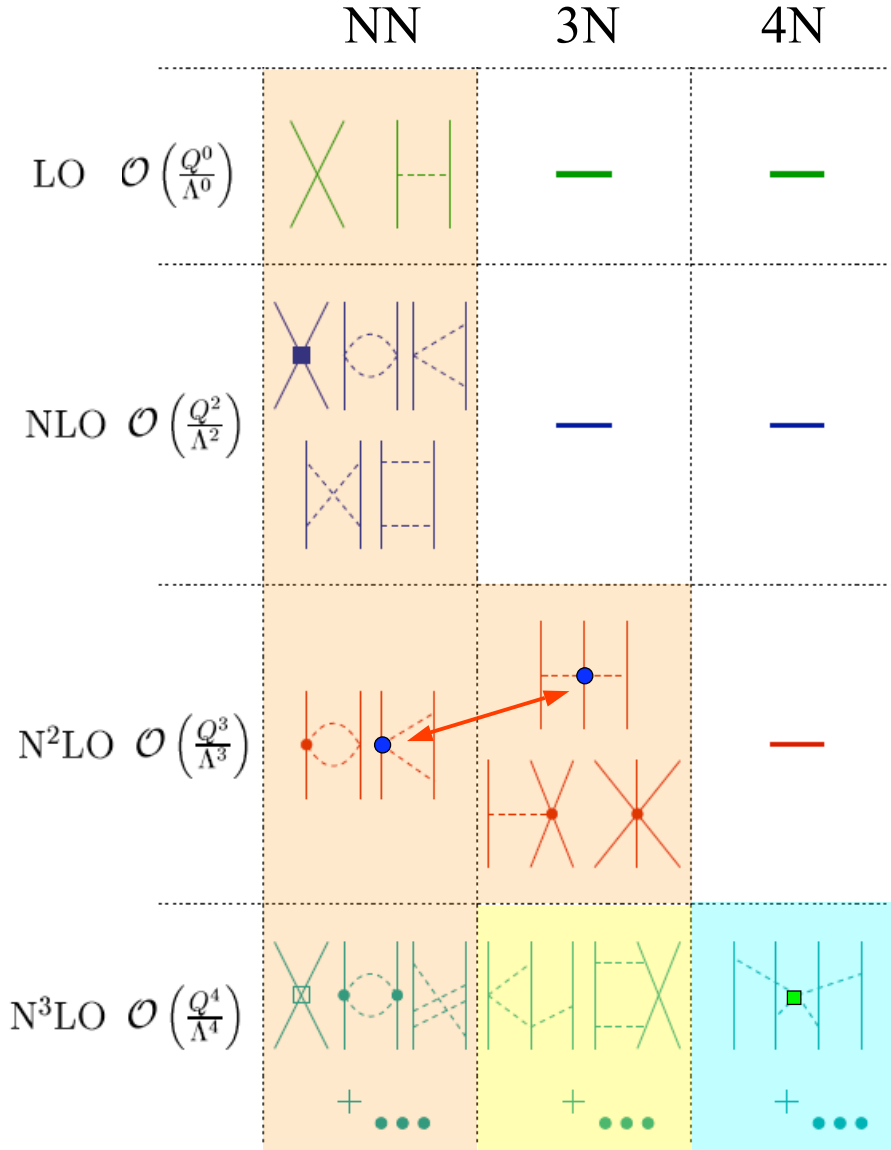
E. Braaten and H.-W. Hammer,  
Universality in few-body systems with large scattering length,  
Phys. Rept. **428**, 259 (2006), cond-mat/0410417.

## Outline

1. Introduction to effective field theory and the renormalization group
2. Chiral effective field theory
3. Renormalization group for nuclear forces
4. EFT and RG for nuclear matter
5. Nuclear matter in astrophysics
6. Neutrino processes in supernovae from chiral EFT

# Chiral EFT for nuclear forces

Separation of scales: low momenta  $\frac{1}{\lambda} = Q \ll \Lambda_b$  breakdown scale  $\sim 500$  MeV

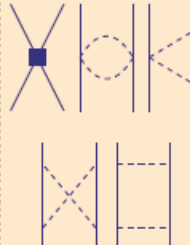
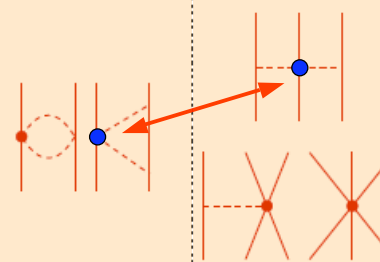
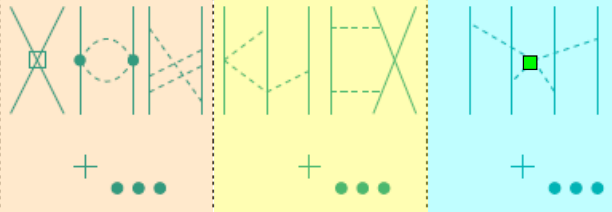
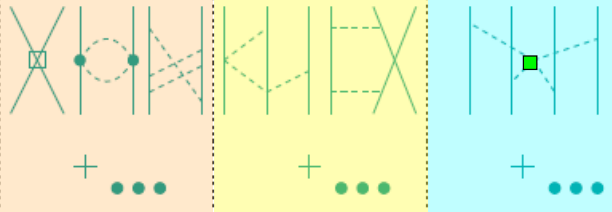
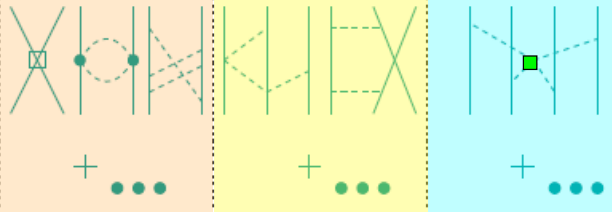


- limited resolution at low energies, can expand in powers  $Q/\Lambda_b$
- include long-range pion physics
- details of short-distance physics not resolved
- capture in few short-range couplings, fit to experiment once (experiment includes all short-range effects)
- systematic: can work to desired accuracy and obtain error estimates

Weinberg, van Kolck, Kaplan, Savage, Wise, Epelbaum, Meissner, Nogga, Machleidt,...

# Chiral EFT for nuclear forces

Separation of scales: low momenta  $\frac{1}{\lambda} = Q \ll \Lambda_b$  breakdown scale  $\sim 500$  MeV

	NN	3N	4N
LO $\mathcal{O}\left(\frac{Q^0}{\Lambda^0}\right)$		—	—
NLO $\mathcal{O}\left(\frac{Q^2}{\Lambda^2}\right)$		—	—
$\mathcal{N}^2\text{LO } \mathcal{O}\left(\frac{Q^3}{\Lambda^3}\right)$		—	—
$\mathcal{N}^3\text{LO } \mathcal{O}\left(\frac{Q^4}{\Lambda^4}\right)$			

explains pheno hierarchy:

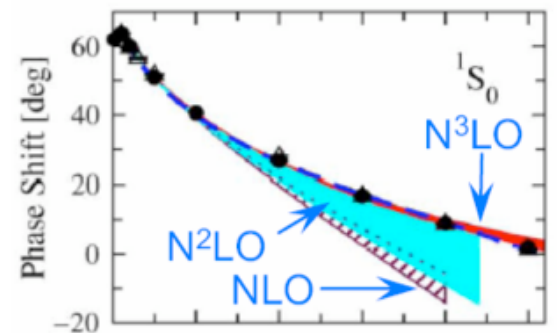
NN > 3N > 4N > ...

consistent NN-3N,  $\pi N$ ,  $\pi\pi$ ,  
electroweak operators

3N,4N: 2 new couplings to  $\mathcal{N}^3\text{LO}$

resolution/ $\Lambda$ -dep. contact interactions

error estimates from truncation order  
and resolution/ $\Lambda$ -variation



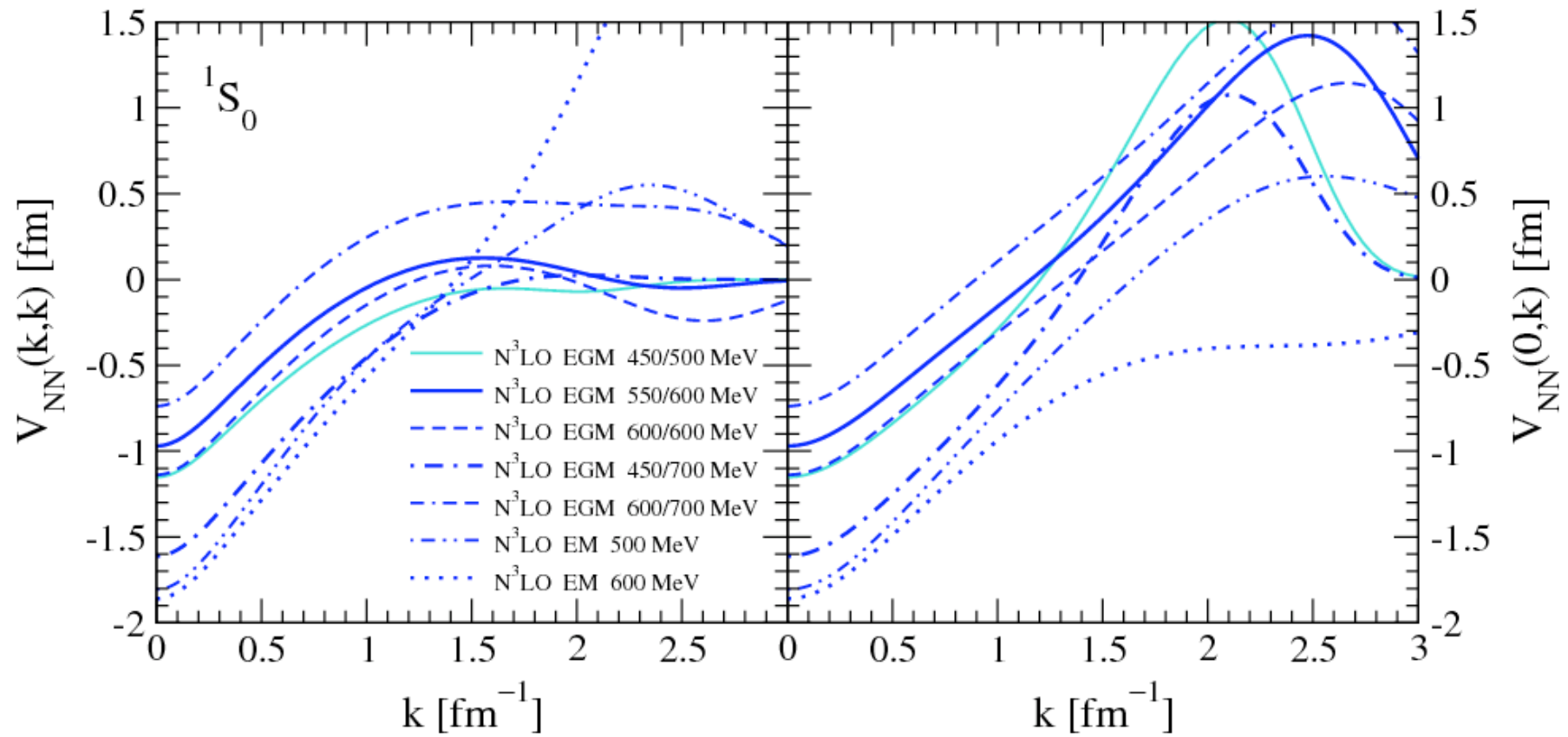
Weinberg, van Kolck, Kaplan, Savage, Wise, Epelbaum, Meissner, Nogga, Machleidt,...

## References

E. Epelbaum, Few-nucleon forces and systems in chiral EFT,  
Prog. Part. Nucl. Phys. **57**, 654 (2006).

R. Machleidt, Nuclear forces from chiral EFT, arXiv:0704.0807.

# Chiral EFT interactions at N<sup>3</sup>LO

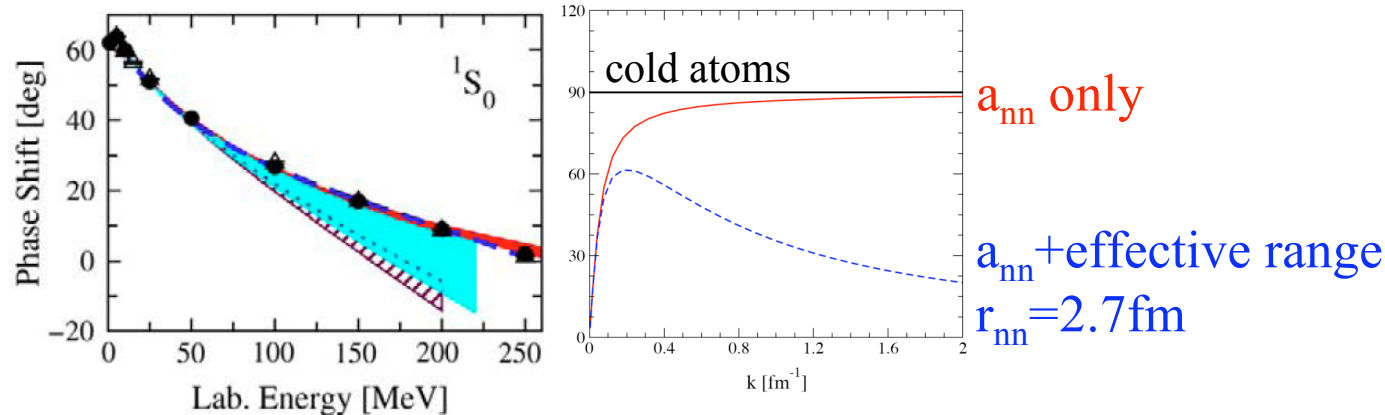


regulator and renormalization scheme and scale dependence

There is not just one N<sup>3</sup>LO potential!

# Chiral EFT phase shifts and NN PWA

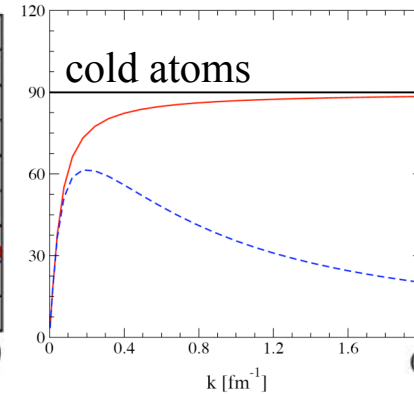
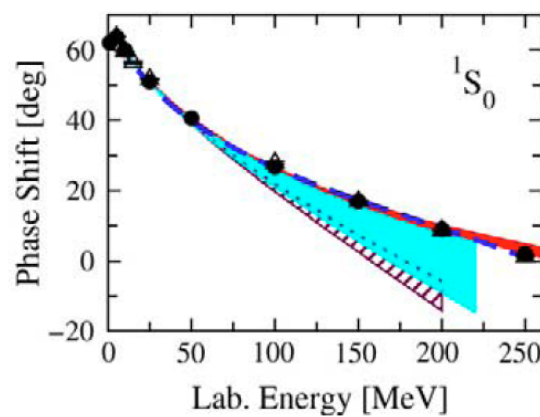
Nijmegen PWA93 (filled circles) <http://www.nn-online.org>



S-waves weaker at higher energies:  
fewer particles interact strongly  
at finite density

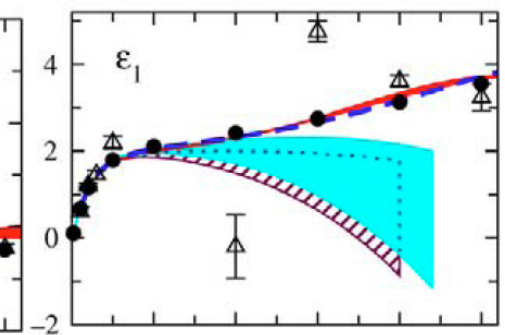
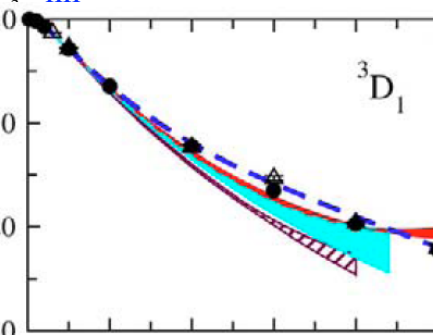
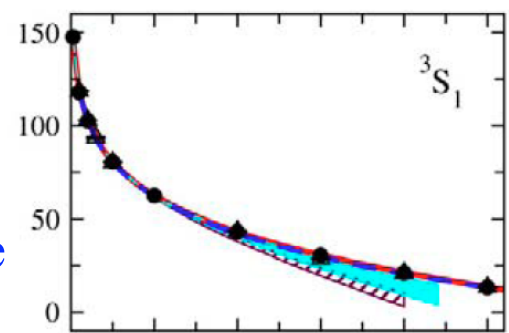
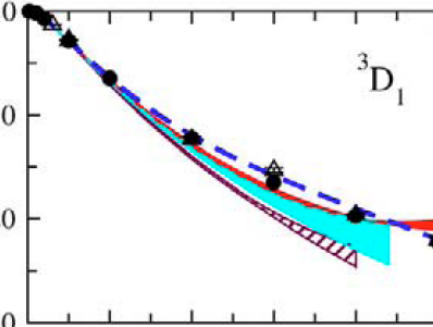
# Chiral EFT phase shifts and NN PWA

Nijmegen PWA93 (filled circles) <http://www.nn-online.org>



$a_{nn}$  only

$a_{nn}$  + effective range  
 $r_{nn} = 2.7 \text{ fm}$



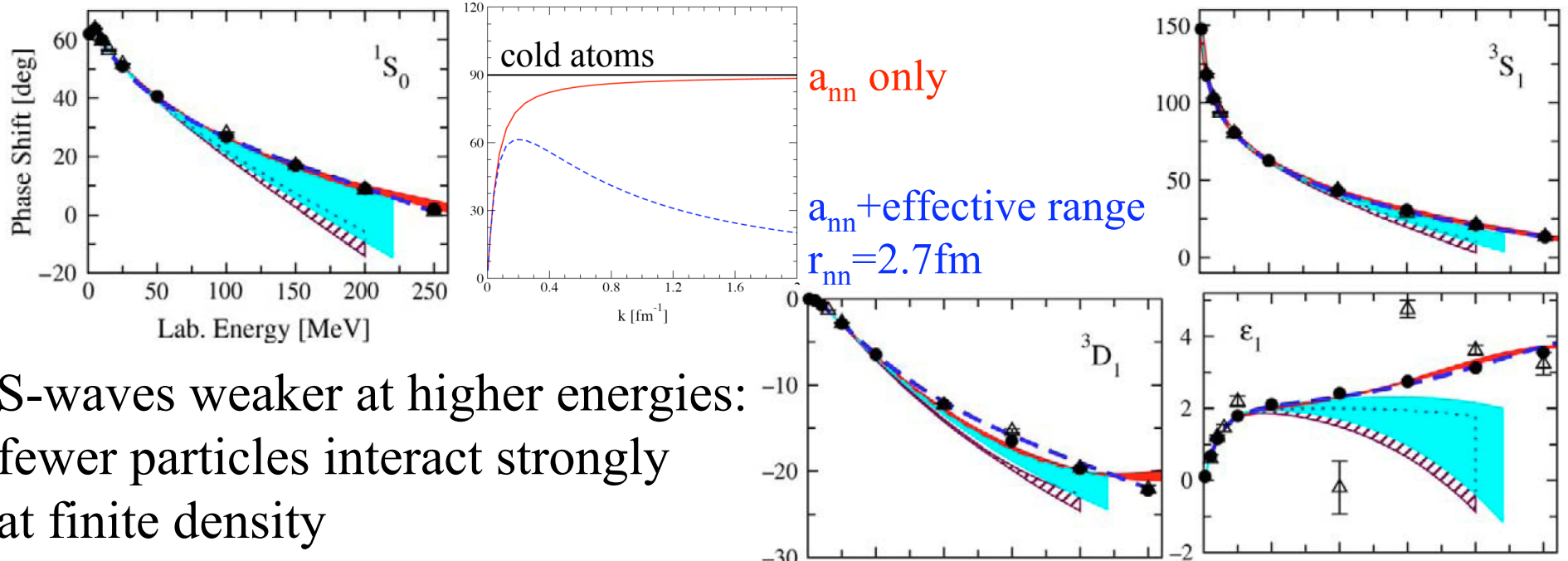
S-waves weaker at higher energies:  
 fewer particles interact strongly  
 at finite density

Tensor force from  $^3S_1$ - $^3D_1$  mixing  $\epsilon_1$  in spin=1 channel

Epelbaum (2006)  
 Machleidt (1998)

# Chiral EFT phase shifts and NN PWA

Nijmegen PWA93 (filled circles) <http://www.nn-online.org>



S-waves weaker at higher energies:  
fewer particles interact strongly  
at finite density

Tensor force from  $^3S_1$ - $^3D_1$  mixing  $\epsilon_1$  in spin=1 channel

Epelbaum (2006)  
Machleidt (1998)

Spin-orbit (LS) force  
from triplet  $^3P_{J=0,1,2}$   
phase shifts  
C=central, T=tensor only

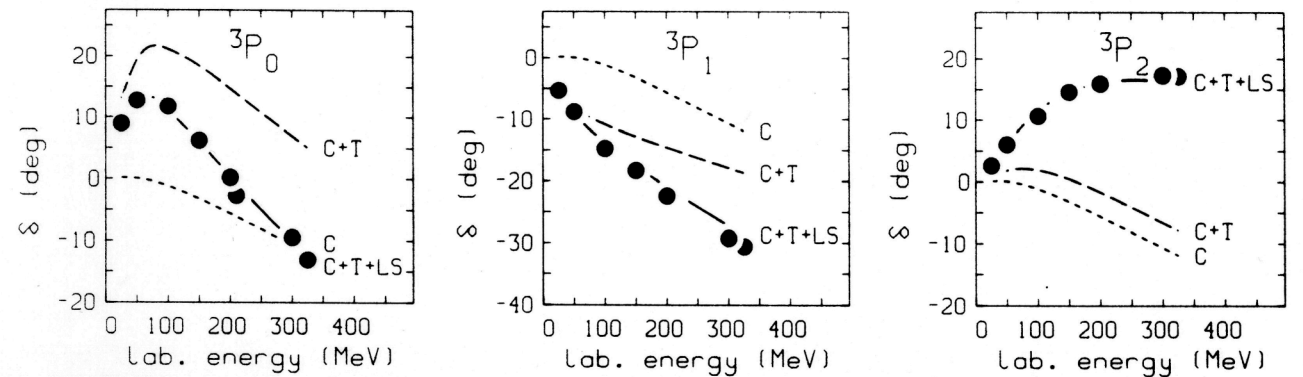
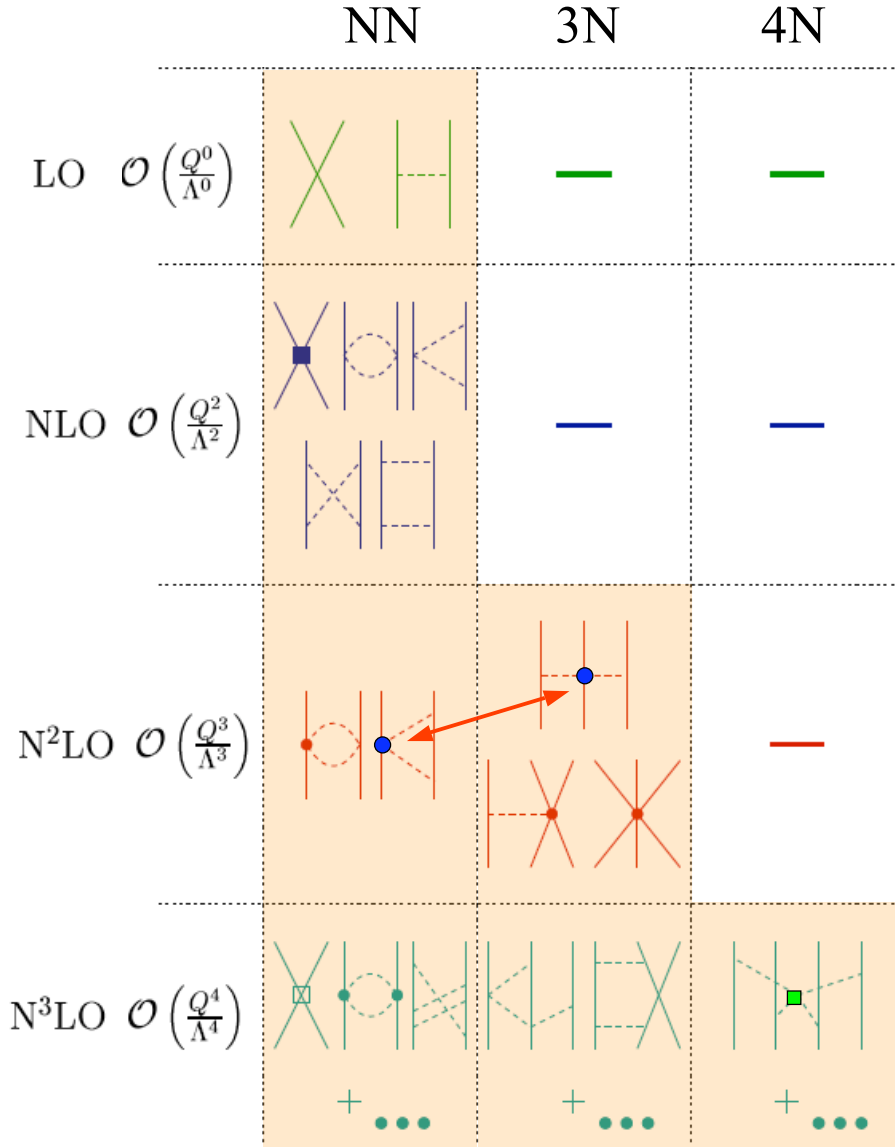


Fig. 3.3. NN phase shifts in triplet  $P$  waves. Shown are predictions using a central

# Chiral EFT for nuclear forces

Separation of scales: low momenta  $\frac{1}{\lambda} = Q \ll \Lambda_b$  breakdown scale  $\sim 500$  MeV



## Open questions:

Power counting with singular pion exchanges, tensor parts  $\sim 1/r^3$  for OPE more singular for higher order pion exch.

promotion of contact interactions

Nogga, Timmermans, van Kolck (2005)

Delta-full  $m_\Delta - m_N \sim m_\pi$   
vs. Delta-less chiral EFT

one- $\Delta$  3N interaction starts at NLO

Counting of  $1/m$  corrections,  
 $m \sim \Lambda^2$  or  $\Lambda$ , could be important for  $A_y$

Lepage plots and breakdown scale

Weinberg, van Kolck, Kaplan, Savage, Wise, Epelbaum, Meissner, Nogga, Machleidt,...

# Lepage plots

Lepage (1997)

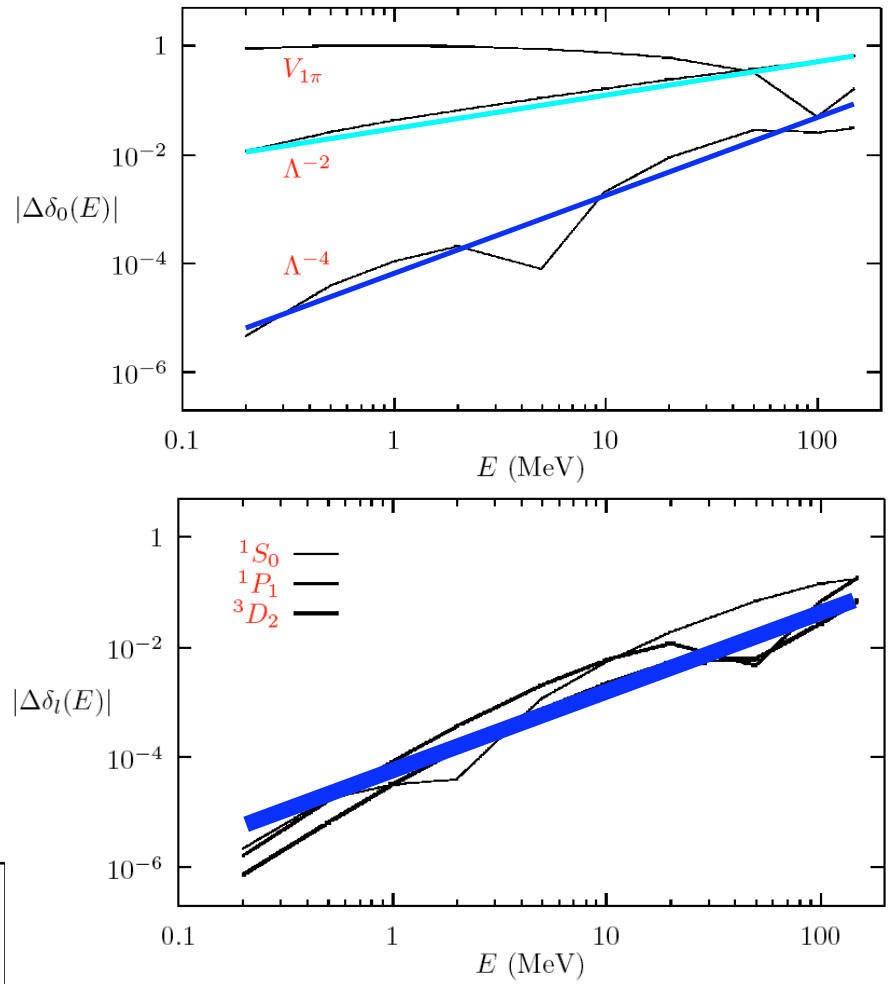
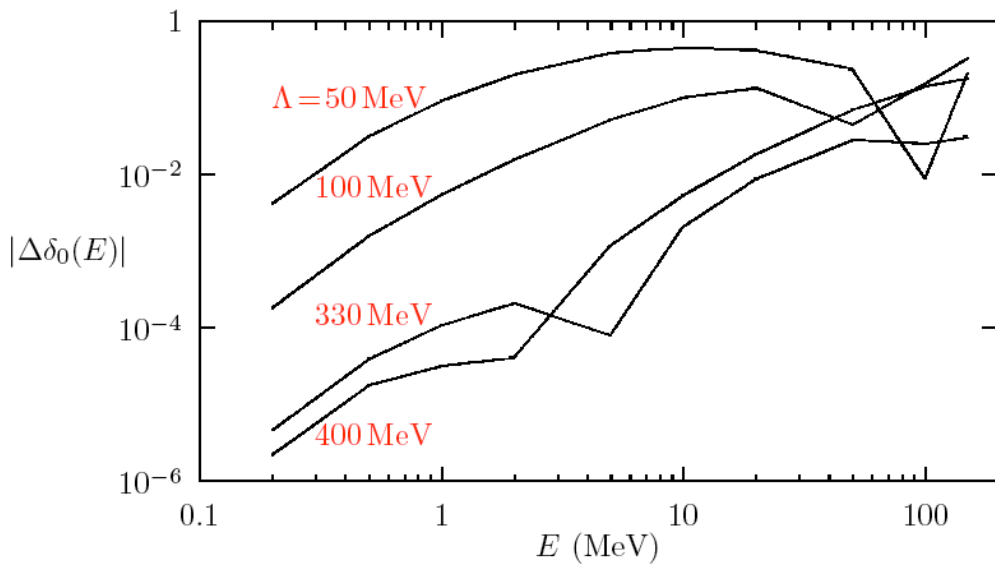
Log-log plots of relative errors vs. E

steeper slope with subsequent orders,  
same in all channels: S,P,D,... waves

$$V(r) = -\alpha_\pi v_\Lambda(r) + c \frac{\delta_{1/\Lambda}^3(\mathbf{r})}{\Lambda^2} - d \frac{\nabla^2 \delta_{1/\Lambda}^3(\mathbf{r})}{\Lambda^4}$$

$$P : \quad V_{\pi,P} + \frac{\nabla \delta_{1/\Lambda}^3 \nabla}{\Lambda^4} + \mathcal{O}(1/\Lambda^6)$$

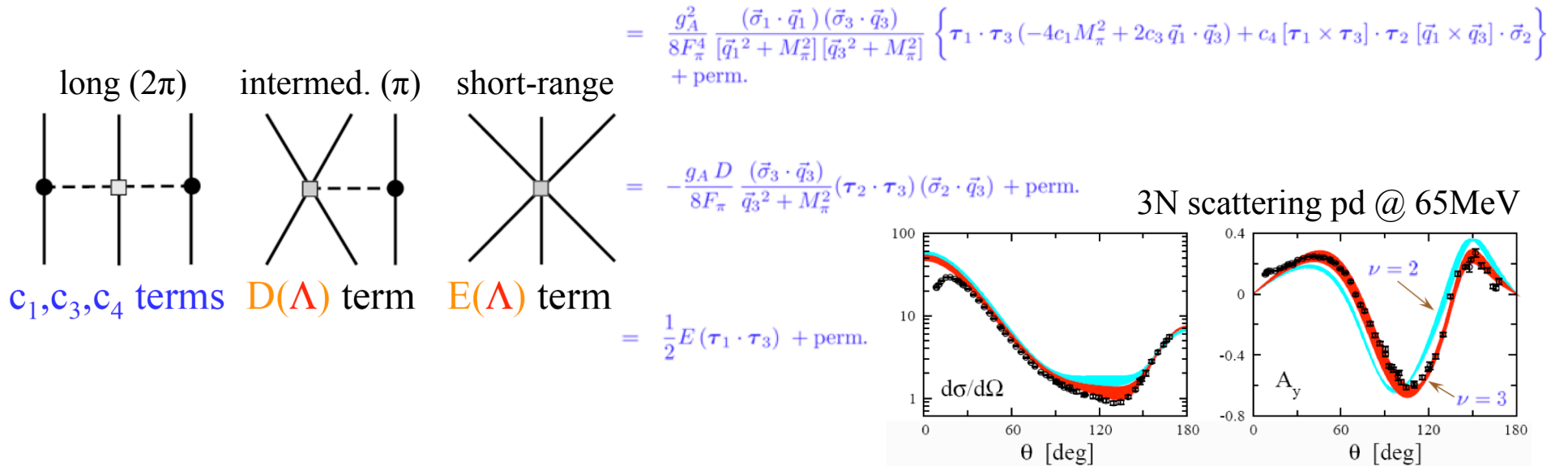
$$D : \quad V_{\pi,D} + \mathcal{O}(1/\Lambda^6)$$



Cutoff dependence:  
truncation errors decrease with  
increasing cutoff  
no advantages for cutoffs >>  
breakdown scale (nonlinearities)

# Chiral EFT 3N interactions

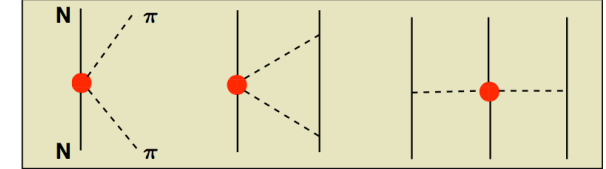
leading  $N^2LO \sim (Q/\Lambda)^3$  van Kolck (1994), Epelbaum et al. (2002)



$c_i$  relate  $\pi N$ ,  $NN$ ,  $3N$ : determination from  $\pi N$

Meissner (2007)

$$c_1 = -0.9^{+0.2}_{-0.5}, \quad c_3 = -4.7^{+1.2}_{-1.0}, \quad c_4 = 3.5^{+0.5}_{-0.2}$$



consistent with  $NN$ :  $c_1 = -0.76(7)$ ,  $c_3 = -4.78(10)$ ,  $c_4 = 3.96(22)$

Rentmeester et al. (2003)

$c_3, c_4$  important for structure, but large uncertainties at present

D,E couplings fixed by  $A>2$  data see Barrett's lectures and next lecture

D term can be fixed by tritium beta decay Gardestig, Phillips (2006) Gazit et al. (2008)

# Subleading chiral EFT 3N interactions

parameter-free N<sup>3</sup>LO Bernard et al. (2007), Ishikawa, Robilotta (2007)

- 1/m-corrections to 1 insertion from  $\mathcal{L}_{1/m}^{(2)} =$   +  $\mathcal{O}(\pi^3)$

— rich operator structure (includes spin-orbit interactions)

- 1-loop diagrams with all vertices from  $\mathcal{L}_{\text{eff}}^{(0)}$

**2π – exchange**

$$\text{Diagram: two vertical lines with a central dot.} = \text{Diagram: two vertical lines with a central dot, one line has a horizontal dash.} + \text{Diagram: two vertical lines with a central dot, one line has a vertical dash.} + \text{Diagram: two vertical lines with a central dot, one line has a diagonal dash.} + \text{Diagram: two vertical lines with a central dot, one line has a vertical dash.} + \text{Diagram: two vertical lines with a central dot, one line has a diagonal dash.} + \dots \text{ decrease } c_i \text{ constants}$$

The calculated corrections simply shift the LECs  $c_i$  as follows:

$$\delta c_1 = \frac{g_A^2 M_\pi}{64\pi F_\pi^2} \sim 0.13 \text{ GeV}^{-1} \quad \delta c_3 = \frac{3g_A^4 M_\pi}{16\pi F_\pi^2} \sim 2.5 \text{ GeV}^{-1} \quad \delta c_4 = -\frac{g_A^4 M_\pi}{16\pi F_\pi^2} \sim -0.85 \text{ GeV}^{-1}$$

**2π-1π – exchange**

$$\text{Diagram: two vertical lines with a central dot, one line has a circle around it.} = \text{Diagram: two vertical lines with a central dot, one line has a circle around it, one line has a horizontal dash.} + \text{Diagram: two vertical lines with a central dot, one line has a circle around it, one line has a vertical dash.} + \text{Diagram: two vertical lines with a central dot, one line has a circle around it, one line has a diagonal dash.} + \text{Diagram: two vertical lines with a central dot, one line has a circle around it, one line has a vertical dash.} + \text{Diagram: two vertical lines with a central dot, one line has a circle around it, one line has a diagonal dash.} + \dots$$

**ring diagrams**

$$\text{Diagram: two vertical lines with a central dot, one line has a circle around it, the other line has a circle around it.} = \text{Diagram: two vertical lines with a central dot, one line has a circle around it, the other line has a circle around it, one line has a horizontal dash.} + \text{Diagram: two vertical lines with a central dot, one line has a circle around it, the other line has a circle around it, one line has a vertical dash.} + \text{Diagram: two vertical lines with a central dot, one line has a circle around it, the other line has a circle around it, one line has a diagonal dash.} + \text{Diagram: two vertical lines with a central dot, one line has a circle around it, the other line has a circle around it, one line has a vertical dash.} + \text{Diagram: two vertical lines with a central dot, one line has a circle around it, the other line has a circle around it, one line has a diagonal dash.} + \dots$$

**contact-1π – exchange**

$$\text{Diagram: two vertical lines with a central dot, one line has a circle around it, the other line has a circle around it, the central dot is connected to the top line by a horizontal line.} = \text{Diagram: two vertical lines with a central dot, one line has a circle around it, the other line has a circle around it, the central dot is connected to the top line by a horizontal line, one line has a horizontal dash.} + \text{Diagram: two vertical lines with a central dot, one line has a circle around it, the other line has a circle around it, the central dot is connected to the top line by a horizontal line, one line has a vertical dash.} + \text{Diagram: two vertical lines with a central dot, one line has a circle around it, the other line has a circle around it, the central dot is connected to the top line by a horizontal line, one line has a diagonal dash.} + \text{Diagram: two vertical lines with a central dot, one line has a circle around it, the other line has a circle around it, the central dot is connected to the top line by a horizontal line, one line has a vertical dash.} + \text{Diagram: two vertical lines with a central dot, one line has a circle around it, the other line has a circle around it, the central dot is connected to the top line by a horizontal line, one line has a diagonal dash.} + \dots$$

3N interactions involving  
NN contacts in progress

**contact-2π – exchange**

$$\text{Diagram: two vertical lines with a central dot, one line has a circle around it, the other line has a circle around it, the central dot is connected to the top line by a horizontal line, the central dot is connected to the bottom line by a horizontal line.} = \text{Diagram: two vertical lines with a central dot, one line has a circle around it, the other line has a circle around it, the central dot is connected to the top line by a horizontal line, the central dot is connected to the bottom line by a horizontal line, one line has a horizontal dash.} + \text{Diagram: two vertical lines with a central dot, one line has a circle around it, the other line has a circle around it, the central dot is connected to the top line by a horizontal line, the central dot is connected to the bottom line by a horizontal line, one line has a vertical dash.} + \text{Diagram: two vertical lines with a central dot, one line has a circle around it, the other line has a circle around it, the central dot is connected to the top line by a horizontal line, the central dot is connected to the bottom line by a horizontal line, one line has a diagonal dash.} + \text{Diagram: two vertical lines with a central dot, one line has a circle around it, the other line has a circle around it, the central dot is connected to the top line by a horizontal line, the central dot is connected to the bottom line by a horizontal line, one line has a vertical dash.} + \text{Diagram: two vertical lines with a central dot, one line has a circle around it, the other line has a circle around it, the central dot is connected to the top line by a horizontal line, the central dot is connected to the bottom line by a horizontal line, one line has a diagonal dash.} + \dots$$

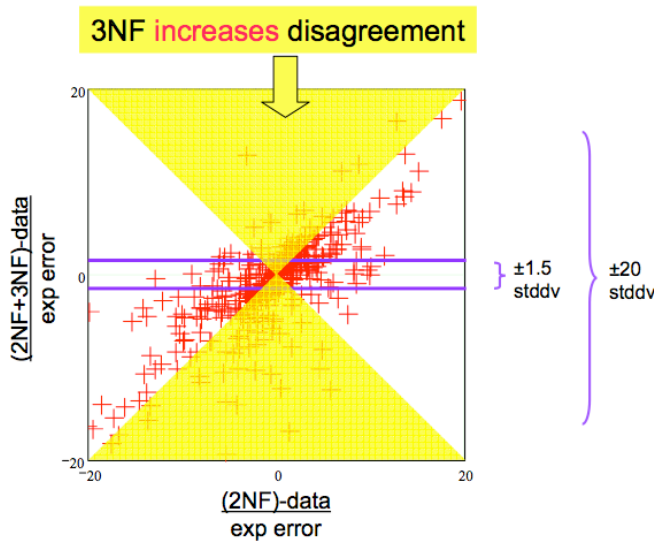
Epelbaum et al.

# 3N interactions: a frontier

from H.-O. Meyer @ TRIUMF 3N workshop (2007)

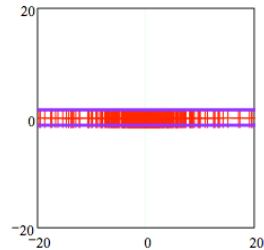
pd scattering

a way to look at  
880 data points...

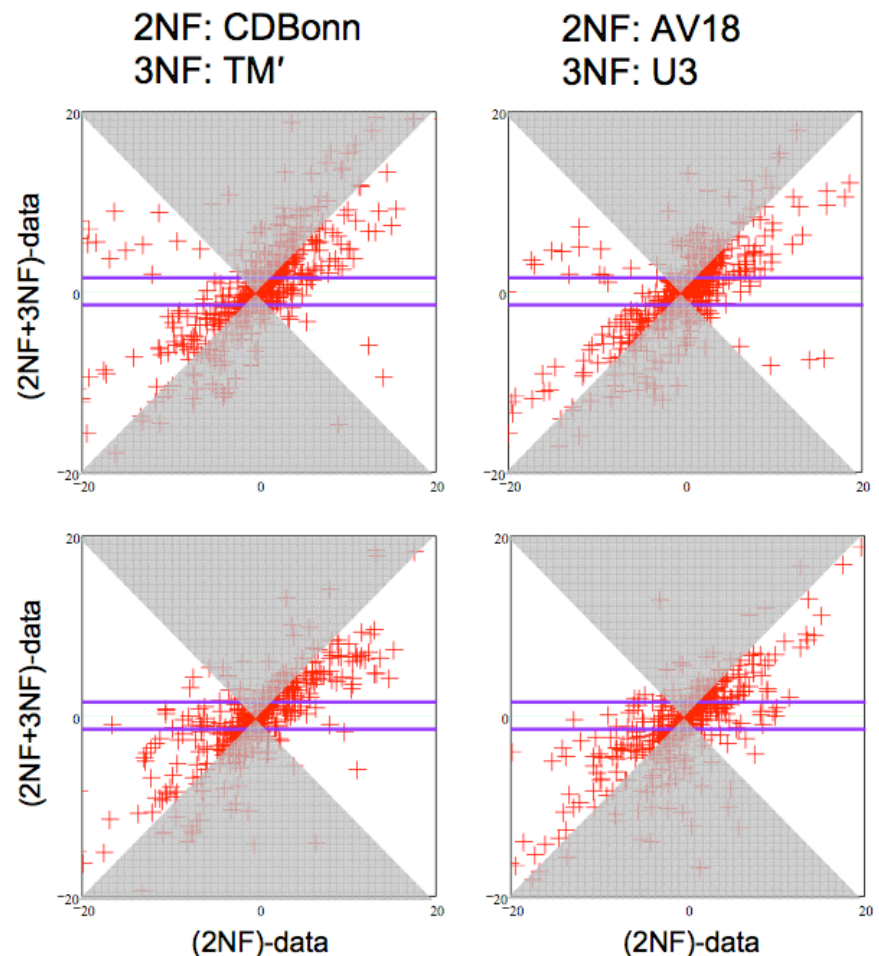
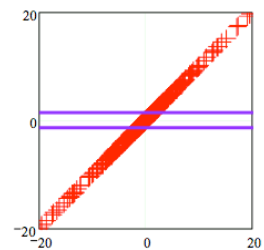


135 MeV

b) 3NF explains data



a) 3NF has no effect



coherent 3N effort needed with theoretical uncertainties

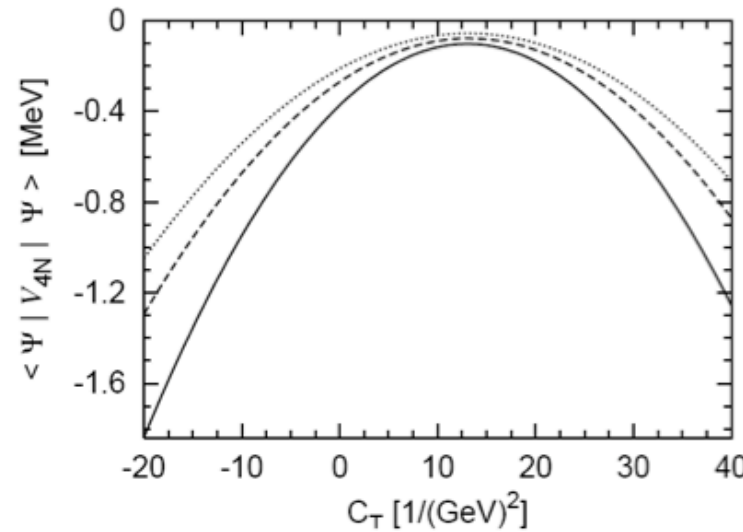
# Chiral EFT 4N interactions - first estimate

from Epelbaum @ TRIUMF 3N workshop (2007)

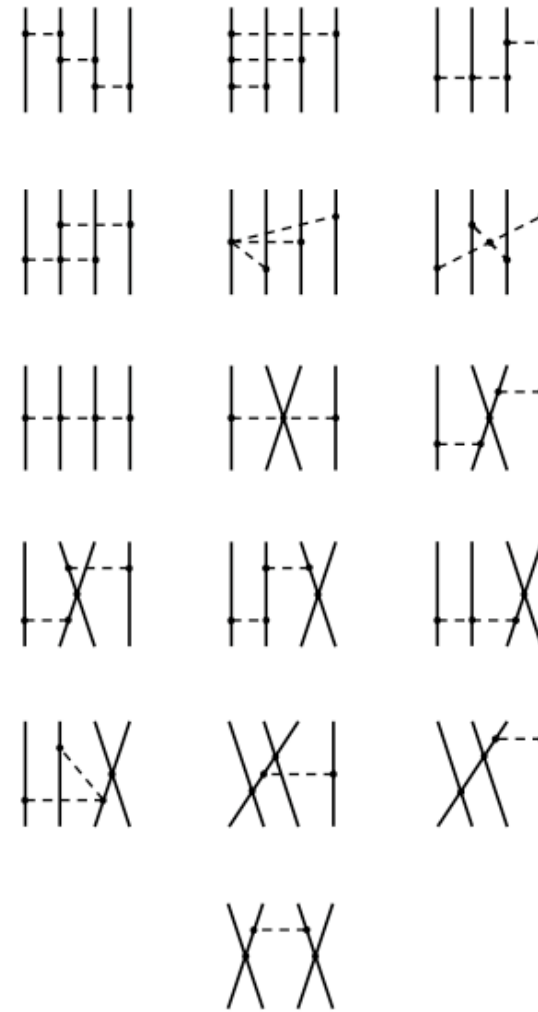
## Four-nucleon force (E.E. '05)

- first shows up at order  $\nu = 4$
- chiral symmetry plays a crucial role
- parameter-free

Contribution of the 4NF to the  ${}^4\text{He}$  BE is attractive and of the order of few 100 keV  
(Rozpedzik et al. '06)

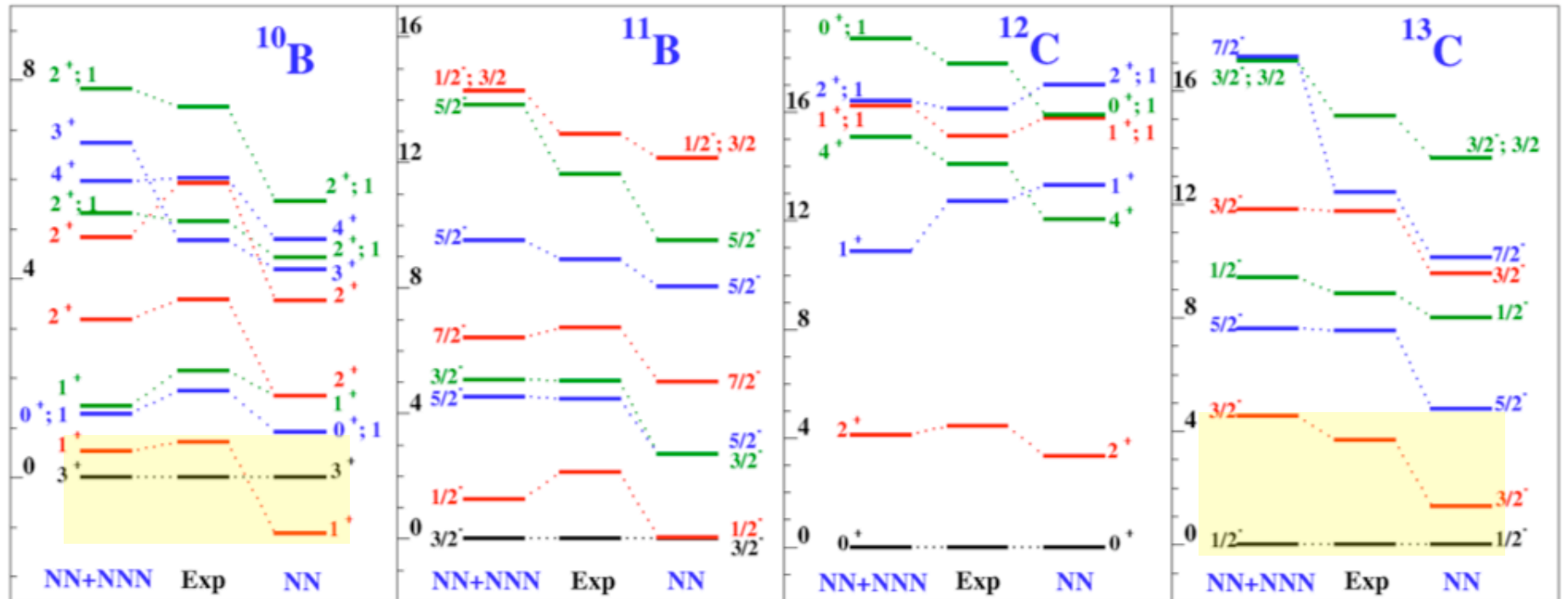


Results from: Rozpedzik et al., nucl-th/0606017



4N contributions  $\sim 1$  MeV at saturation density not unreasonable

# 3N interactions and nuclear structure



No-Core Shell Model: Navratil et al. (2007)

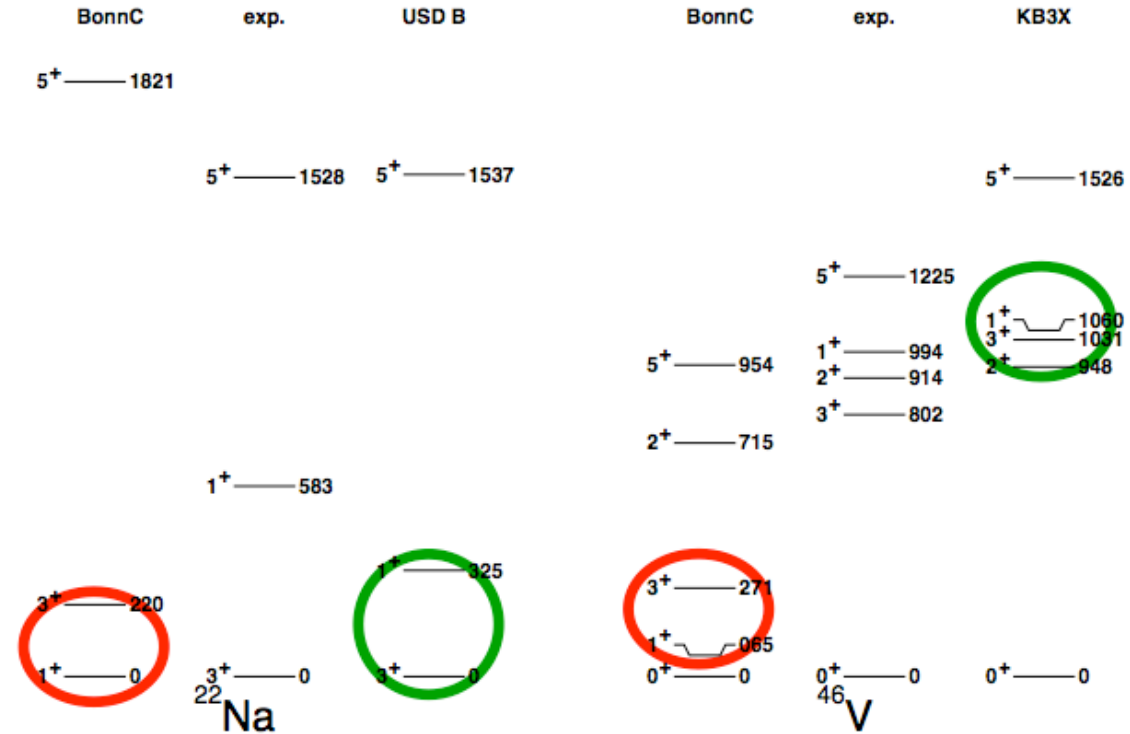
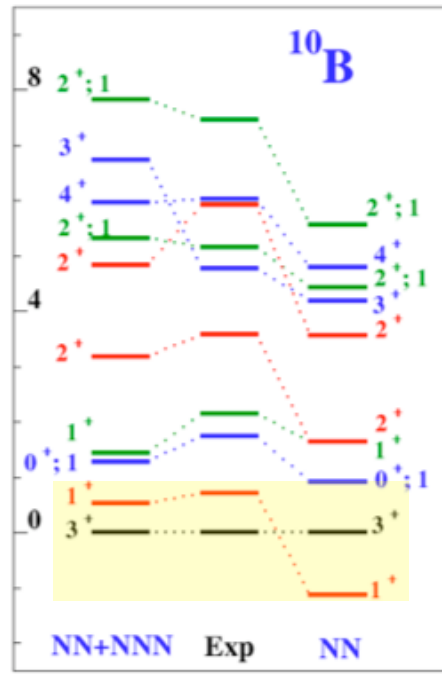
agreement supports chiral EFT interactions

highlights the importance of 3N interactions

# 3N interactions and nuclear structure

microscopic calculations highlight the importance of 3N interactions

Navratil et al. (2007)



same  $1^+$  vs.  $3^+$  inversion in closed shell  $+3p+3n$  without 3N interactions  
Nowacki @ Oslo 2008

3N crucial for  $T=1$  spin-orbit shell closures in  $^{22}\text{O}$ ,  $^{48}\text{Ca}$ ,...

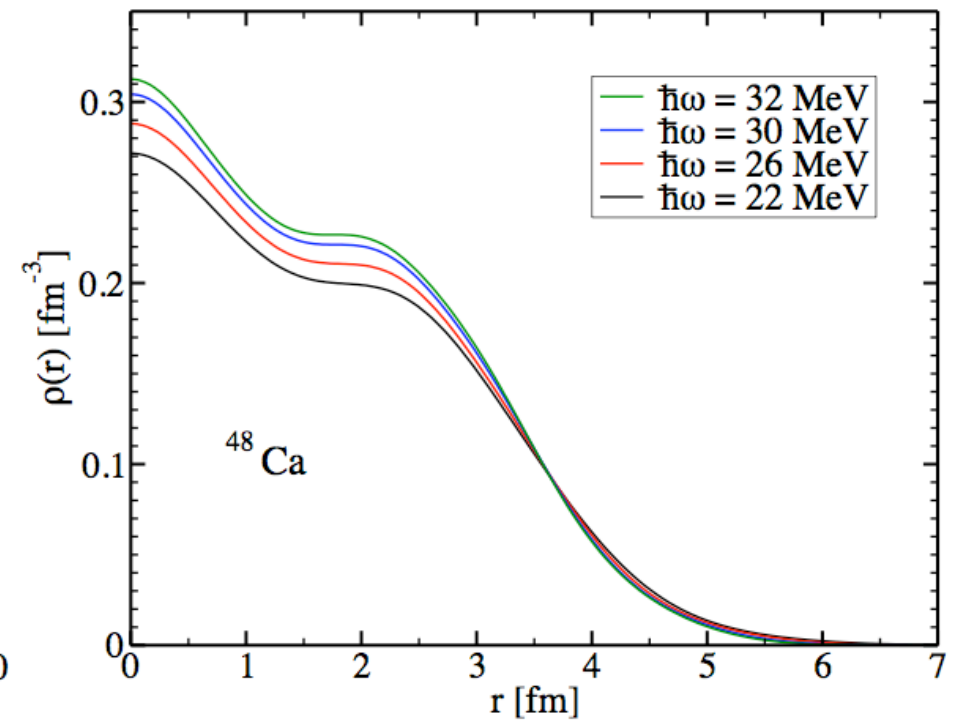
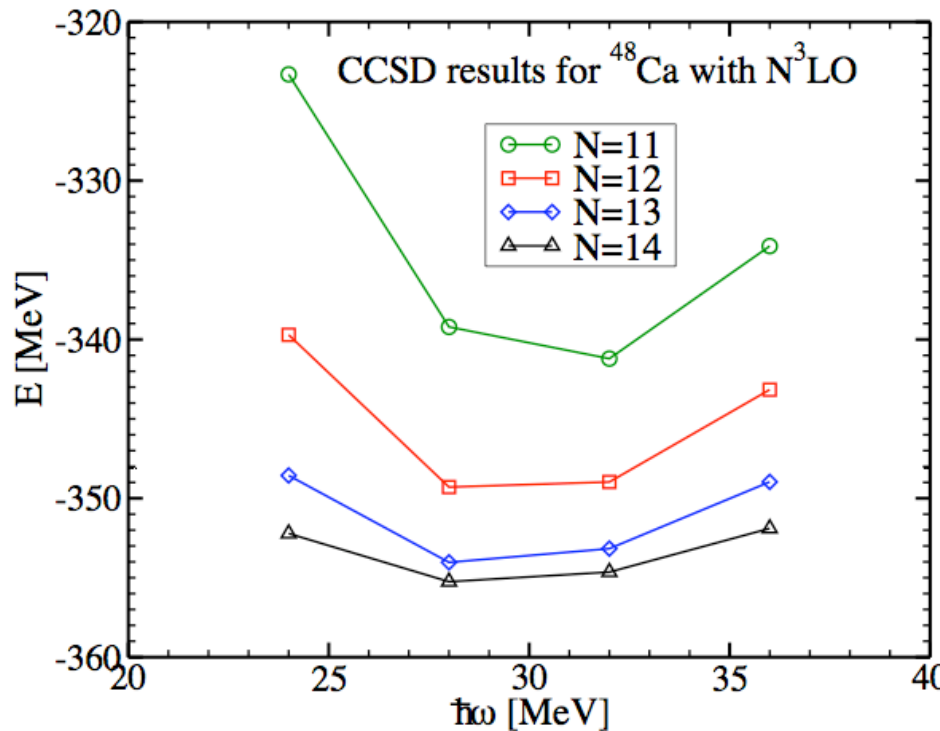
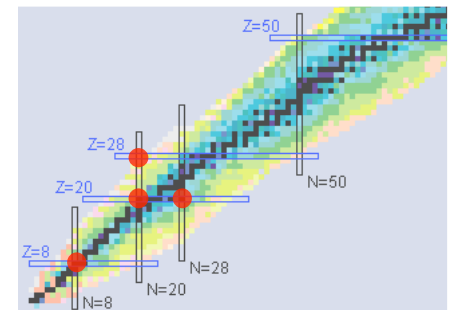
see e.g., AS, Zuker (2006)

# Medium-mass nuclei from chiral NN interactions Hagen et al. (2008)

spherical coupled-cluster theory:  $\sim 10^5$  speed-up

$^{40,48}\text{Ca}$  and  $^{48}\text{Ni}$  in 15 major shells on single processor

near converged ground states for  $\text{N}^3\text{LO}$  NN potentials



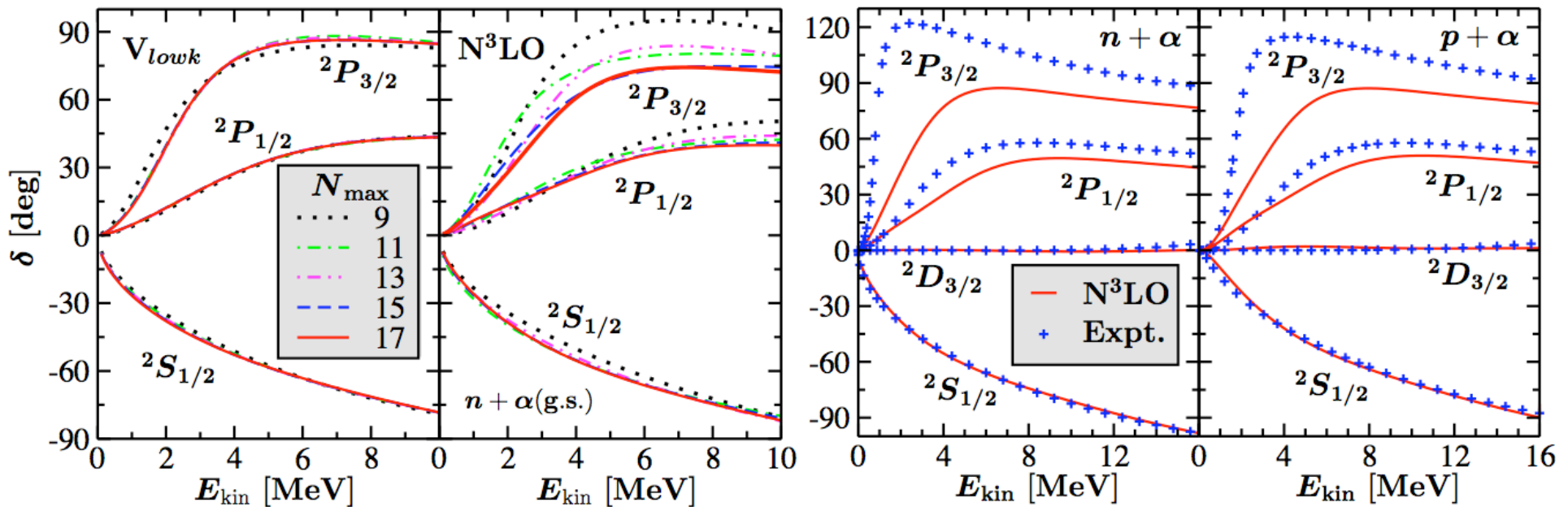
future: first calculations with 3N interactions for medium-mass nuclei

$^{100}\text{Sn}$  and  $^{208}\text{Pb}$ , ab-initio calc of Pb neutron radius from chiral EFT

# First nuclear reactions from chiral interactions Quaglioni, Navratil (2008)

Resonating group method combined with No-Core Shell Model

n/p- $^4\text{He}$  scattering,... n- $^{10}\text{Be}$  scattering



future: include 3N interactions, inelastic scattering,...

## Outline

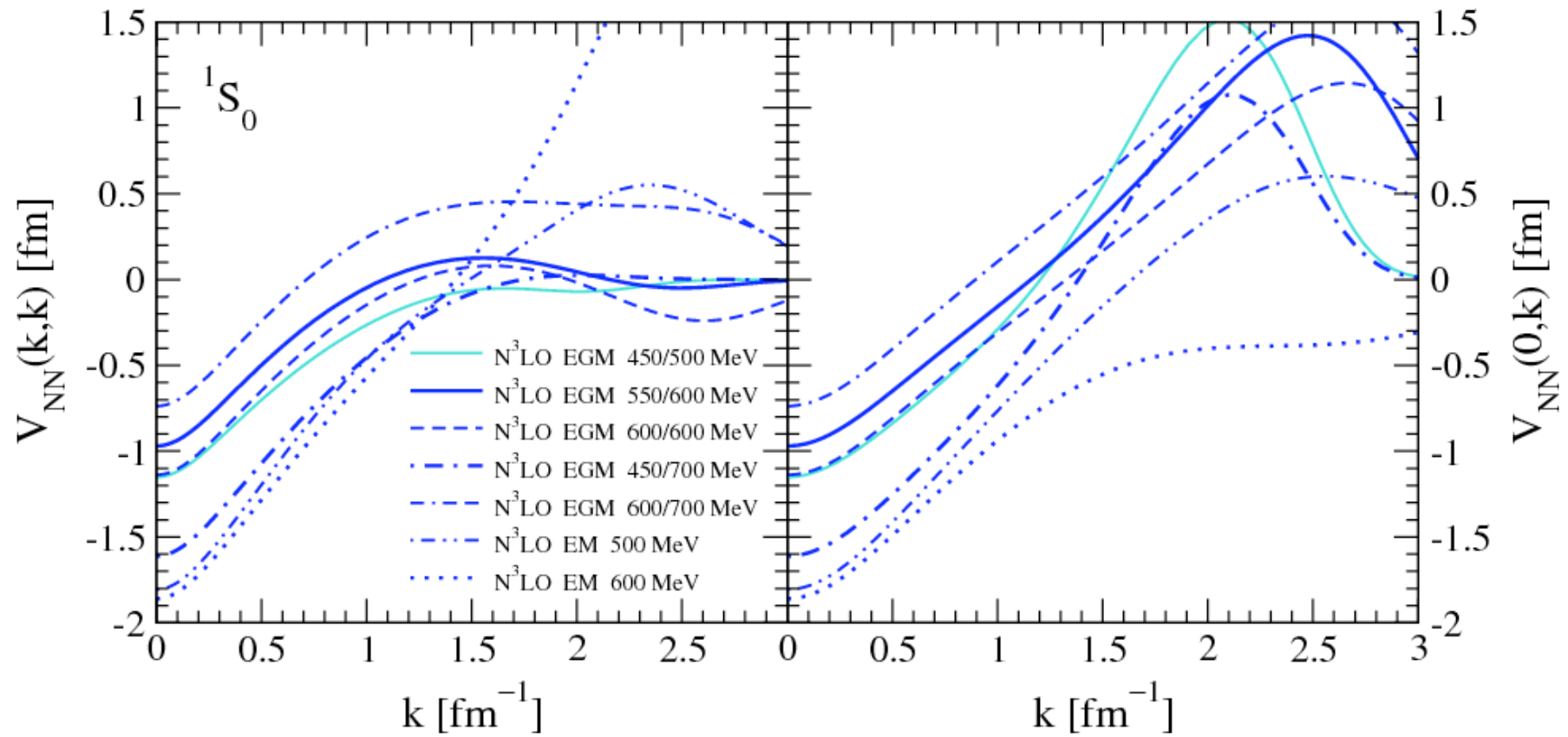
1. Introduction to effective field theory and the renormalization group
2. Chiral effective field theory
3. Renormalization group for nuclear forces
4. EFT and RG for nuclear matter
5. Nuclear matter in astrophysics
6. Neutrino processes in supernovae from chiral EFT

## References

S.K. Bogner, T.T.S. Kuo and AS, Phys. Rept. **386**, 1 (2003).

S.K. Bogner, R.J. Furnstahl, S. Ramanan and AS,  
Low-momentum interactions with smooth cutoffs,  
Nucl. Phys. **A784**, 79 (2007).

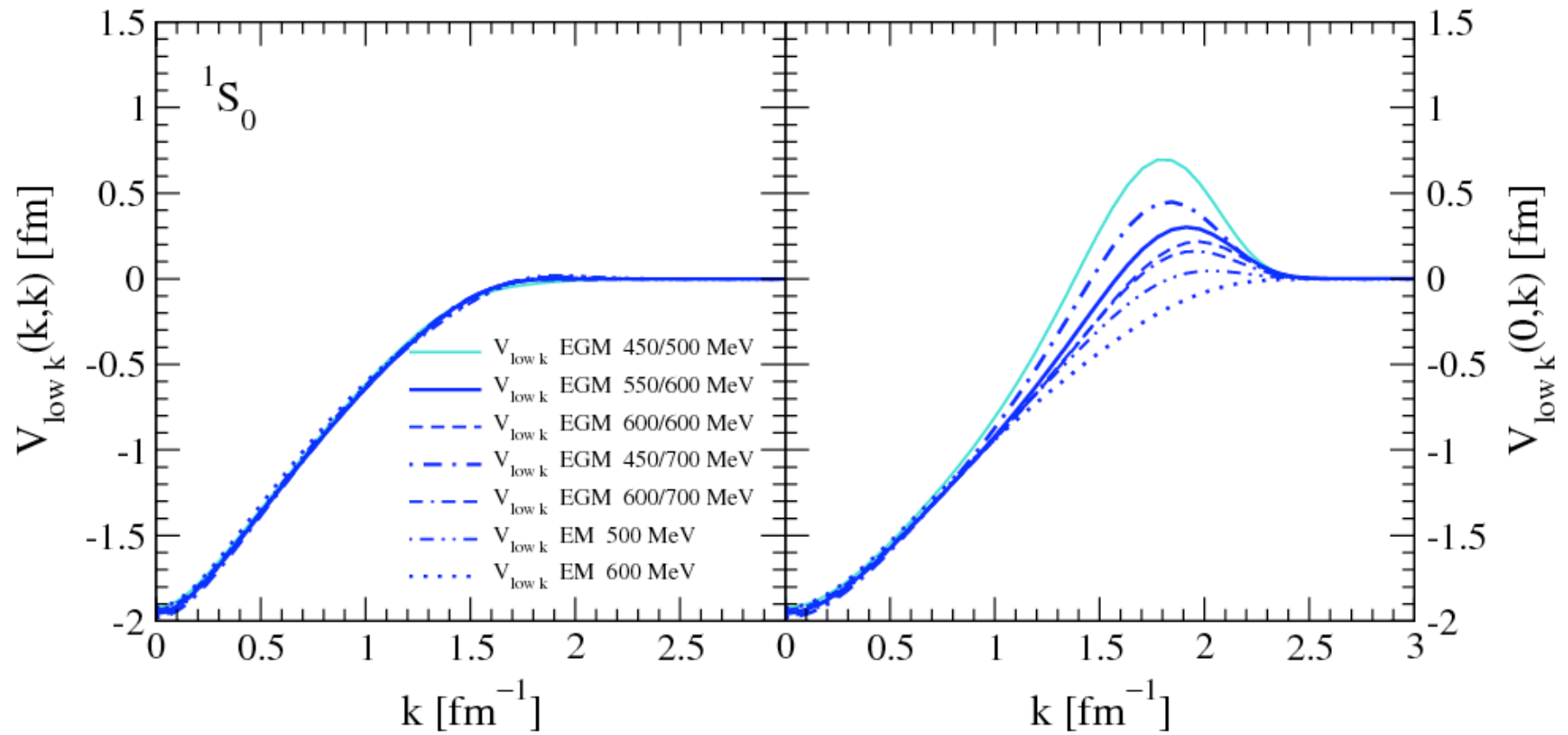
# Chiral EFT interactions at N<sup>3</sup>LO



regulator and renormalization scheme and scale dependence

There is not just one N<sup>3</sup>LO potential!

# RG evolution of chiral EFT interactions at N<sup>3</sup>LO



find  $\approx$  universality from different N<sup>3</sup>LO potentials

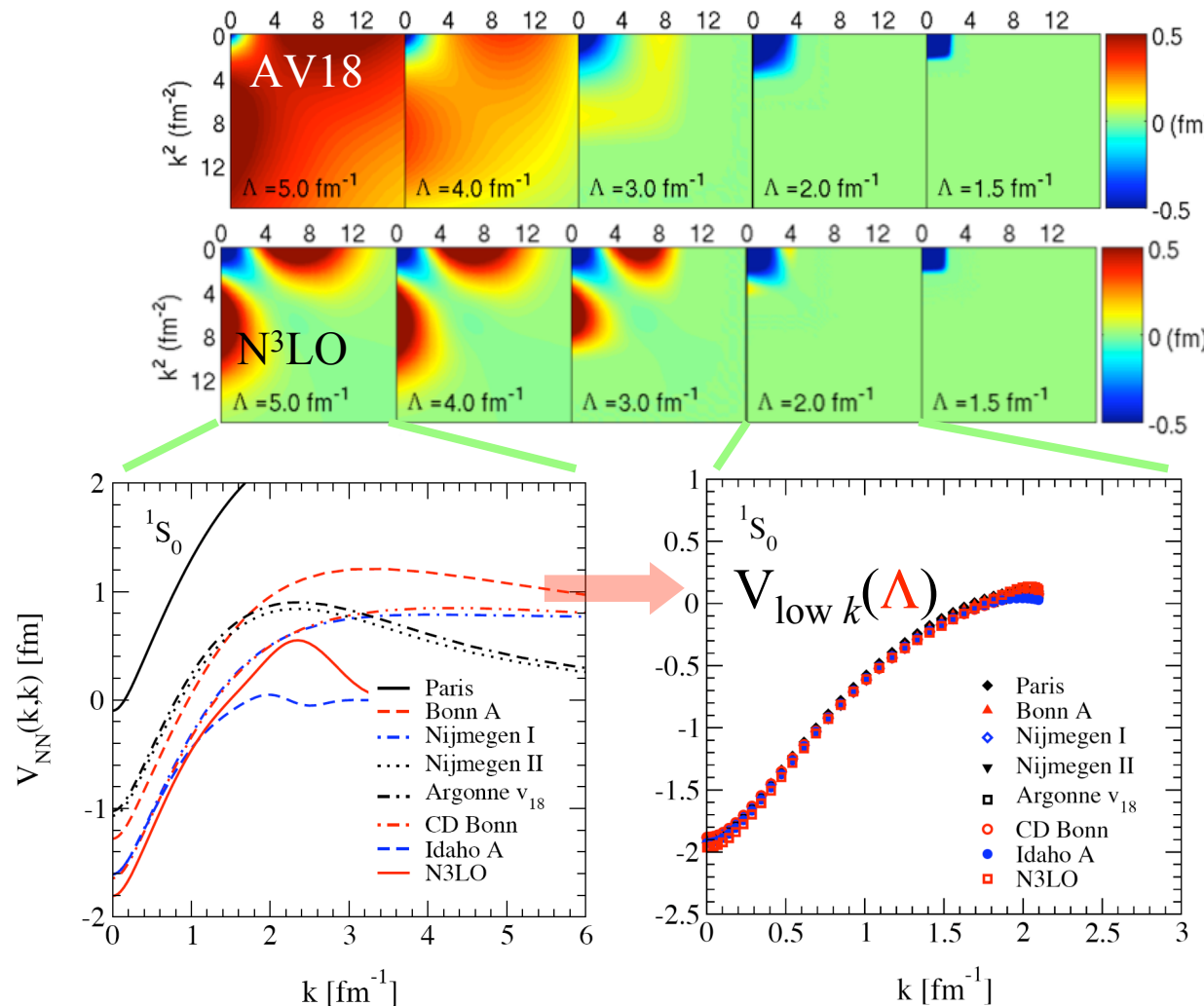
RG evolution weakens off-diagonal coupling,  
decouples high momenta

# Low-momentum interactions from the Renormalization Group

## RG evolution to lower resolution/cutoffs

$$H(\Lambda) = T + V_{\text{NN}}(\Lambda) + V_{3\text{N}}(\Lambda) + V_{4\text{N}}(\Lambda) + \dots$$

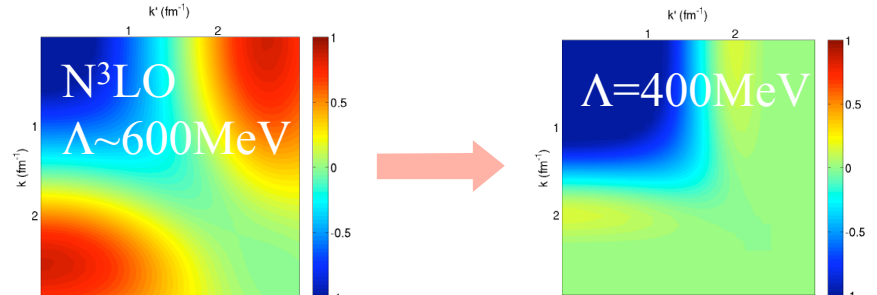
$\approx$  universal interaction for low momenta  $V_{\text{low } k}(\Lambda)$  Bogner, Kuo, AS (2003)



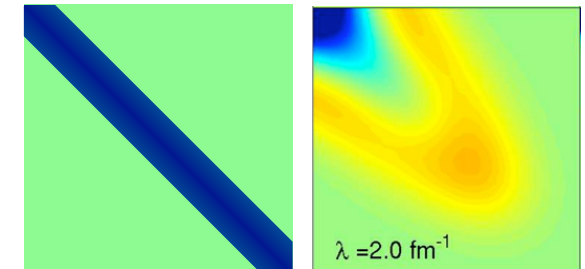
# Advantages of low-momentum interactions for nuclei

lower cutoffs need smaller basis

Bogner et al. (2007...)

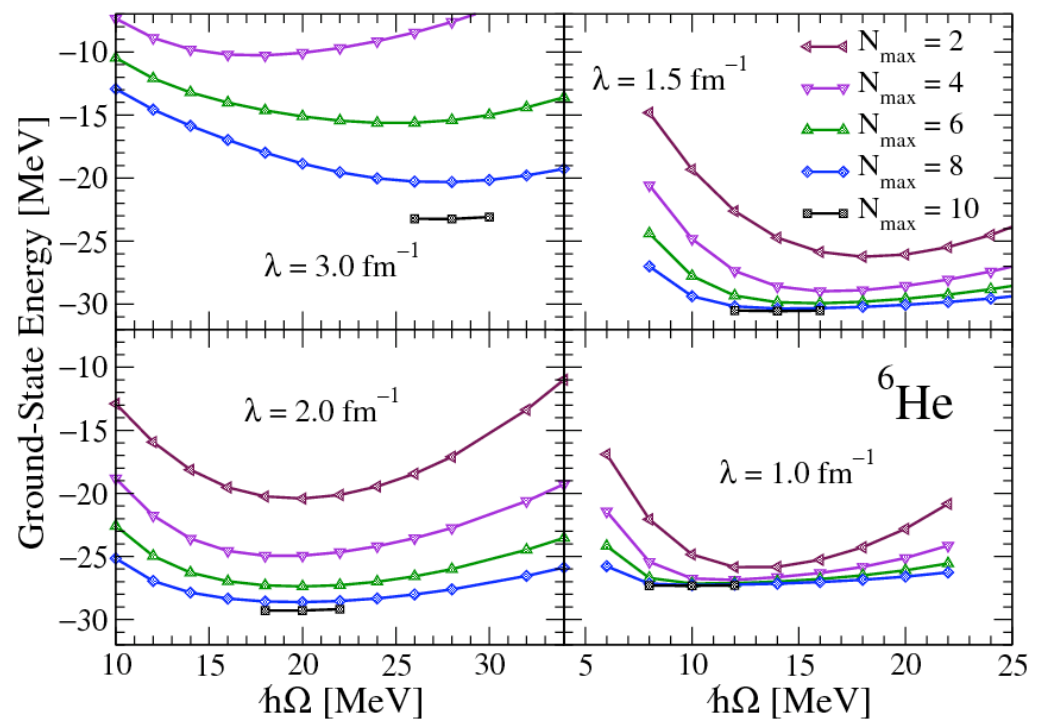


Similarity Renormalization Group (SRG)  
evolution towards band diagonal  $V_{\text{SRG}}(\lambda)$



improved convergence for nuclei

$10^3$  states for  $N_{\text{max}}=2$  vs.  
 $10^7$  states for  $N_{\text{max}}=10$



# Similarity RG interactions

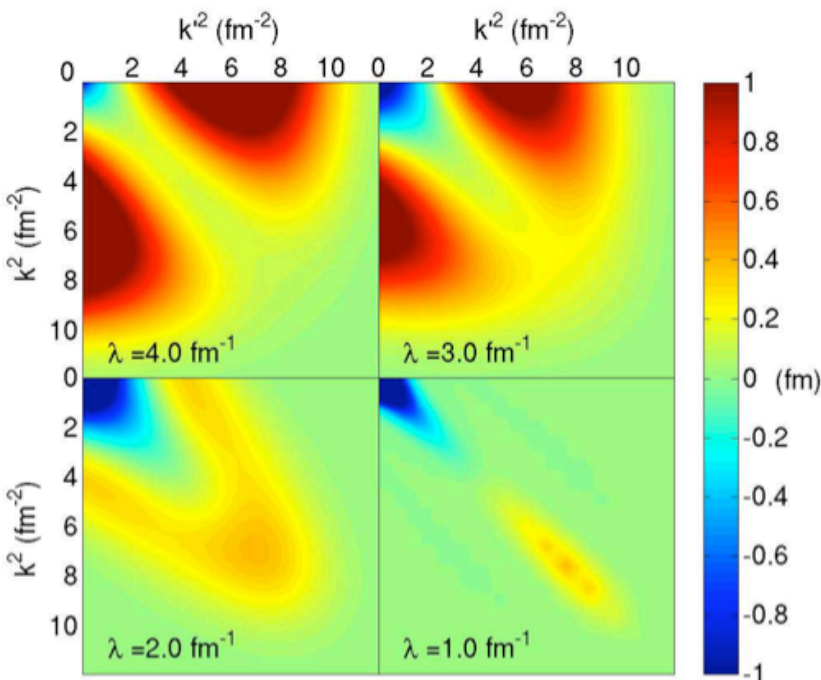
Unitary transformations to band-diagonal  $V_{\text{srg}}(\lambda)$  from flow equations

Glazek, Wilson (1993), Wegner (1994)

$$\frac{dH_s}{ds} = [\eta_s, H_s] = [[G_s, H_s], H_s]$$

with flow operator  $G_s = T_{\text{rel}}$  and resolution  $\lambda = s^{-1/4}$  Bogner et al. (2007)

$$\frac{dV_s(k, k')}{ds} = -(k^2 - k'^2)^2 V_s(k, k') + \frac{2}{\pi} \int_0^\infty q^2 dq (k^2 + k'^2 - 2q^2) V_s(k, q) V_s(q, k')$$



# Similarity RG interactions

Unitary transformations to band-diagonal  $V_{\text{srg}}(\lambda)$  from flow equations

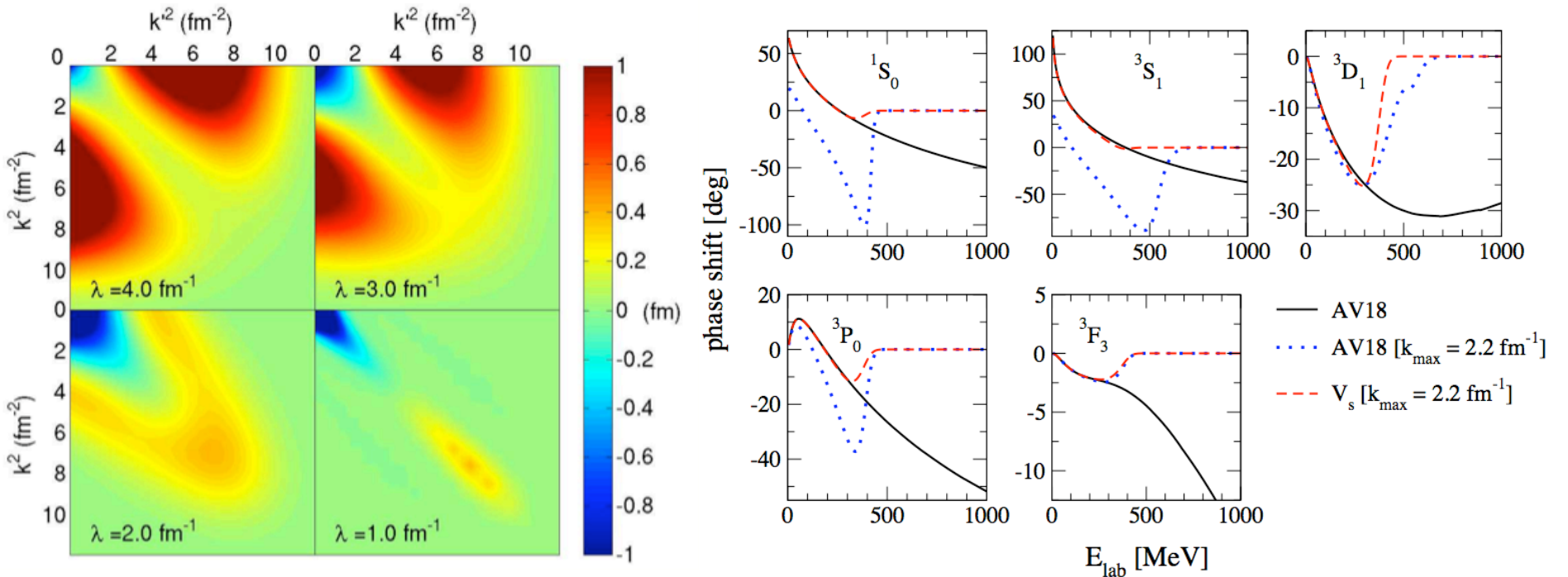
Glazek, Wilson (1993), Wegner (1994)

$$\frac{dH_s}{ds} = [\eta_s, H_s] = [[G_s, H_s], H_s]$$

with flow operator  $G_s = T_{\text{rel}}$  and resolution  $\lambda = s^{-1/4}$  Bogner et al. (2007)

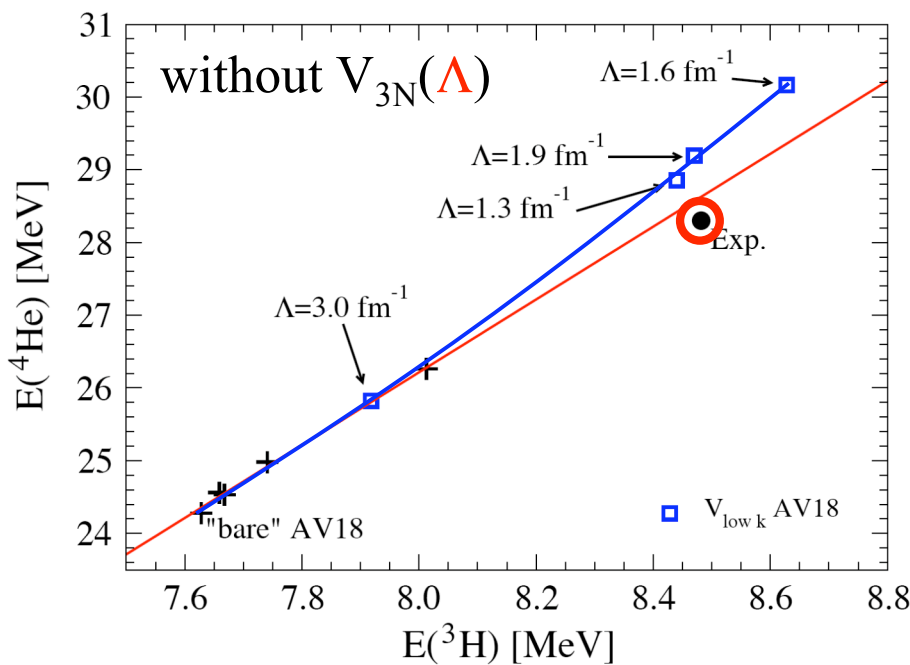
$$\frac{dV_s(k, k')}{ds} = -(k^2 - k'^2)^2 V_s(k, k') + \frac{2}{\pi} \int_0^\infty q^2 dq (k^2 + k'^2 - 2q^2) V_s(k, q) V_s(q, k')$$

intermediate momenta  $k > k_{\text{max}} \sim \lambda$  decouple for low energies

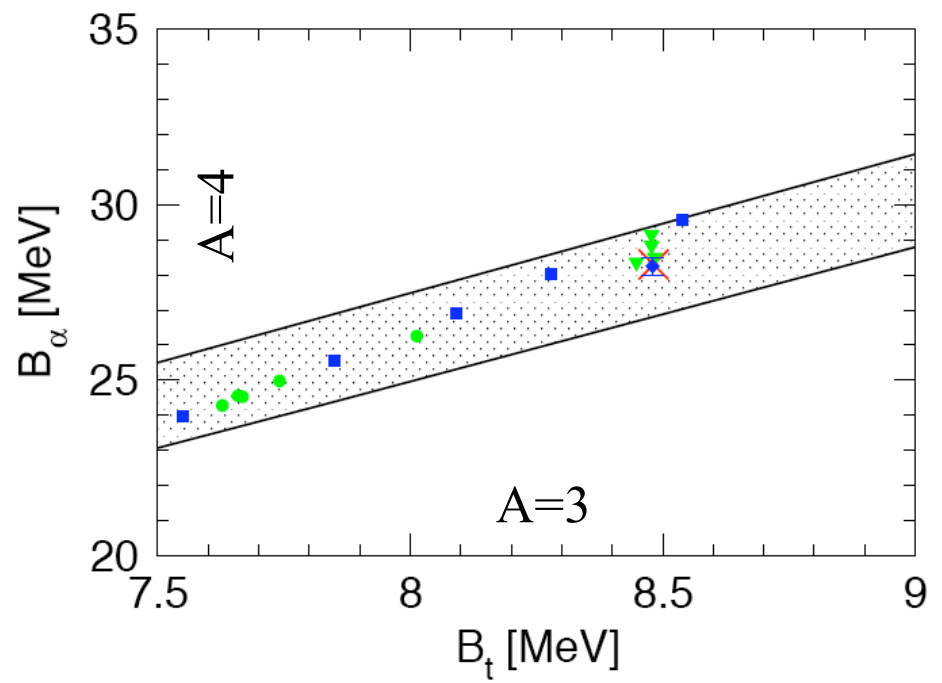


## 3N interactions required for renormalization

$V_{NN}(\Lambda)$  defines NN interactions with cutoff-independent NN observables  
cutoff variation estimates errors due to neglected parts in  $H(\Lambda)$   
cutoff dependence explains “Tjon line”  $\rightarrow$  3N for renormalization



Nogga, Bogner, AS (2004)



pionless EFT: Platter, Hammer, Meissner (2005)

large scattering lengths drive correlation

## Low-momentum 3N fits

fit D,E couplings to A=3,4 binding energies  
for range of cutoffs

linear dependences in fits to triton binding

3N interactions perturbative for  $\Lambda \lesssim 2 \text{ fm}^{-1}$

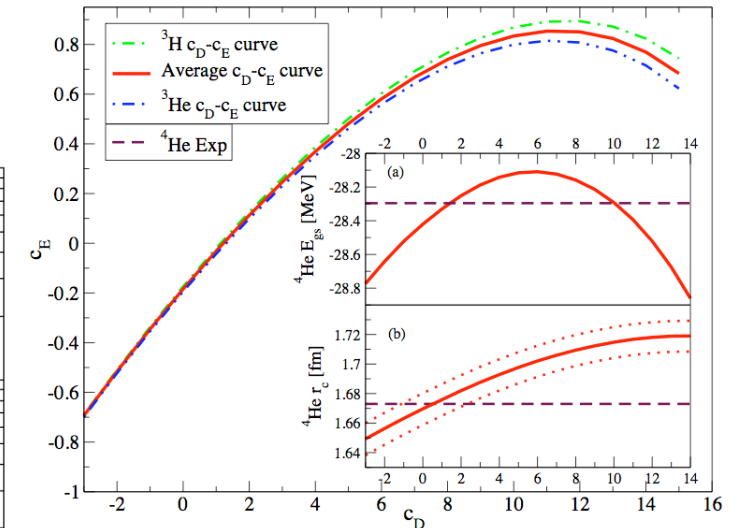
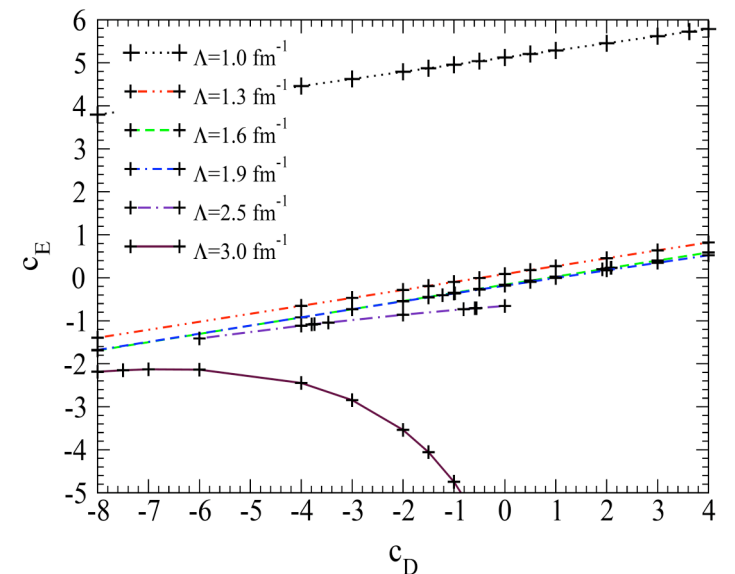
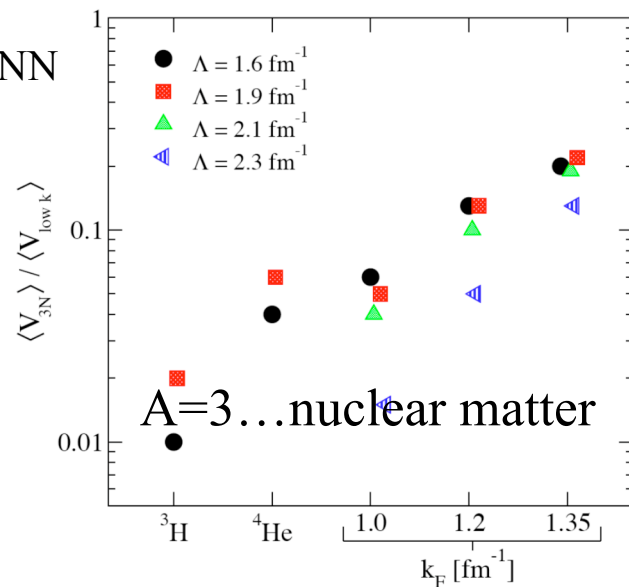
Nogga, Bogner, AS (2004)

nonperturbative at larger cutoffs

cf. chiral EFT  $\Lambda \approx 3 \text{ fm}^{-1}$

3N exp. values natural

$\sim (Q/\Lambda)^3 V_{\text{NN}} \sim 0.1 V_{\text{NN}}$

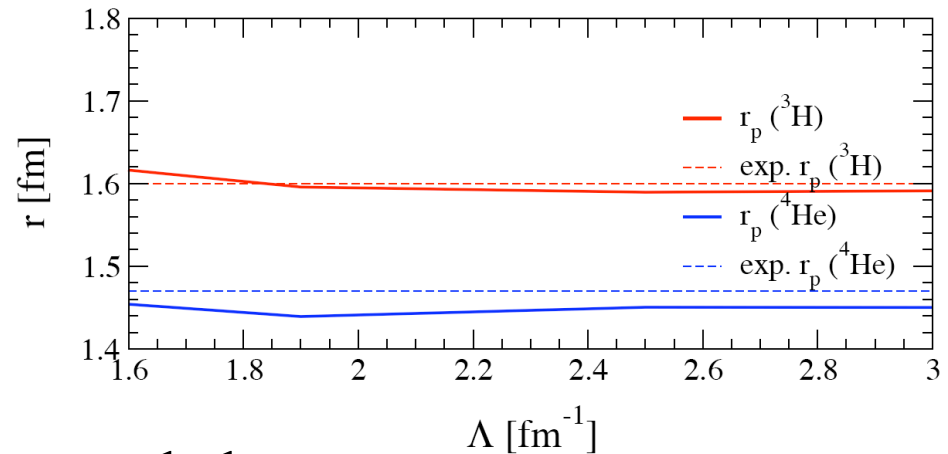


Navratil et al. (2007)

## Theoretical uncertainties

EFT/RG interactions: more accurate with higher orders  
and cutoff variation estimates theoretical uncertainties

Radii of light nuclei approximately  
cutoff-independent, agree with exp.



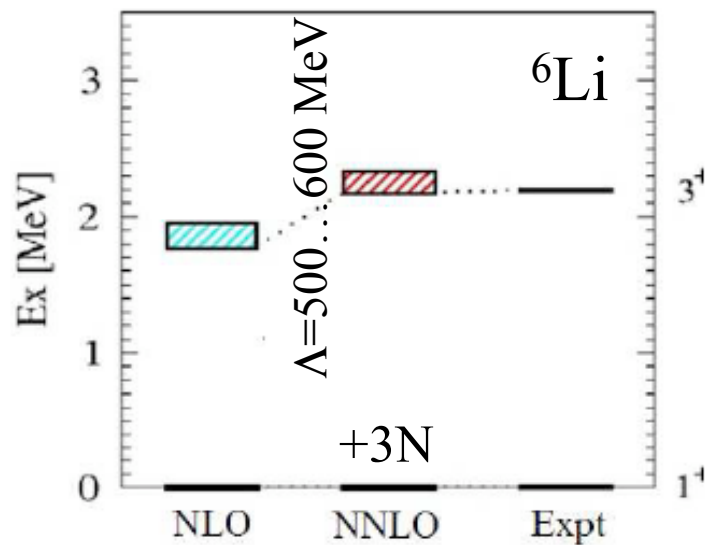
goal: apply to pivotal matrix elements needed  
to constrain beyond Standard Model physics

isospin-symmetry breaking corrections  
for superallowed beta decay

$V_{ud} = 0.97416(13)$  (14/18)theo.

nuclear matrix elements for  $0\nu\beta\beta$  decay

octupole EDM enhancement

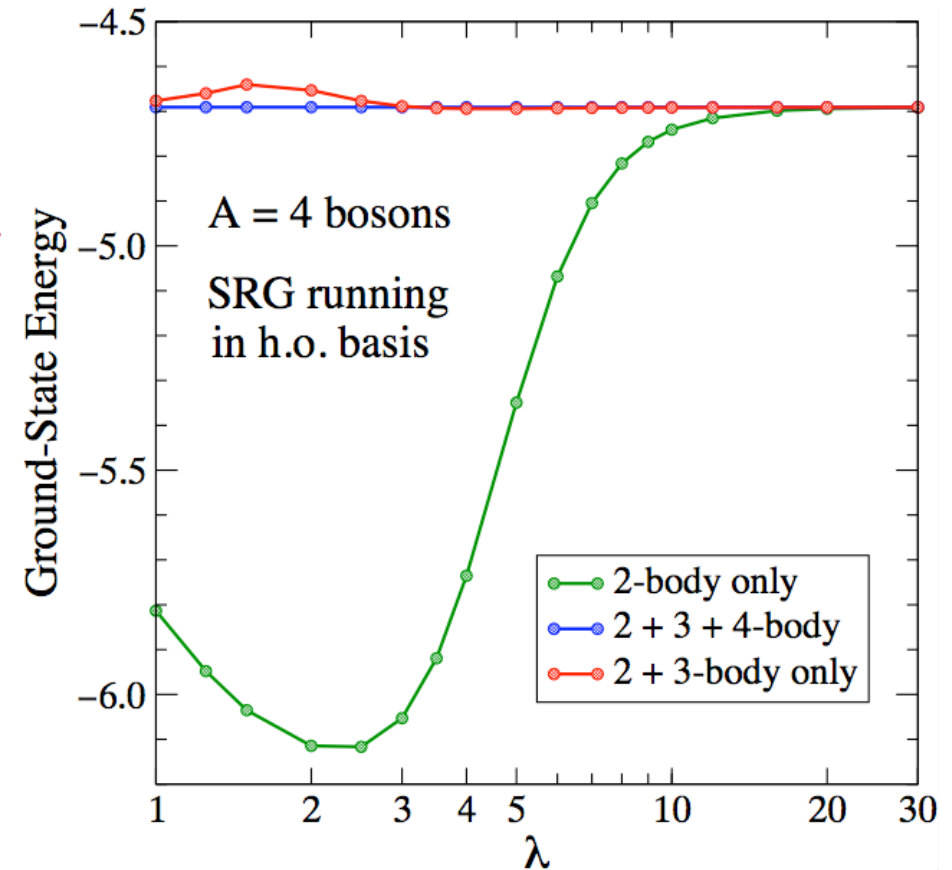
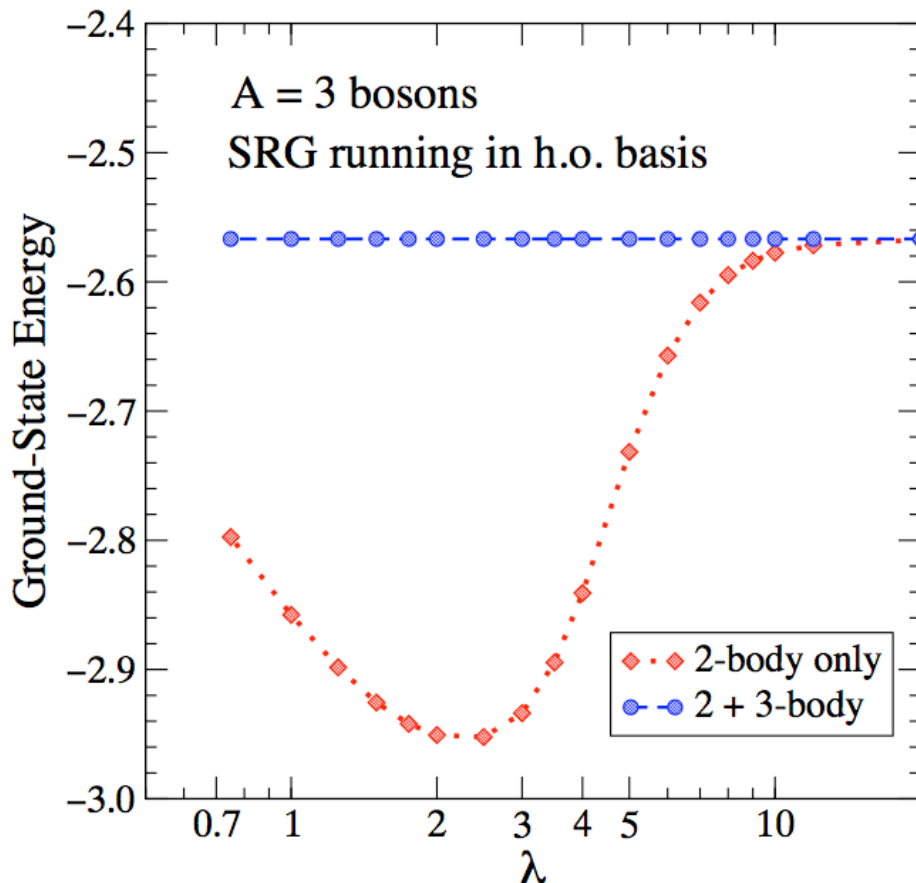


from A. Nogga

# Towards evolving 3N interactions

Similarity RG evolution for 1d systems in harmonic oscillator basis

Jurgenson, Furnstahl (2008)

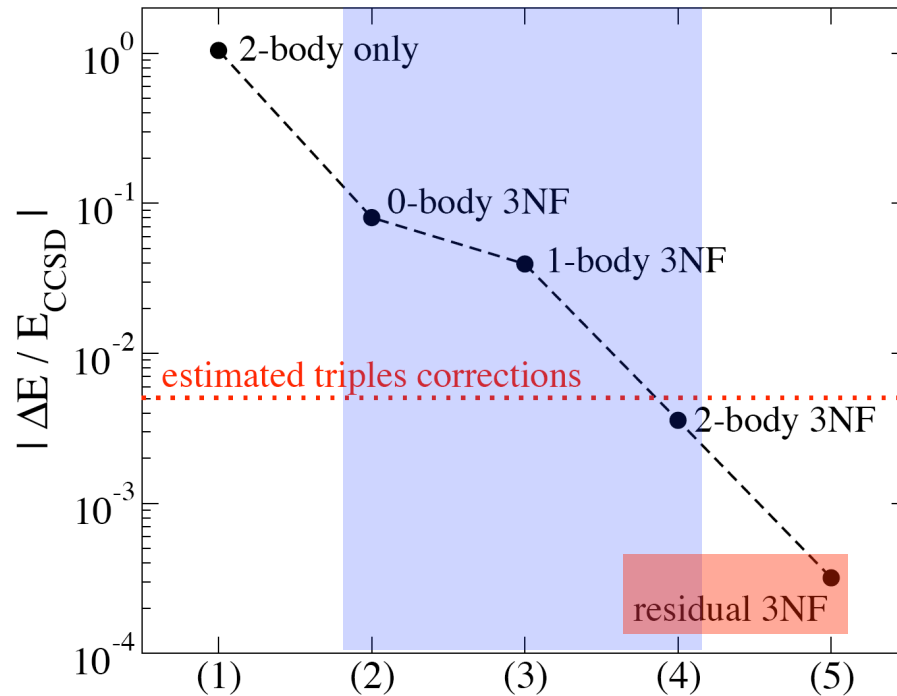


gearing up to evolve chiral 3N interactions

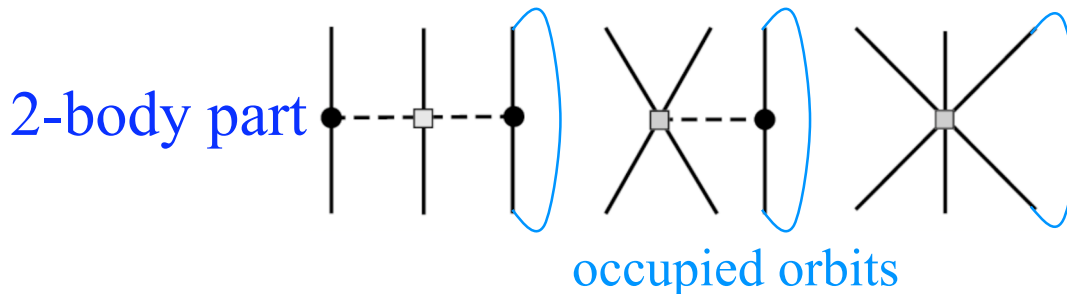
for now: use chiral EFT is complete basis,  $V_{3N}(\Lambda)$  fits for lower cutoffs

# Towards 3N interactions in medium-mass nuclei

developed coupled-cluster theory with 3N interactions [Hagen et al. \(2007\)](#)  
first benchmark for  ${}^4\text{He}$  based on low-momentum interactions



show that 0-, 1- and 2-body parts of 3N interaction dominate



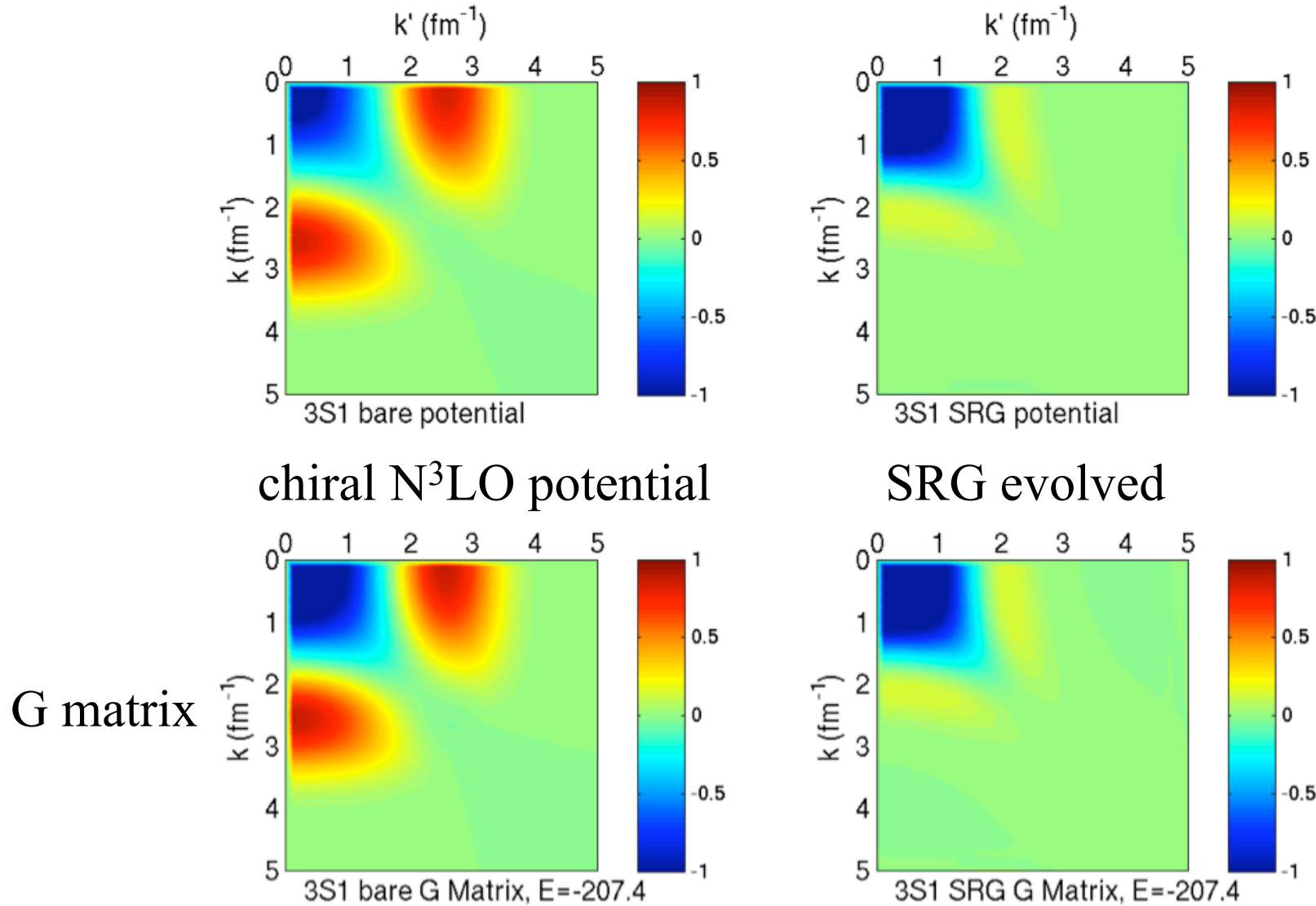
residual 3N interaction can be neglected: very promising

## Outline

1. Introduction to effective field theory and the renormalization group
2. Chiral effective field theory
3. Renormalization group for nuclear forces
4. EFT and RG for nuclear matter
5. Nuclear matter in astrophysics
6. Neutrino processes in supernovae from chiral EFT

# Advantages of low-momentum interactions for nuclei

conventional G matrix approach does not solve off-diagonal coupling,  
renders Bethe-Brueckner-Goldstone expansion necessarily nonperturb.



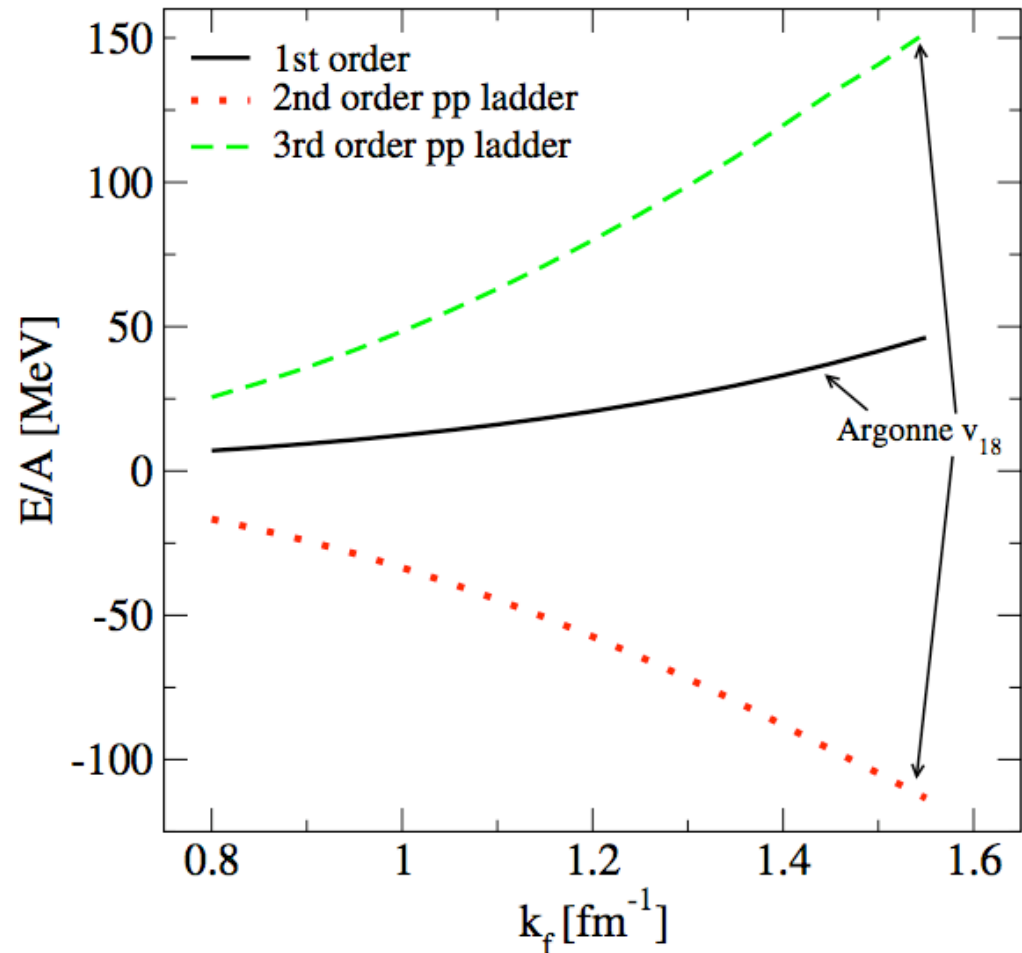
# Is nuclear matter perturbative with chiral EFT and RG?

conventional Bethe-Brueckner-Goldstone expansion:

no, due to nonpert. cores (flipped-V bound states) and off-diag coupling

start from chiral EFT and RG evolution:

nuclear matter converged at  $\approx$  2nd order



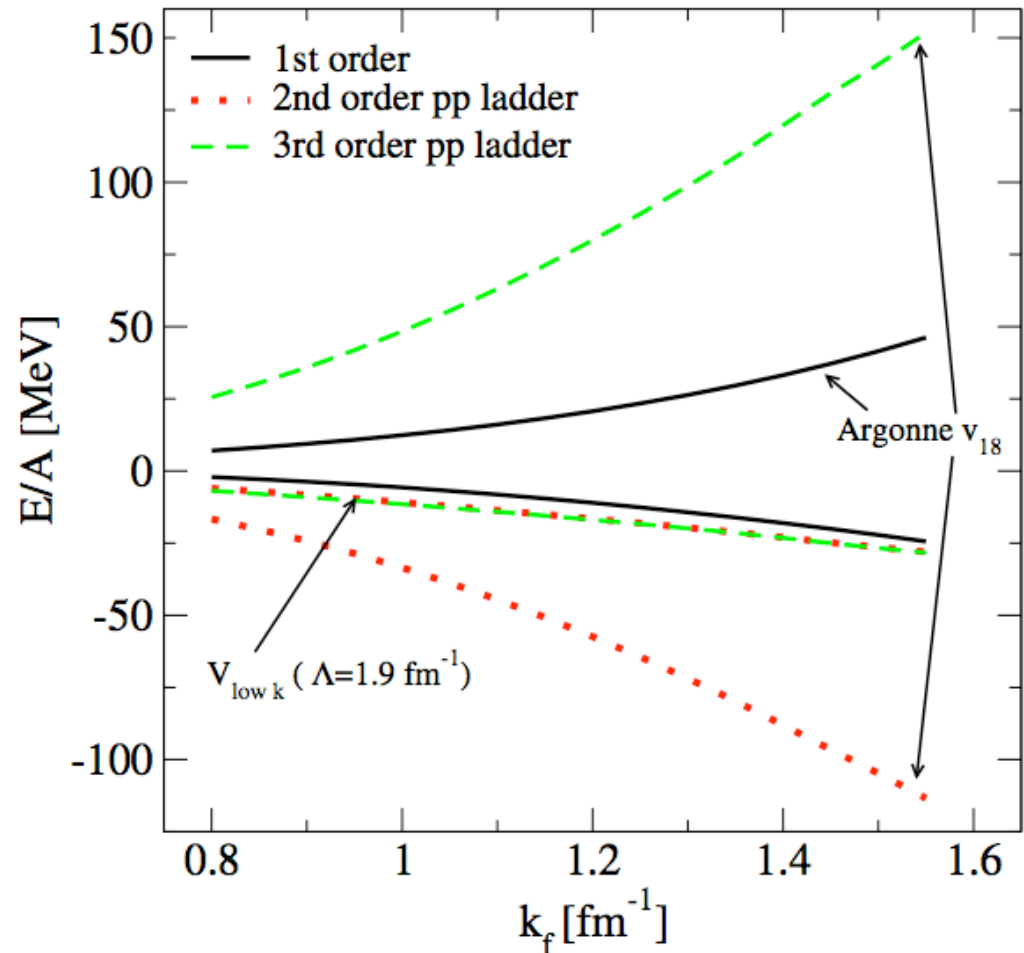
# Is nuclear matter perturbative with chiral EFT and RG?

conventional Bethe-Brueckner-Goldstone expansion:

no, due to nonpert. cores (flipped-V bound states) and off-diag coupling

start from chiral EFT and RG evolution:

nuclear matter converged at  $\approx$  2nd order



# Is nuclear matter perturbative with chiral EFT and RG?

conventional Bethe-Brueckner-Goldstone expansion:

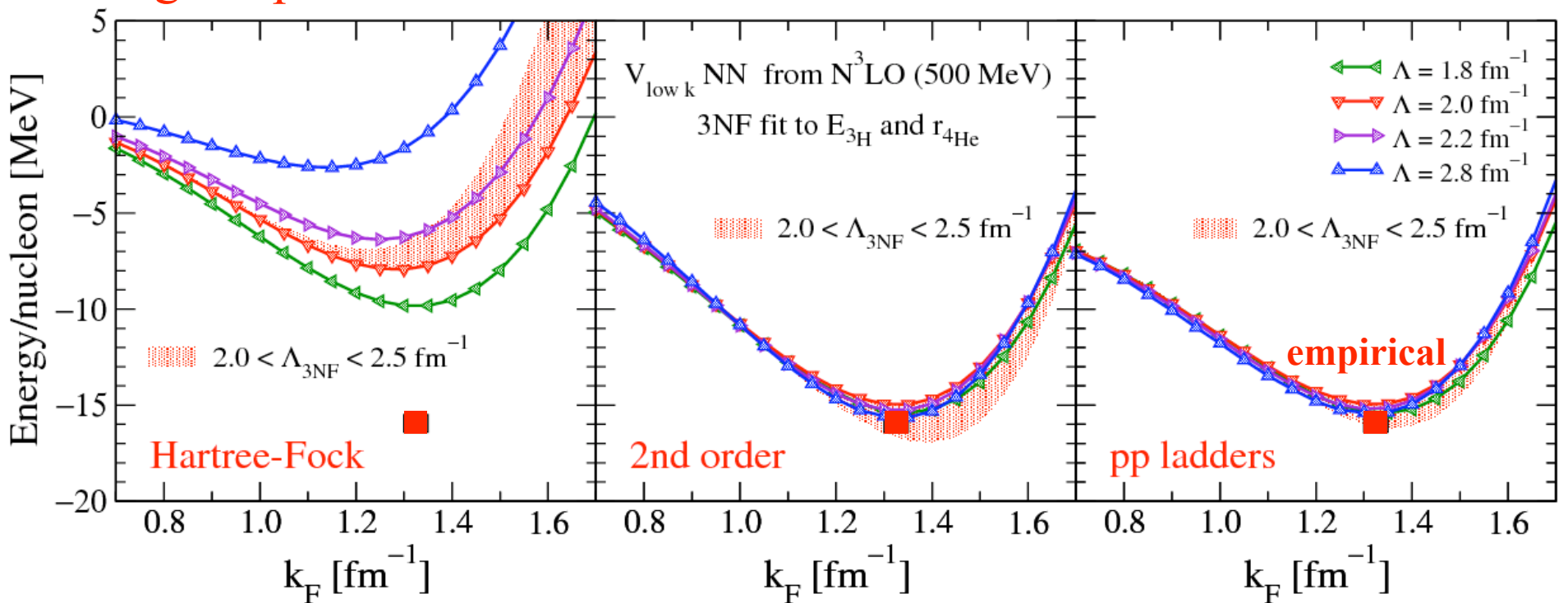
no, due to nonpert. cores (flipped-V bound states) and off-diag coupling

start from chiral EFT and RG evolution:

nuclear matter converged at  $\approx$  2nd order, 3N drives saturation

weak cutoff dependence, improved by 3N fits to  ${}^4\text{He}$  radius

**exciting: empirical saturation within theoretical uncertainties**

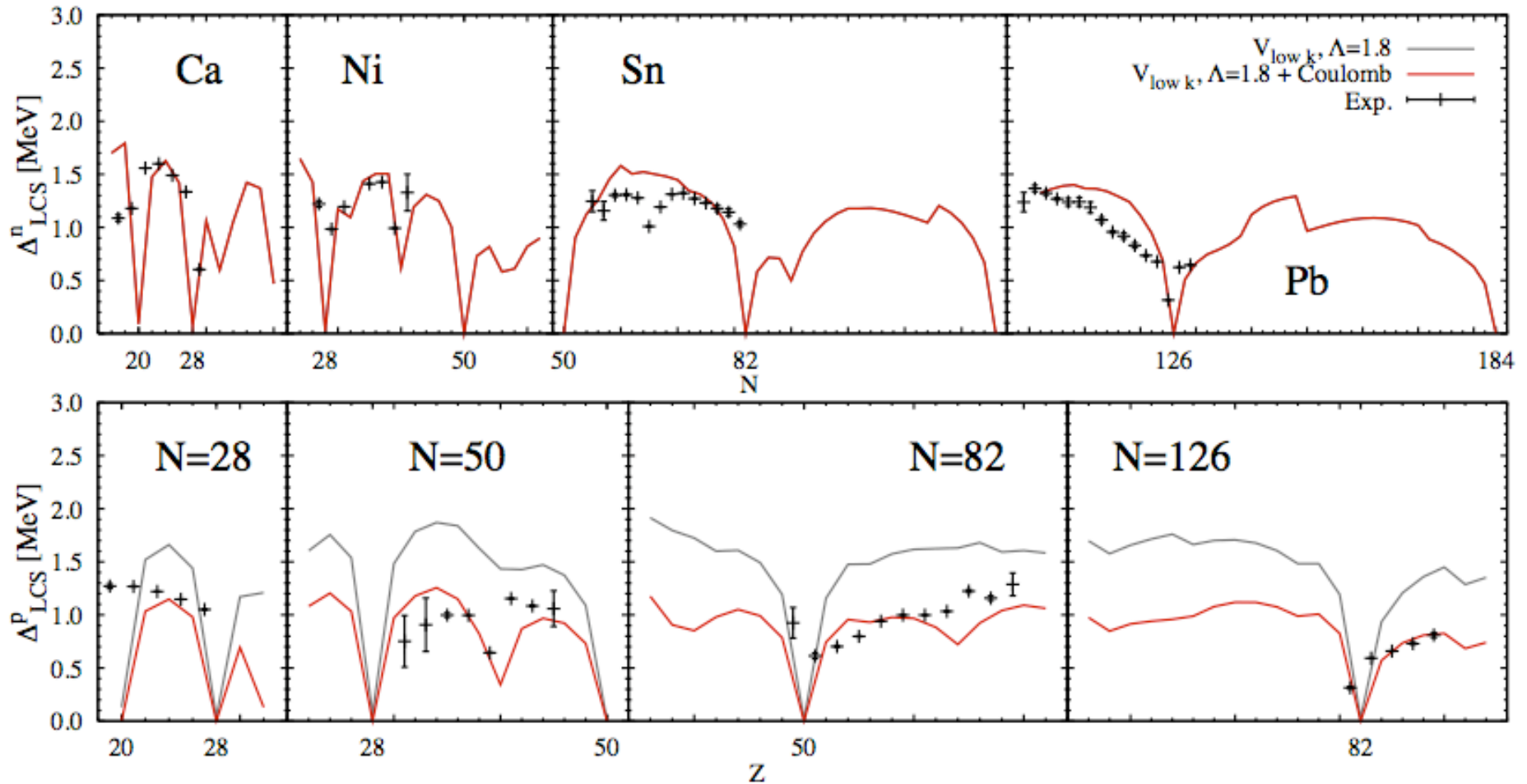


Bogner, AS, Furnstahl, Nogga (2005) + improvements, in prep.

# Pairing gaps

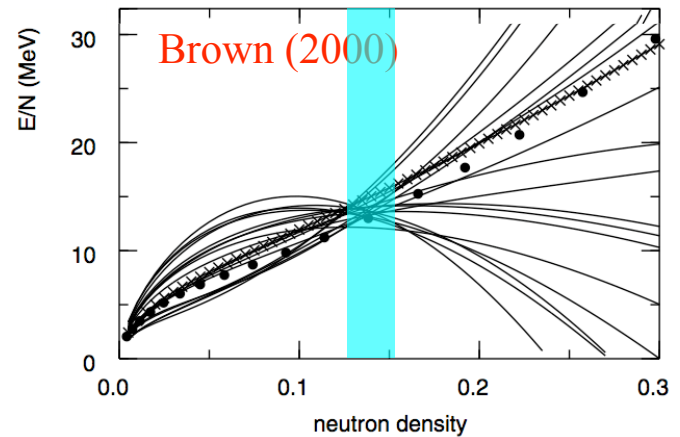
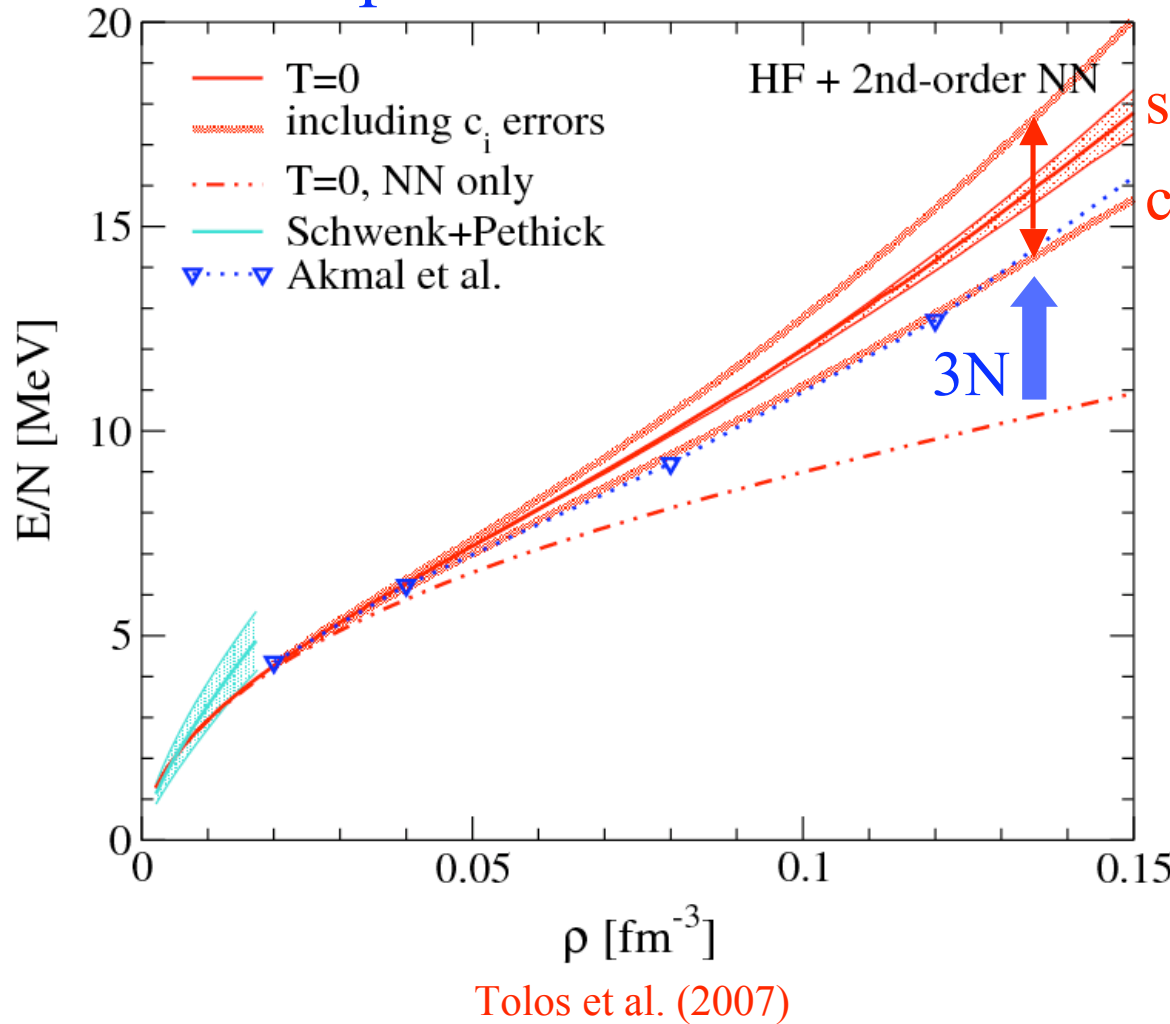
first density functional theory results with microscopic pairing functional  
from  $V_{\text{low } k}$  + Coulomb interaction

Lesinski, Duguet et al. (2008)



current limitations: no 3N forces, no density/spin/isospin fluctuations

# Impact of 3N interactions on neutron matter



uncertainties from  $c_i$  overwhelm errors due to cutoff variation, mainly  $c_3$   
combine with knowledge of nuclear properties  
important for dense matter in astrophysics

# Towards a universal nuclear energy density functional

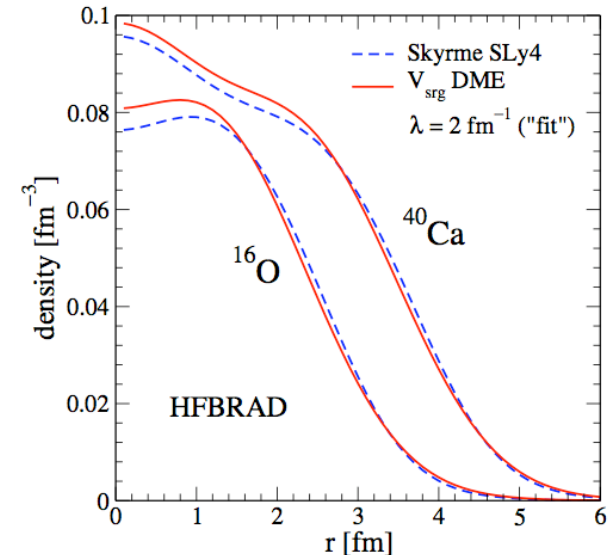
low-momentum interactions  
provide key input to SciDAC



using density matrix expansion

Bogner, Furnstahl, Platter (2008), Finelli, Kaiser, Weise,...

$$\mathcal{E} = \frac{\tau}{2M} + \textcolor{red}{A}[\rho] + \textcolor{blue}{B}[\rho]\tau + \textcolor{green}{C}[\rho]|\nabla\rho|^2 + \dots$$

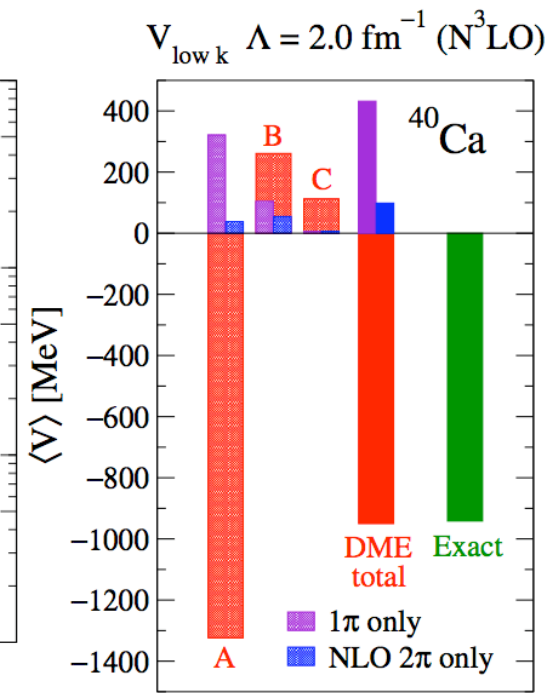
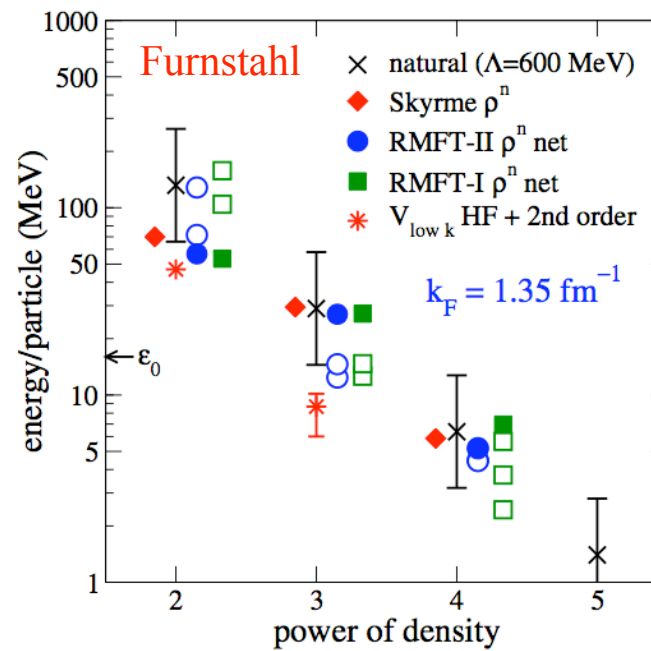


use EFT/RG interactions:

to identify new terms  
in density functional

to quantify theoretical  
errors for extrapolations

to benchmark with  
ab-initio methods



# Three-nucleon interactions

3N interactions crucial for:

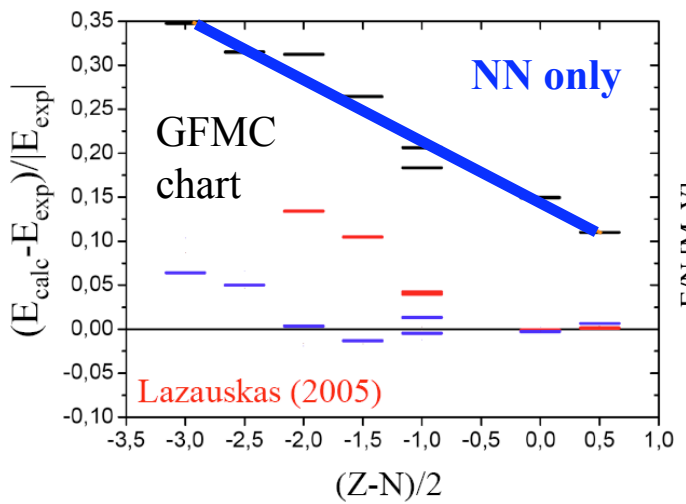
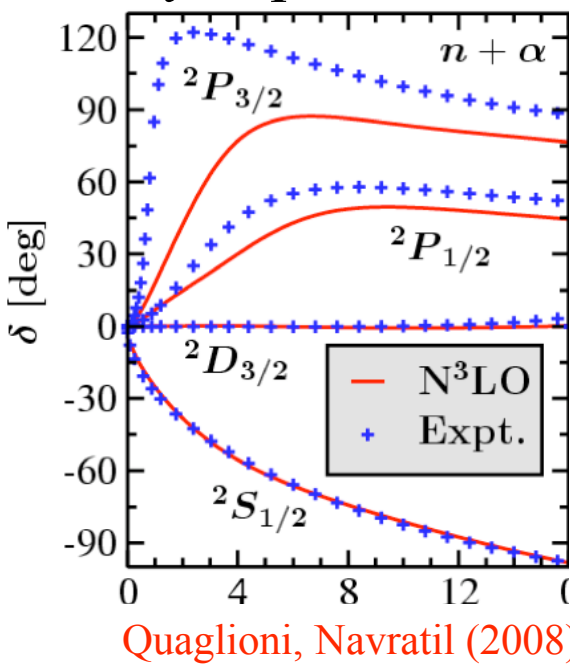
binding energies

cutoff dependence explains Tjon line due to neglected parts in  $H(\Lambda)$ , 3N required

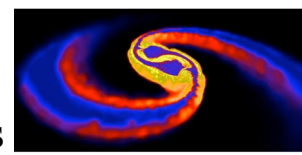
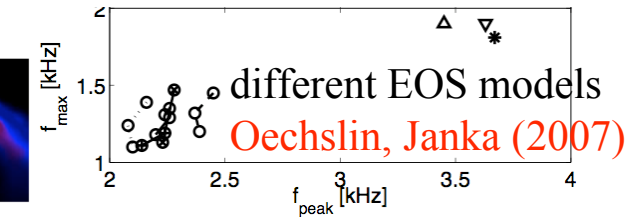
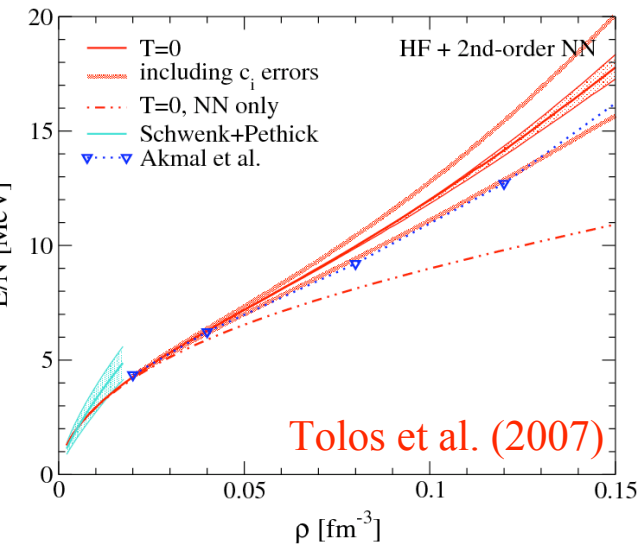
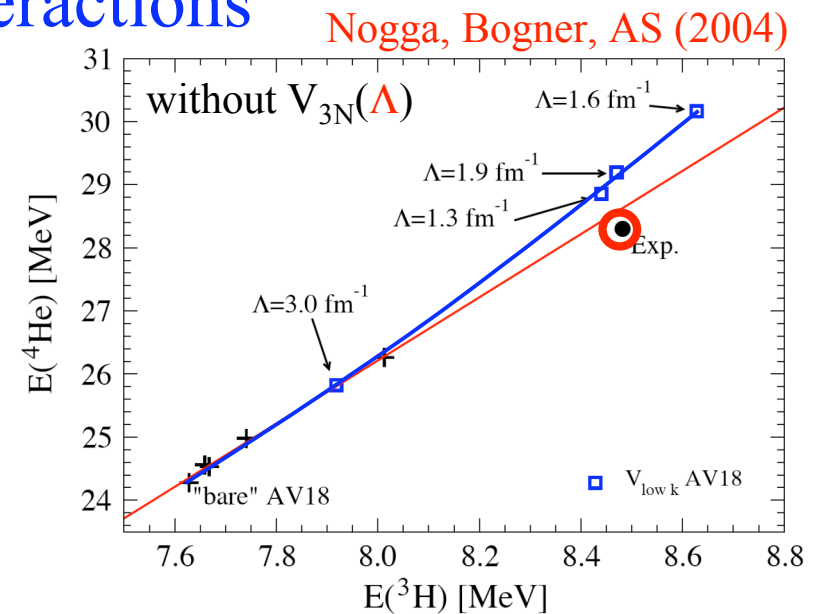
spin-orbit effects

isospin dependence

density dependence



neutron star mergers  
→ gravitational waves



## Outline

1. Introduction to effective field theory and the renormalization group
2. Chiral effective field theory
3. Renormalization group for nuclear forces
4. EFT and RG for nuclear matter
5. The virial equation of state and light nuclei
6. Neutrino processes in supernovae from chiral EFT

## Motivation

Core-collapse supernovae most sensitive to low-density nucleonic matter

Conditions at neutrinosphere (surface of last scattering of neutrinos):

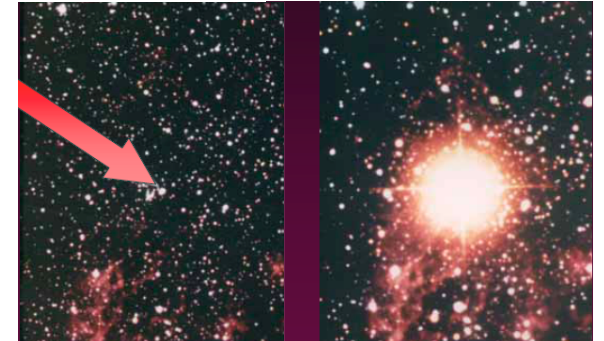
$T \sim 4$  MeV from  $\sim 20$  SN1987a events

$n \sim 10^{11}\text{-}10^{12}$  g/cm<sup>3</sup> from  $n\sigma \sim n(G_F E_\nu)^2 \sim R^{-1}$

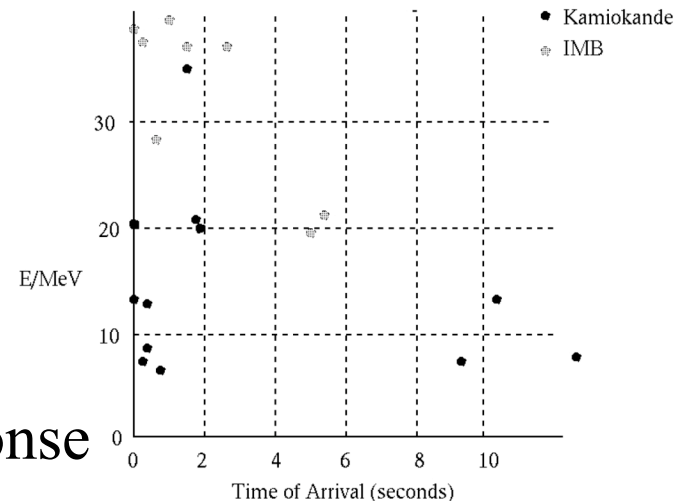
What is the equation of state and neutrino response of nuclear matter near the neutrinosphere?

Fugacity small  $z = e^{\mu/T} \lesssim 0.5$  for  $n \lesssim 4 \cdot 10^{11} (T/\text{MeV})^{3/2}$  g/cm<sup>3</sup>

Virial expansion gives model-independent answers for SN neutrinosphere  
**Horowitz, AS (2006)**



Before and after SN1987A



Virial expansion: general formalism for low  $n$ , high  $T$

assumptions: gas phase,  $T >$  any  $T_{\text{crit}}$ , fugacity  $z = e^{\mu/T}$  small

Neutron matter

$$P = \frac{2T}{\lambda^3} (z + z^2 b_n + z^3 b_n^{(3)} + \mathcal{O}(z^4)) \quad n = \frac{2}{\lambda^3} (z + 2z^2 b_n + 3z^3 b_n^{(3)} + \mathcal{O}(z^4))$$

Second virial coefficient  $\sim$  2-particle partition fn

$$b_n(T) = \frac{1}{2^{1/2} \pi T} \int_0^\infty dE e^{-E/2T} \delta^{\text{tot}}(E) - 2^{-5/2}$$

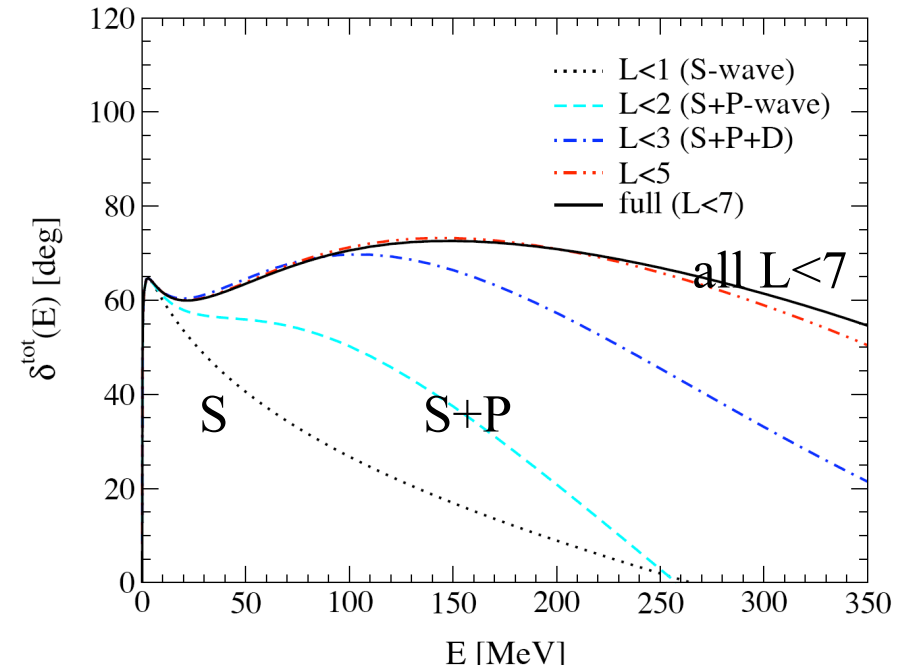
For infinite scattering length  $a = \pm\infty$

$b_n = 3/2^{5/2} = 0.53$ , not  $k_F a$  expansion,  
tested in cold atoms Ho, Mueller (2004);

Thomas et al. (2005)

Second virial coefficient for neutrons  
approx  $T$  independent  $b_n = 0.30$ , leads  
to scaling  $E/E_{\text{free}} = P/P_{\text{free}} = \xi(T/T_F)$

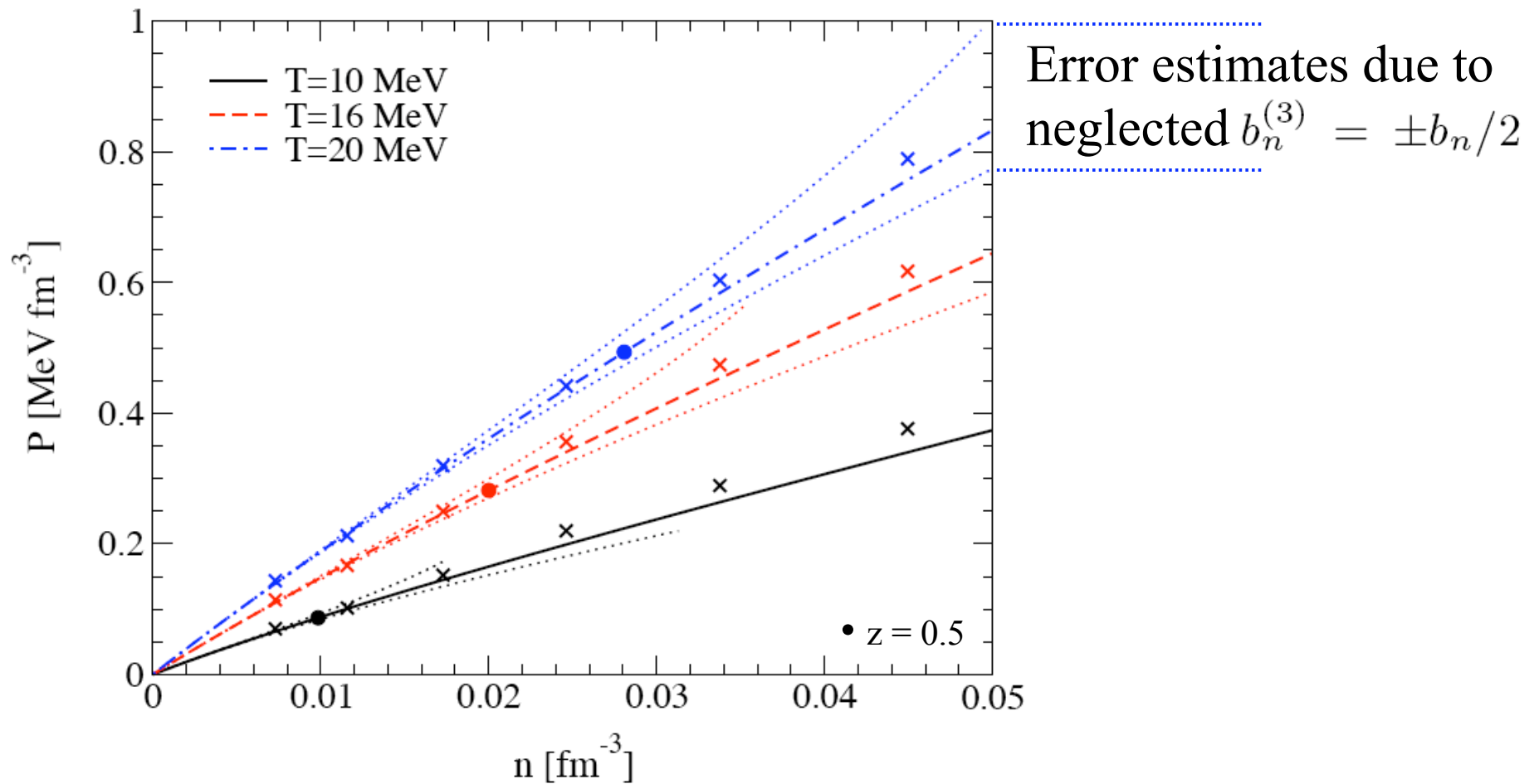
Previous work Buchler, Coon (1977); Pratt et al. (1987); Venugopalan, Prakash (1992); Roepke et al.



# Neutron matter equation of state

Fugacity small for  $n \lesssim 4 \cdot 10^{11} (T/\text{MeV})^{3/2} \text{ g/cm}^3$

Comparison to Friedman, Pandharipande ( $\times$ )



## Nuclear matter

deuterons enter as bound state contribution to  $b_2 \sim e^{E_d/T}$   
nuclei as bound state contributions to  $b_A$ , limits nucleon virial expansion  
at low densities, nuclear matter mainly composed of n,p and  $\alpha$  particles,  
include  $\alpha$  particles explicitly, to second-order in fugacities  $z_n, z_p, z_\alpha$

$$\frac{P}{T} = \frac{2}{\lambda^3} (z_n + z_p + (z_n^2 + z_p^2)b_n + 2z_p z_n b_{pn}) + \frac{1}{\lambda_\alpha^3} (z_\alpha + z_\alpha^2 b_\alpha + 2z_\alpha (z_n + z_p) b_{\alpha n})$$

second virial coefficients directly from NN, N $\alpha$ ,  $\alpha\alpha$  phase shifts and  $E_d$   
model-independent description of matter in thermal equilibrium

consider chemical equilibrium  $z_\alpha = z_p^2 z_n^2 e^{E_\alpha/T}$   
adjust  $z_n, z_p$  to reproduce desired baryon density and proton fraction

can include heavy nuclei at higher densities with  $z_A$   
virial  $b_{NA}, \dots$  correct NSE models for strong interactions between nuclei

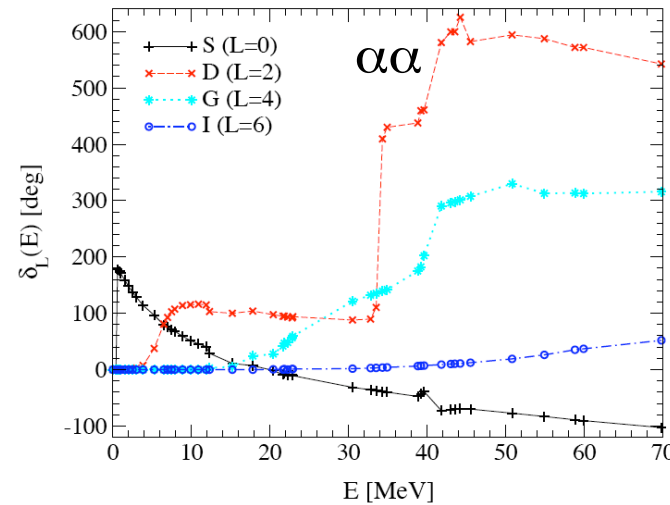
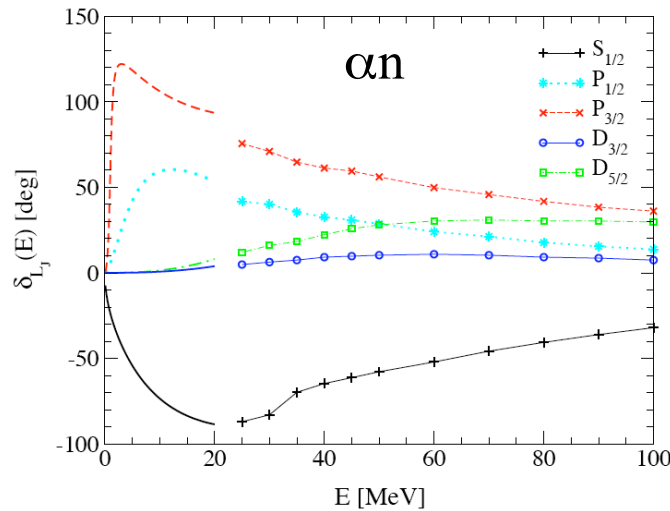
## Virial coefficients

neglected Coulomb (use  $np, n\alpha$  phase shifts;  $b_2$  for plane wave bc), mixing parameters and inelasticities in scattering, can improve this

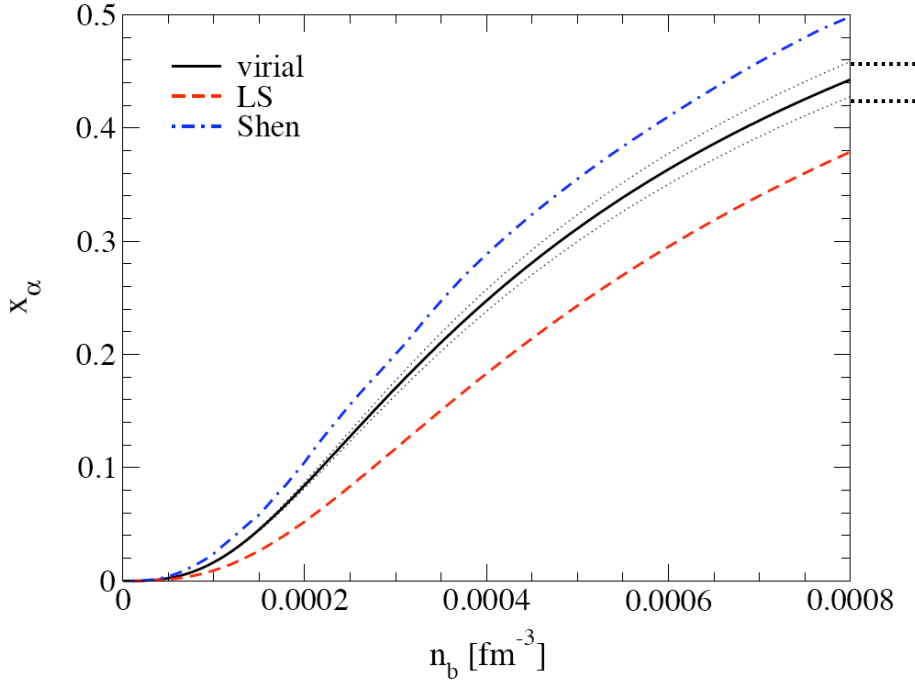
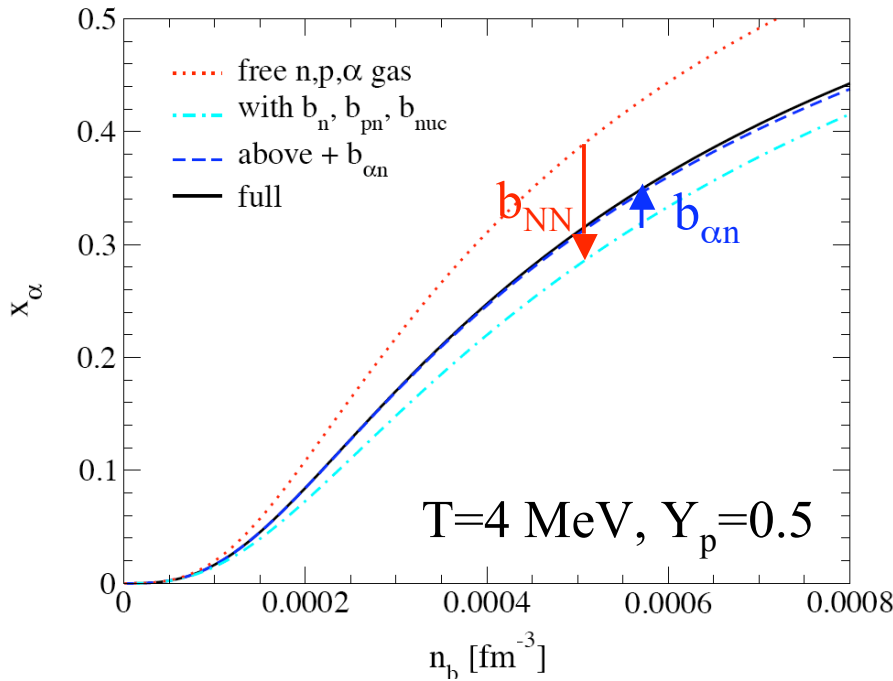
for  $b_{NN}$ : all  $L \leq 6$  from [Nijmegen PWA93](#), includes deuteron and large  $^1S_0$  scattering lengths on equal footing

for  $b_{\alpha n}$ : all  $L \leq 3$  from [Arndt, Roper \(1970\)](#) for  $E < 20$  MeV, [Amos, Karataglidis \(2005\)](#) optical model for higher E, includes  $P_{3/2}$  resonance

for  $b_{\alpha\alpha}$ : all  $L \leq 6$  from [Afzal et al. \(1969\)](#) for  $E < 30$  MeV, [Bacher et al. \(1972\)](#) for  $30 < E < 70$  MeV includes  $0^+, 2^+$  resonances



virial coefficients dominated by resonant (large a) interactions



## Composition: $\alpha$ mass fraction

Hierarchy of virial contributions:

$b_{NN}$  more important than  $b_{\alpha n}$ ,  $b_\alpha$

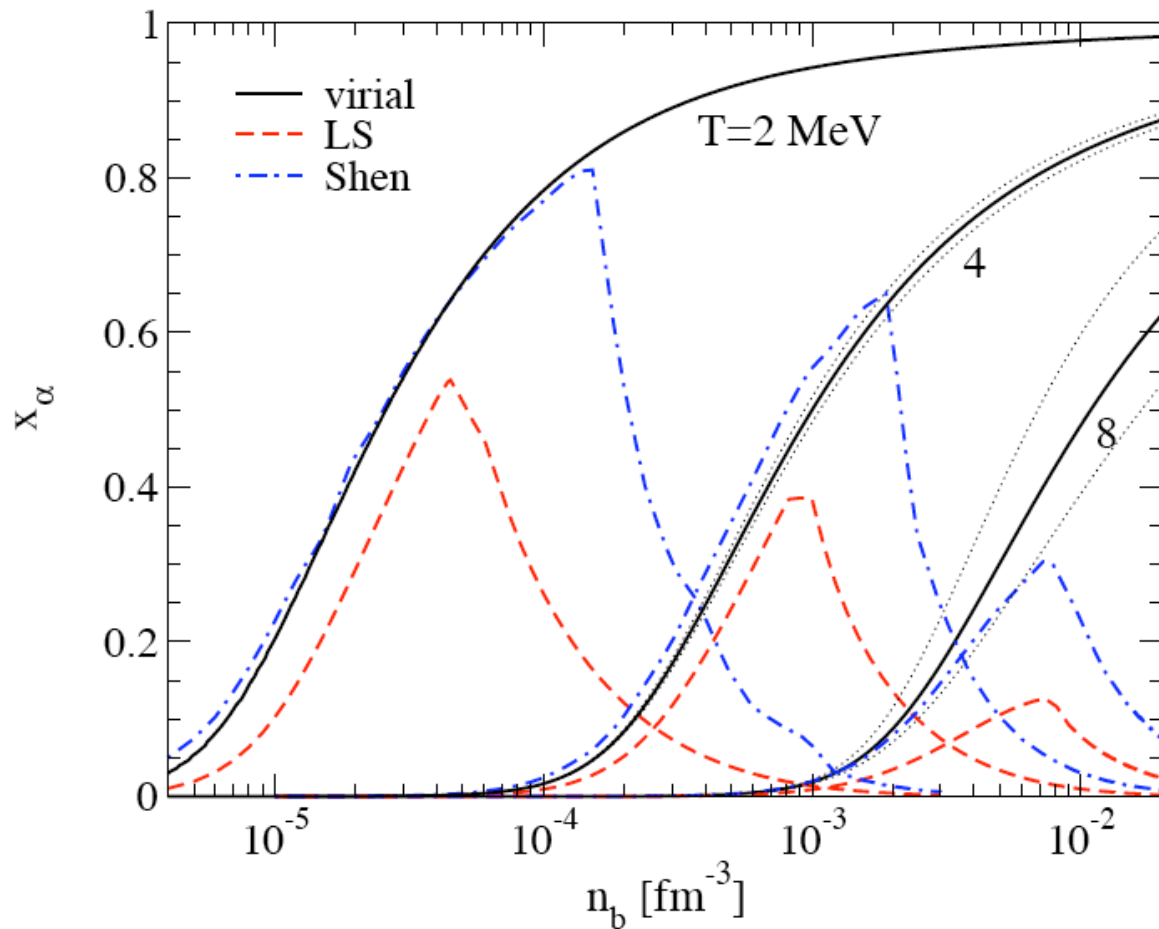
$b_{\alpha n}$  attractive due to  $P_{3/2}$  resonance

Estimate errors due to neglected third virial coefficient  $b_3 \sim \pm 10$

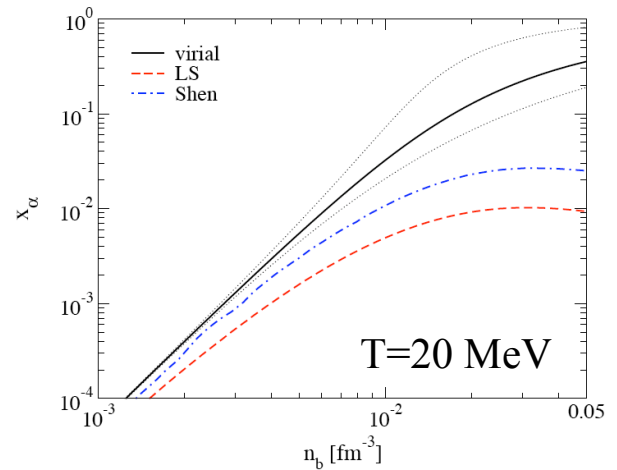
$\alpha$  mass fraction differs from LS=Lattimer-Swesty, Shen et al. EOS used in SN simulations

LS models no  $\alpha$  interaction with repulsive excluded volume

## $\alpha$ mass fraction for various T

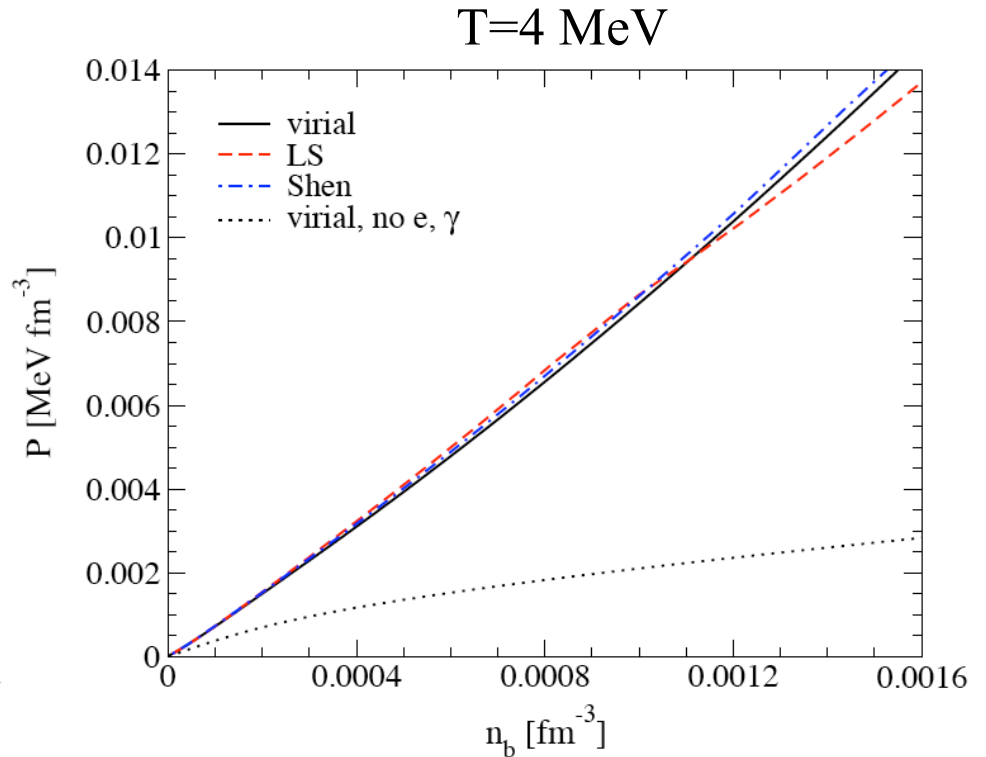
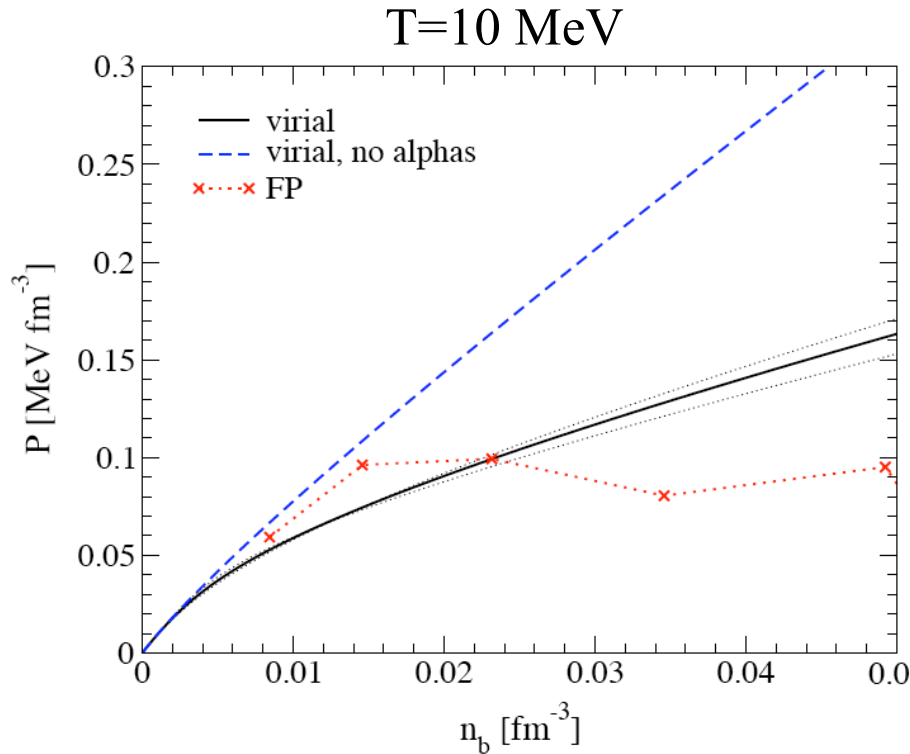


$\alpha$  fractions drop in LS/Shen at high density due to formation of heavy A limits validity of n,p, $\alpha$  virial EOS  
for  $T>10$  MeV, models underestimate  $\alpha$  fraction



$x_\alpha$  important for spin/neutrino response, since  $\alpha$  particles have  $J=0$

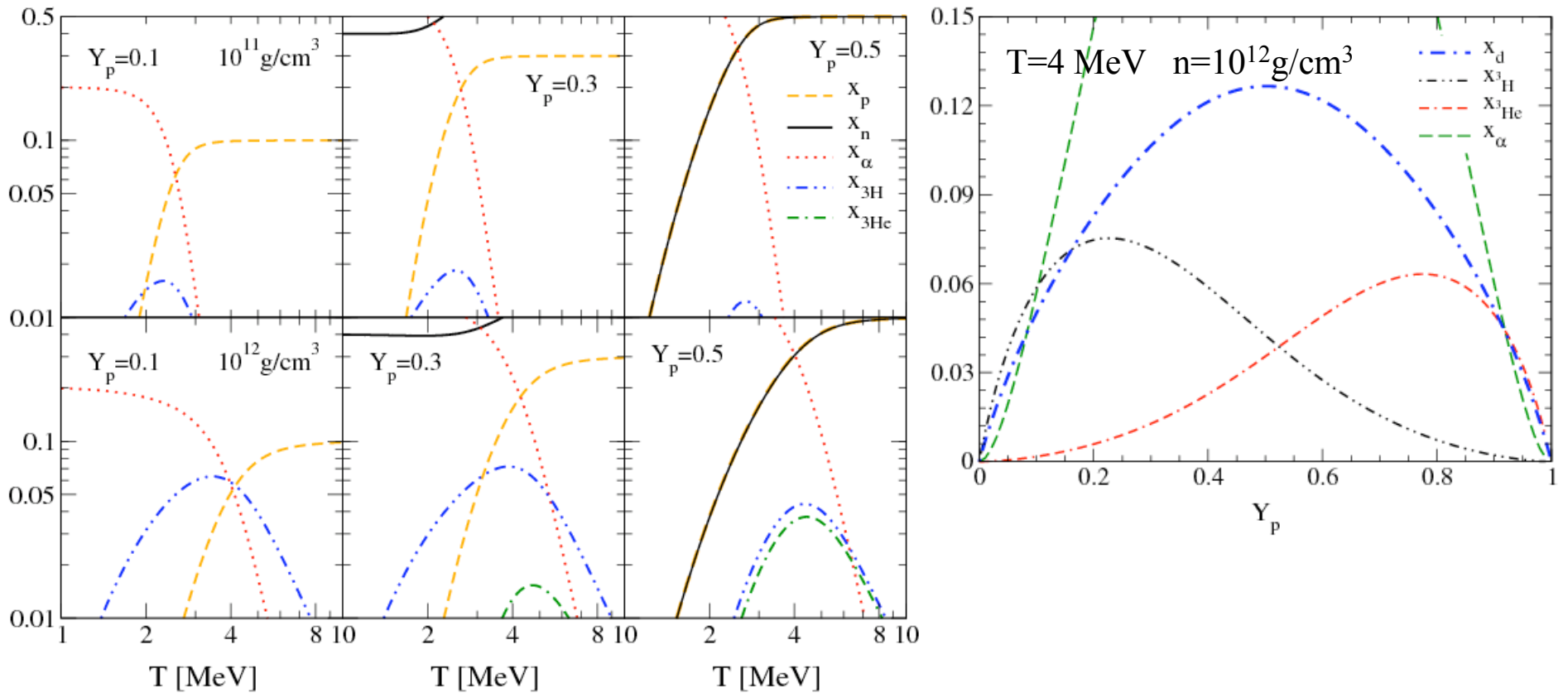
# Pressure



Variational calculations [Friedman, Pandharipande](#) fail to describe  $\alpha$  contributions

Pressure agrees well with LS, Shen et al. EOS

# Virial equation of state with light nuclei



O'Connor et al. (2007)

included  $A=3$  nuclei and nucleon- $A=3$  virial coefficients

$A=3$  nuclei decrease alpha mass fraction, small effects of  $b_{N-A=3}$

near neutrinosphere  $\sim 10\%$  in  $A=3$

$d$ ,  $^3\text{H}$ ,  $^4\text{He}$  mass fractions can be comparable for neutron-rich matter

# Neutrino breakup of A=3

## energy transfer

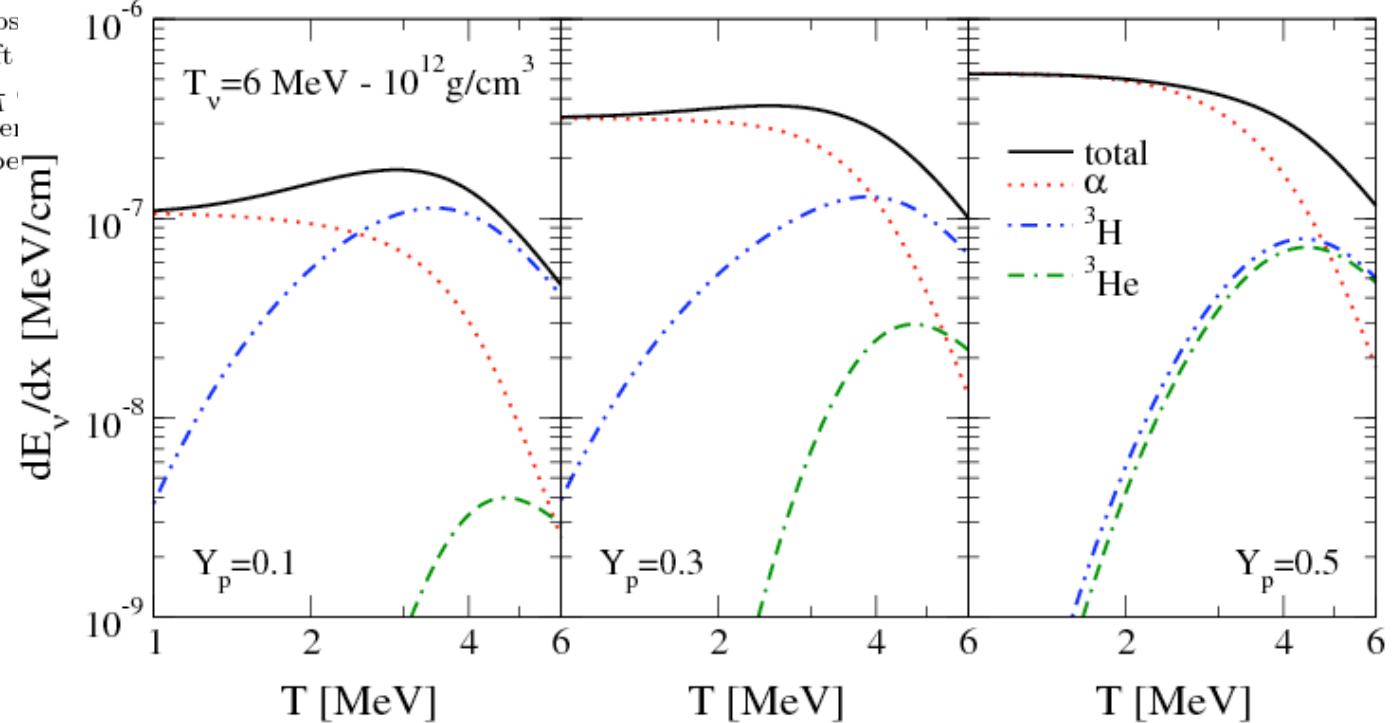
$T_\nu$ [MeV]	${}^3\text{H}$		${}^3\text{He}$	
1	$1.97 \times 10^{-6}$	$1.68 \times 10^{-5}$	$3.49 \times 10^{-6}$	$2.76 \times 10^{-5}$
2	$4.62 \times 10^{-4}$	$4.73 \times 10^{-3}$	$6.15 \times 10^{-4}$	$5.94 \times 10^{-3}$
3	$5.53 \times 10^{-3}$	$6.38 \times 10^{-2}$	$6.77 \times 10^{-3}$	$7.41 \times 10^{-2}$
4	$2.68 \times 10^{-2}$	$3.37 \times 10^{-1}$	$3.14 \times 10^{-2}$	$3.77 \times 10^{-1}$
5	$8.48 \times 10^{-2}$	1.14	$9.70 \times 10^{-2}$	1.25
6	$2.09 \times 10^{-1}$	2.99	$2.35 \times 10^{-1}$	3.21
7	$4.38 \times 10^{-1}$	6.61	$4.87 \times 10^{-1}$	7.03
8	$8.20 \times 10^{-1}$	13.0	$9.03 \times 10^{-1}$	13.7
9	1.41	23.4	1.54	24.6
10	2.27	39.3	2.47	41.2

$$\frac{dE_\nu}{dx} = n_b \sum_{i={}^3\text{H}, {}^3\text{He}, {}^4\text{He}} x_i \langle \omega \sigma \rangle_{i, T_\nu}$$

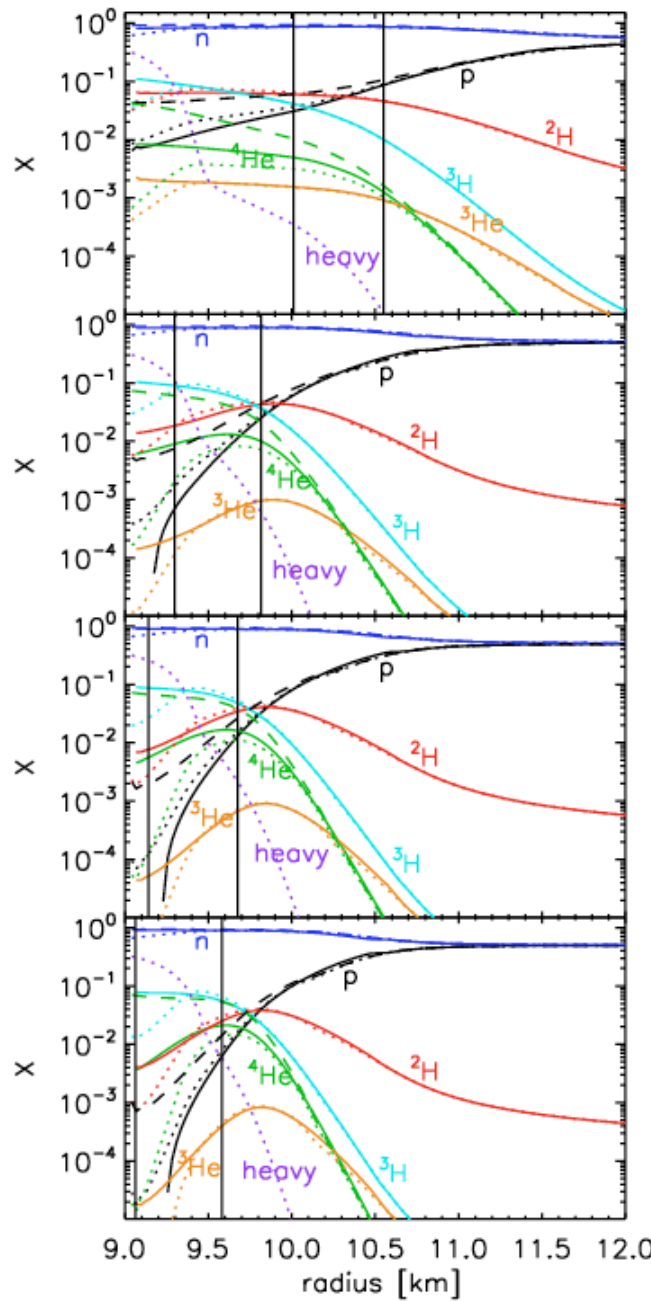
can be dominated by breakup of loosely-bound A=3 nuclei

TABLE II: Averaged neutrino- and anti-neutrino- ${}^3\text{H}$  and  ${}^3\text{He}$  neutral-current inclusive inelastic cross (A=3),  $\langle \sigma \rangle_{T_\nu} = \frac{1}{2A} \langle \sigma_\nu + \sigma_{\bar{\nu}} \rangle_{T_\nu}$  (left transfer cross-sections,  $\langle \omega \sigma \rangle_{T_\nu} = \frac{1}{2A}$  columns), as a function of neutrino temperature  $10^{-42} \text{ cm}^2$  and  $10^{-42} \text{ MeV cm}^2$  respectively.

O'Connor et al. (2007)



# Light nuclei and neutrino-driven supernova outflows



$t=2\text{s}$  Arcones et al. (2008)  
 dashed=simulation →  
 dotted=NSE  
 solid=virial

$t=5\text{s}$

$t=7\text{s}$

$t=10\text{s}$

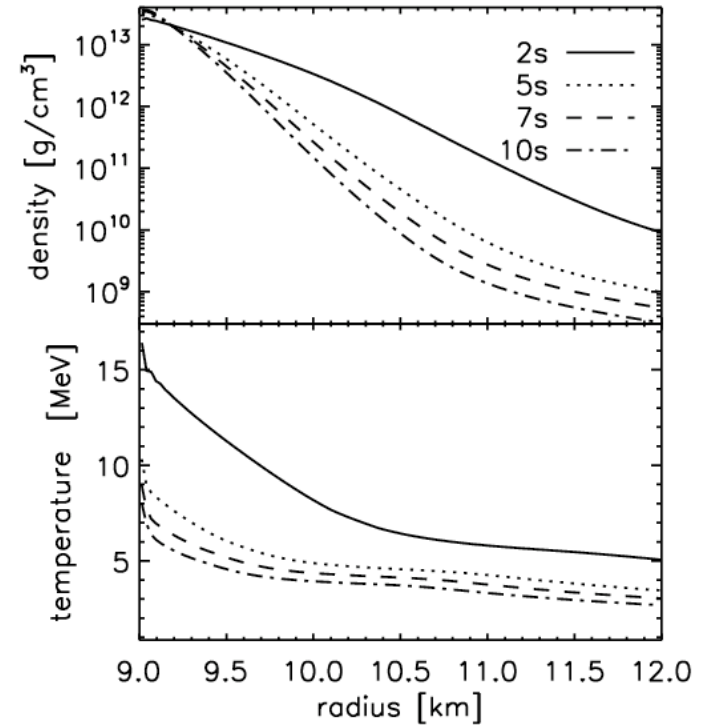
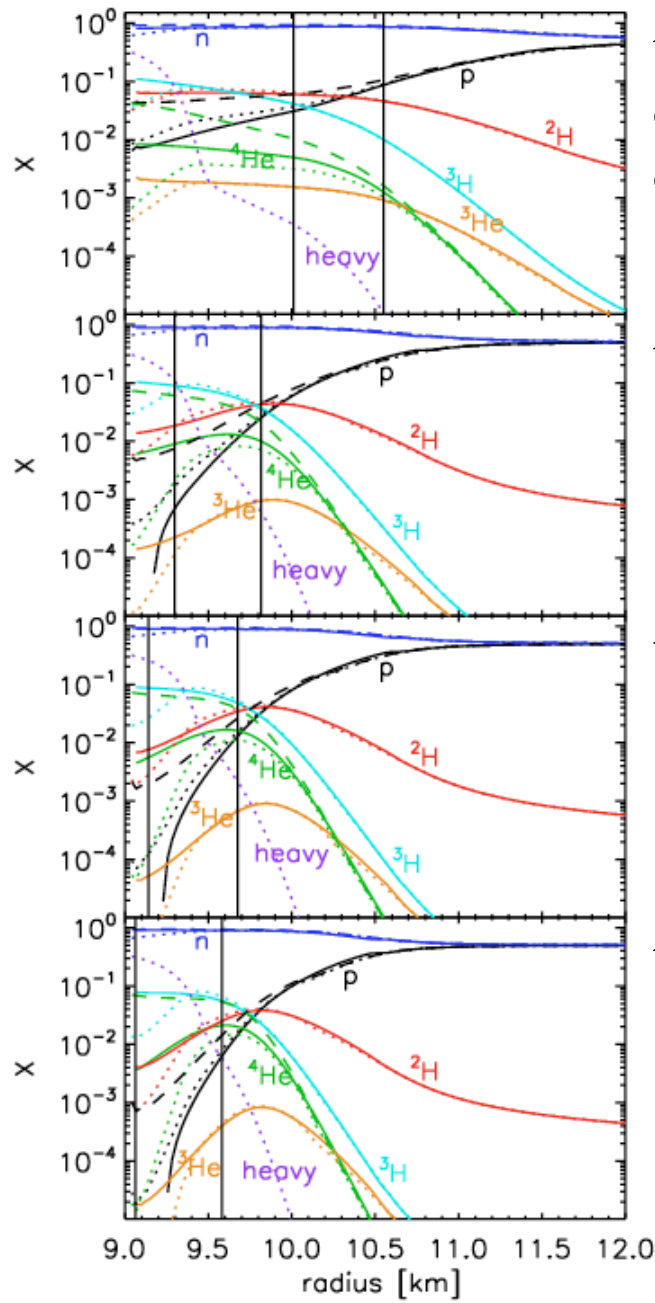


FIG. 1: Neutron star atmosphere profiles of density and temperature corresponding to model M15-II-r1 of Ref. [7] for times  $t = 2, 5, 7$  and  $10\text{s}$  post bounce.

Light nuclei present in substantial amounts in outer layers of protoneutron star dominated by  $d$ ,  $^3\text{H}$  (and  $^4\text{He}$ )

# Light nuclei and neutrino-driven supernova outflows



t=2s Arcones et al. (2008)

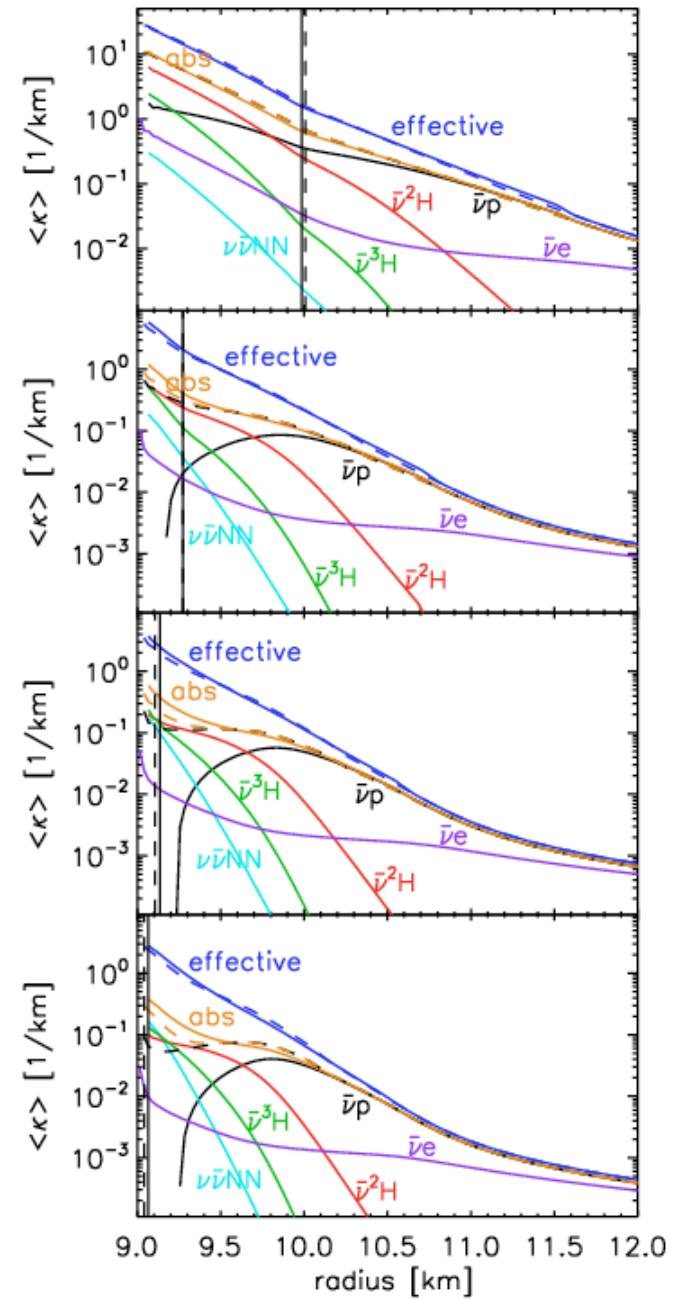
dashed=simulation  
 dotted=NSE  
 solid=virial

t=5s

t=7s

t=10s

absorption of electron antineutrinos on d,  $^3\text{H}$  dominates over p



# Light nuclei and neutrino-driven supernova outflows

TABLE II: Different cases explored in Sect. III.

Case	$Y_e$ determined from	EOS and composition
A	beta equilibrium	NSE (n, p, $^4\text{He}$ )
B	case A	NSE (nucleons and nuclei)
C	beta equilibrium	NSE (nucleons and nuclei)
D	beta equilibrium	virial (n, p, $A \leq 4$ nuclei)

Arcones et al. (2008)

impact of light nuclei on electron antineutrino emission and wind  $Y_e$  compared to reference case A

TABLE III: Neutrinosphere radii  $R_{\bar{\nu}_e, \nu_e}$ , neutrino spectral temperatures  $T_{\bar{\nu}_e, \nu_e}$ , and average energies  $\langle \epsilon_{\bar{\nu}_e, \nu_e} \rangle$ , as well as number luminosities  $L_n$ , spectral parameter  $\eta_{\nu_e}$ , and wind electron fractions  $Y_e^w$  at four different times post bounce.

	$R_{\bar{\nu}_e}$ [km]	$T_{\bar{\nu}_e}$ [MeV]	$\langle \epsilon_{\bar{\nu}_e} \rangle$ [MeV]	$L_n$ $[10^{56} \text{ s}^{-1}]$	$\eta_{\nu_e}$	$R_{\nu_e}$ [km]	$T_{\nu_e}$ [MeV]	$\langle \epsilon_{\nu_e} \rangle$ [MeV]	$Y_e^w$
$t = 2 \text{ s}$									
A	10.01	8.14	25.64	6.05	0.72	10.55	6.34	20.71	0.514
B	9.977	8.30	26.16	6.38	0.79	10.55	6.34	20.80	0.507
C	10.00	8.17	25.73	6.10	0.73	10.55	6.35	20.75	0.513
D	9.979	8.29	26.12	6.36	0.77	10.53	6.37	20.87	0.509
$t = 5 \text{ s}$									
A	9.272	7.17	22.60	3.55	1.01	9.821	5.14	17.10	0.478
B	9.260	7.24	22.83	3.65	1.04	9.819	5.15	17.16	0.475
C	9.295	7.04	22.17	3.37	0.94	9.814	5.16	17.07	0.487
D	9.272	7.17	22.60	3.55	1.00	9.813	5.16	17.15	0.480
$t = 7 \text{ s}$									
A	9.107	6.88	21.69	3.03	1.15	9.683	4.73	15.90	0.462
B	9.095	6.97	21.95	3.13	1.19	9.681	4.74	15.96	0.458
C	9.139	6.68	21.04	2.78	1.04	9.676	4.75	15.82	0.475
D	9.134	6.71	21.14	2.82	1.05	9.675	4.75	15.85	0.473
$t = 10 \text{ s}$									
A	9.041	6.94	21.86	3.06	1.49	9.592	4.37	15.05	0.431
B	9.039	7.02	22.12	3.17	1.53	9.590	4.37	15.12	0.427
C	9.063	6.49	20.44	2.51	1.23	9.582	4.39	14.82	0.456
D	9.065	6.45	20.32	2.47	1.20	9.581	4.39	14.80	0.458

## Summary

virial equation of state provides model-independent constraints for low-density nuclear matter and neutrino response

based directly on scattering phase shifts, includes bound states and resonant interactions on equal footing

important for supernova neutrinosphere

light nuclei can be present in significant amounts,  
 $d$  and  $^3H$  favored for neutron-rich conditions

include light nuclei and interactions with neutrinos in supernova and neutrino-driven wind simulations

## Outline

1. Introduction to effective field theory and the renormalization group
2. Chiral effective field theory
3. Renormalization group for nuclear forces
4. EFT and RG for nuclear matter
5. The virial equation of state and light nuclei
6. Neutrino processes in supernovae from chiral EFT

## Motivation and basics

Neutrino processes in supernovae and neutron stars:  
important for explosion, neutrino spectra, neutron star cooling,...

processes involving two nucleons play a special role

neutrino-pair bremsstrahlung and absorption: key for production of muon and tau neutrinos, and for equilibrating neutrino number densities

Suzuki, Nakamura, Raffelt, Janka, Keil, Seckel, Hannestad, Thompson, Burrows, Horvath,...

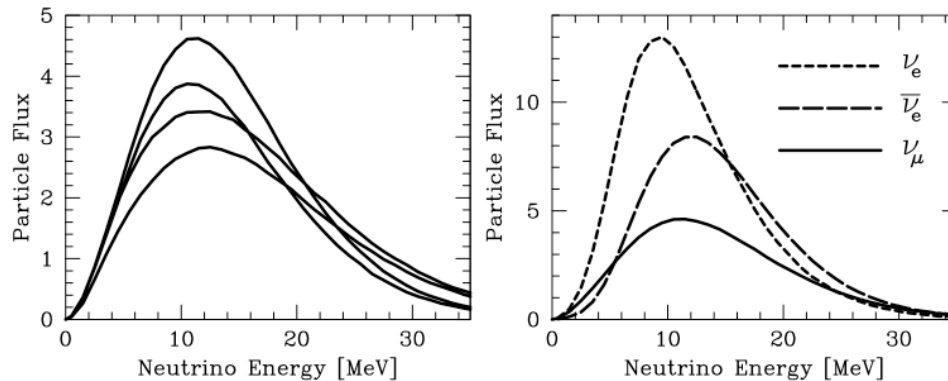
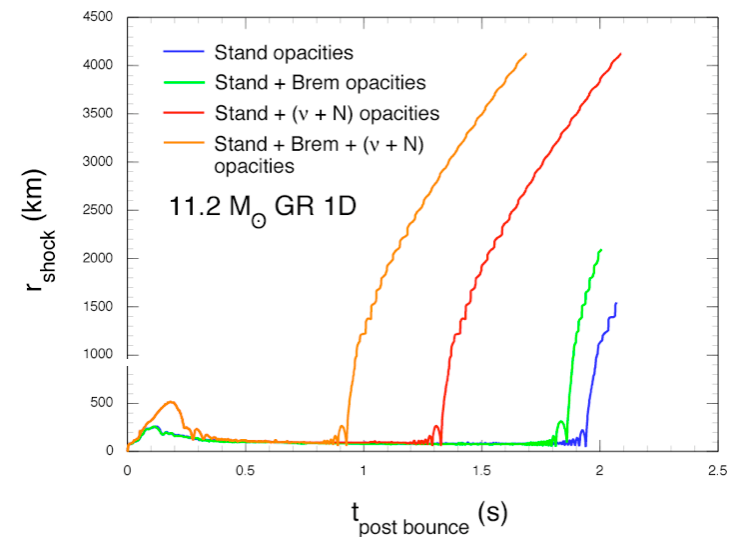


Figure 1. Neutrino fluxes for an accretion-phase model. *Left panel*, curves from bottom to top: Flux of  $\nu_\mu$  with traditional neutrino interaction channels, then adding nucleon bremsstrahlung, next adding nucleon recoils, and finally adding  $\nu_e\bar{\nu}_e$  annihilation. *Right panel*: Fluxes for all flavors; the  $\nu_\mu$  curve includes all reaction channels.

from Raffelt et al. (2003)



from Mezzacappa (2008)

but standard rates based on one-pion exchange for NN interactions,  
nobody uses only OPE for nuclear structure

## Single- and two-nucleon processes

elastic scattering from nucleons (space-like  $\omega < q$ )

initial and final state interactions, inelastic scattering  $\nu nn \leftrightarrow \nu nn$   
Landau-Pomeranchuk-Migdal effect

neutrino-pair bremsstrahlung/absorption  $nn \leftrightarrow nn\nu\bar{\nu}$  (time-like  $\omega > q$ )

need collisions between nucleons for the latter processes

noncentral contributions, due to tensor forces from pion exchanges and spin-orbit forces, are essential for the two-nucleon response

follows from direct calculations Friman, Maxwell (1979)  
and from conservation laws Olsson, Pethick (2002) (see later)

develop a unified treatment that consistently includes one- and two-quasiparticle-quasihole pair states Lykasov, Pethick, AS, PRC 78, 045803 (2008)

## Neutrino processes and dynamical structure factors

neutrinos interact weakly → rates for neutrino scattering, emission and absorption determined by dynamical structure factors of nucleon matter

generally axial/spin response most important, ~ factor 3

rate for bremsstrahlung  $\Gamma_{NN \leftrightarrow NN\nu\bar{\nu}} = 2\pi n G_F^2 C_A^2 (3 - \cos \theta) S_A(\omega, \mathbf{q})$

with spin dynamical structure factor  $S_A(\omega, \mathbf{q}) = \frac{1}{\pi n} \frac{1}{1 - e^{-\omega/T}} \text{Im} \chi_\sigma(\omega, \mathbf{q})$

response is diagonal in spin for long wavelengths

problem is to calculate structure factors of nucleon matter

not included:

reduction of axial coupling  $g_a$  for nucleon quasiparticles  
by 5-10% in neutron matter [Cowell, Pandharipande \(2003\)](#)

beyond quasiparticle contributions (incoherent parts)

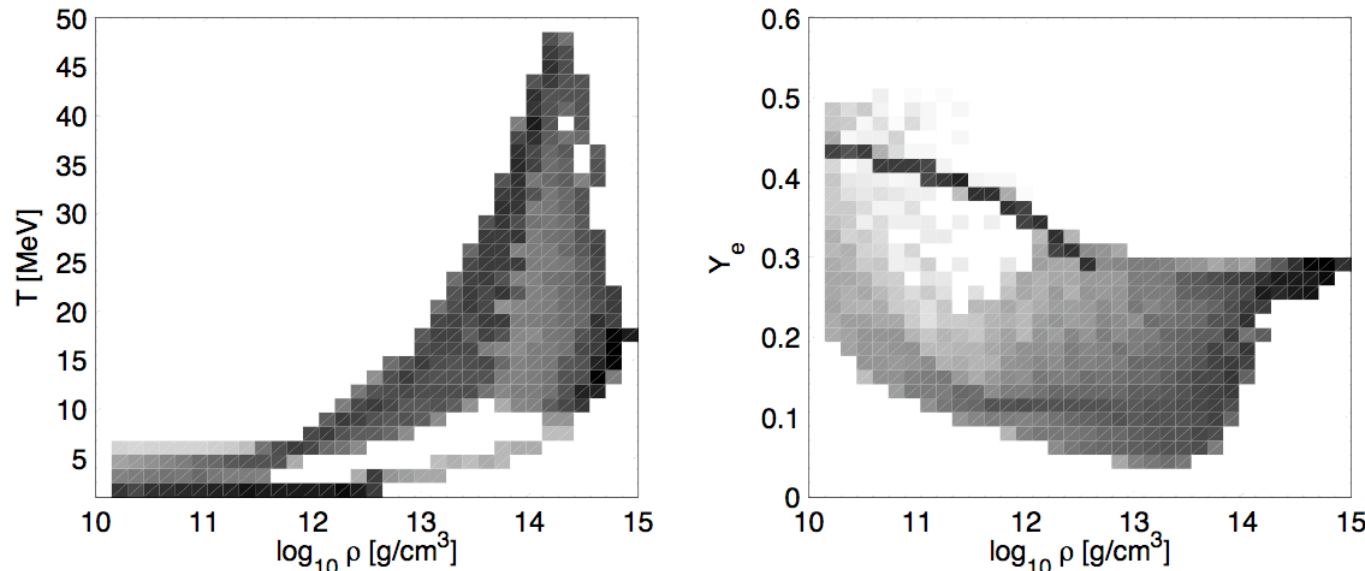
## Relevant conditions

crucial densities seem to be below nuclear matter density  $\rho \sim \rho_0/10$   
(high densities: neutrinos trap; low densities: few interactions)

energy, momentum transfers  $\omega, q$  small compared with Fermi momentum  
temperatures  $\sim$  Fermi temperature or less

→ Landau Fermi liquid theory is a reasonable first approximation

conditions for muon and tau neutrino production: higher T and low  $Y_e$



from Liebendoerfer (2008)

## Unified approach to structure factors, qp transport equation

Linearized quasiparticle transport equation for the spin response  $\delta\mathbf{s}_\mathbf{p}$

$$(\omega - \varepsilon_{\mathbf{p}+\mathbf{q}/2} + \varepsilon_{\mathbf{p}-\mathbf{q}/2}) \delta\mathbf{s}_\mathbf{p} + (n_{\mathbf{p}+\mathbf{q}/2} - n_{\mathbf{p}-\mathbf{q}/2}) \delta\mathbf{h}_\mathbf{p} = i I_\sigma[\mathbf{s}_{\mathbf{p}'}]$$

includes one-pair states through perturbation of quasiparticle energy

$$\delta\mathbf{h}_\mathbf{p} = \mathbf{U}_\sigma + 2 \int \frac{d\mathbf{p}'}{(2\pi)^3} g_{\mathbf{p}\mathbf{p}'} \delta\mathbf{s}_{\mathbf{p}'}$$

rates involving two nucleons expressed in terms of the collision integral

solution to qp transport equation includes multiple-scattering effects,  
Landau-Pomeranchuk-Migdal effect

qp transport equation can be solved in a relaxation time approximation

## Relaxation time approximation

approximate collision integral as  $I_\sigma[\mathbf{s}_{\mathbf{p}'}] = -\frac{\delta\mathbf{s}_{\mathbf{p}} - \delta\mathbf{s}_{\mathbf{p}'}|_{\text{le}}}{\tau_\sigma}$

with spin relaxation time  $\tau_\sigma = \text{rate of change of nucleon spin through collisions with other nucleons}$

assumes all angular harmonics relax at the same rate

### Spin relaxation rate

spin relaxation rate for frequencies  $|\omega| \gg 1/\tau_\sigma$  and  $q \ll k_F$

$$\frac{1}{\tau_\sigma} = C_\sigma [T^2 + (\omega/2\pi)^2]$$

$$C_\sigma = \frac{\pi^3 m^*}{6k_F^2} \left\langle \frac{1}{12} \sum_{k=1,2,3} \text{Tr} \left[ \mathcal{A}_{\sigma_1, \sigma_2}(\mathbf{k}, \mathbf{k}') \boldsymbol{\sigma}_1^k [(\boldsymbol{\sigma}_1 + \boldsymbol{\sigma}_2)^k, \mathcal{A}_{\sigma_1, \sigma_2}(-\mathbf{k}, \mathbf{k}')] \right] \right\rangle$$

with qp scattering amplitude and average over the Fermi surface

commutator with 2-body spin: only noncentral interactions contribute

## Resulting dynamical structure factors

solution to qp transport equation

$$\text{Im}\chi_\sigma = N(0) \frac{\text{Im} \tilde{X}_\sigma}{|1 + G_0 \tilde{X}_\sigma|^2}$$

isotropic Landau interaction  $G_0$  dominates in neutron matter

$$\text{in relaxation time approximation } \tilde{X}_\sigma = 1 - \frac{\omega}{2v_F q} \ln \left( \frac{\omega + i/\tau_\sigma + v_F q}{\omega + i/\tau_\sigma - v_F q} \right)$$

generalizes earlier work to finite  $q$  and include mean-field effects

### Limits

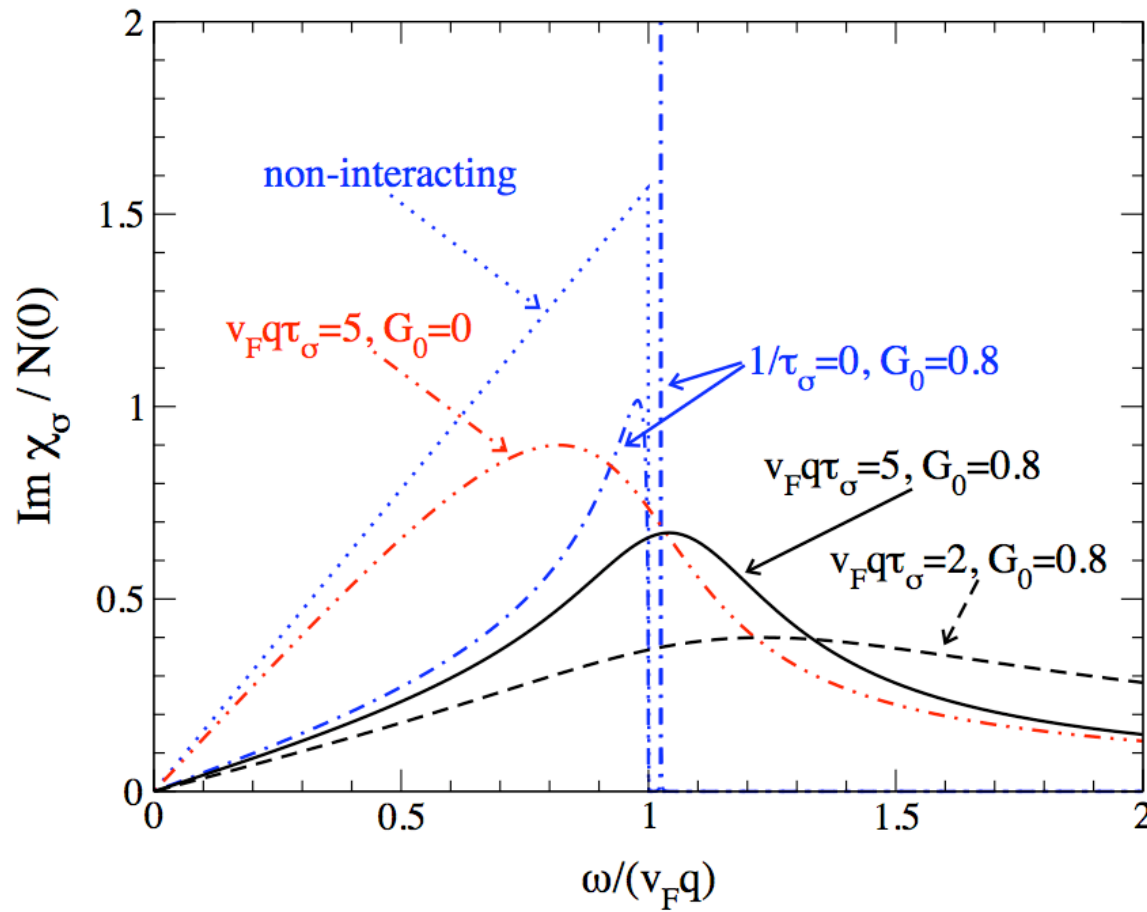
Long-wavelength limit:

$$\text{Im}\chi_\sigma(\omega, q \rightarrow 0) = N(0) \frac{\omega \tau_\sigma}{(1 + G_0)^2 + (\omega \tau_\sigma)^2}$$

without mean-field effects ( $G_0=0$ ): same form as Ansatz of [Raffelt et al.](#)  
but multiple-scattering effects calculated not introduced as parameter

and for  $|\omega| \tau_\sigma \gg 1$  reproduces standard rates with  $\tau_\sigma$  based on OPE

## Spin dynamical structure factor



single-pair mean-field effects ( $G_0=0.8$ ): collective spin-zero-sound pole with increasing spin relaxation rate from  $1/\tau_\sigma = 0$  to  $v_F q/5$  and  $v_F q/2$  spin-zero-sound peak disappears, response pushed to higher frequencies significant for  $1/\tau_\sigma$  comparable to  $v_F q \rightarrow$  recoil effects may be important

# Rates based on chiral effective field theory (EFT) for nuclear forces

Separation of scales: low momenta  $Q \ll \Lambda_b$  breakdown scale  $\sim 500$  MeV

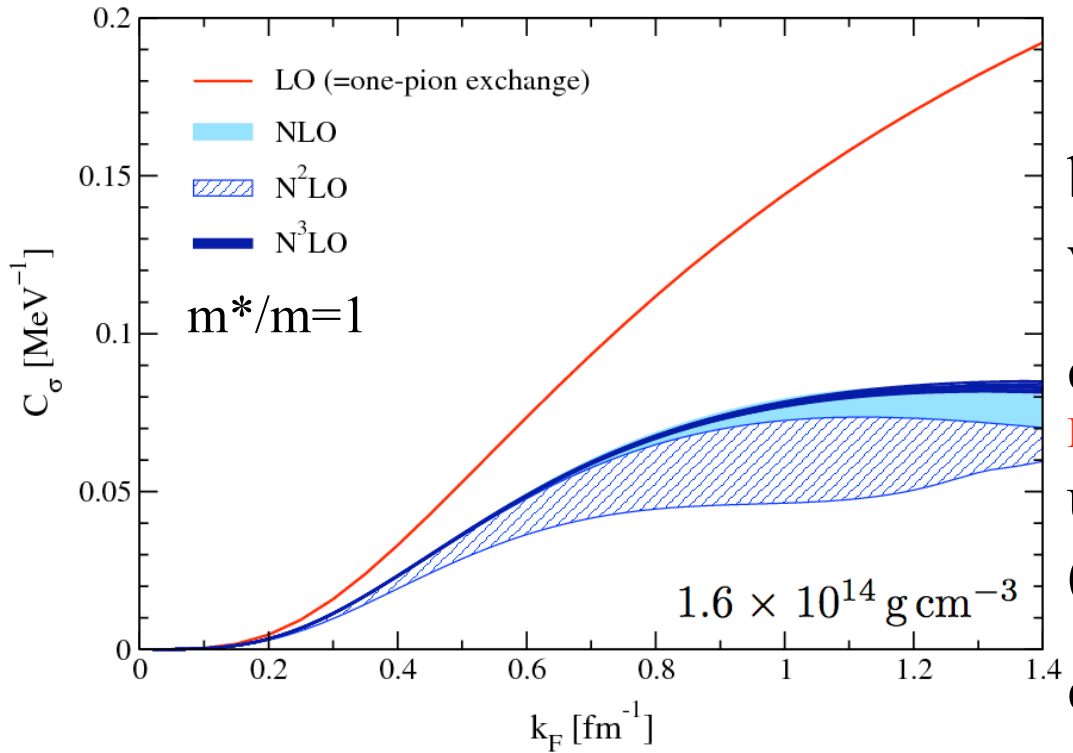
	NN	3N	4N	
LO $\mathcal{O}\left(\frac{Q^0}{\Lambda^0}\right)$			—	limited resolution at low energies, can expand in powers $Q/\Lambda_b$
NLO $\mathcal{O}\left(\frac{Q^2}{\Lambda^2}\right)$		—	—	include long-range pion physics details of short-distance physics not resolved
$N^2LO \mathcal{O}\left(\frac{Q^3}{\Lambda^3}\right)$			—	capture in few short-range couplings, fit to experiment once
$N^3LO \mathcal{O}\left(\frac{Q^4}{\Lambda^4}\right)$				systematic: can work to desired accuracy and obtain error estimates
	+	...	+	...

Weinberg, van Kolck, Kaplan, Savage, Wise, Epelbaum, Meissner, Nogga, Machleidt,...

## Rates based on chiral effective field theory (EFT) for nuclear forces

	NN	3N	4N	
LO $\mathcal{O}\left(\frac{Q^0}{\Lambda^0}\right)$		—	—	standard rates for bremsstrahlung based on one-pion exchange (OPE)
NLO $\mathcal{O}\left(\frac{Q^2}{\Lambda^2}\right)$		—	—	reasonable starting point: long-range part and LO for neutrons
$N^2LO \mathcal{O}\left(\frac{Q^3}{\Lambda^3}\right)$			—	however: subleading contributions crucial for NN scattering at $k_F \sim 1.0 \text{ fm}^{-1} \approx 200 \text{ MeV}$
$N^3LO \mathcal{O}\left(\frac{Q^4}{\Lambda^4}\right)$				3N important for EOS for $k_F \gtrsim 1.5 \text{ fm}^{-1}$ <b>Tolos, Friman, AS (2008)</b>
				go beyond OPE approximation: NN contributions up to $N^3LO$ at subnuclear densities
				<b>Bacca, Hally, Pethick, AS, arXiv:0812.0102.</b>

# Spin relaxation rate in neutron matter from chiral EFT



$$\frac{1}{\tau_\sigma} = C_\sigma [T^2 + (\omega/2\pi)^2]$$

bremsstrahlung rate  $\sim C_\sigma$   
when  $|\omega| \gg 1/\tau_\sigma$

chiral EFT interactions from  
Epelbaum et al. (2005) Entem, Machleidt (2003)  
used in Born approximation  
(will justify later)

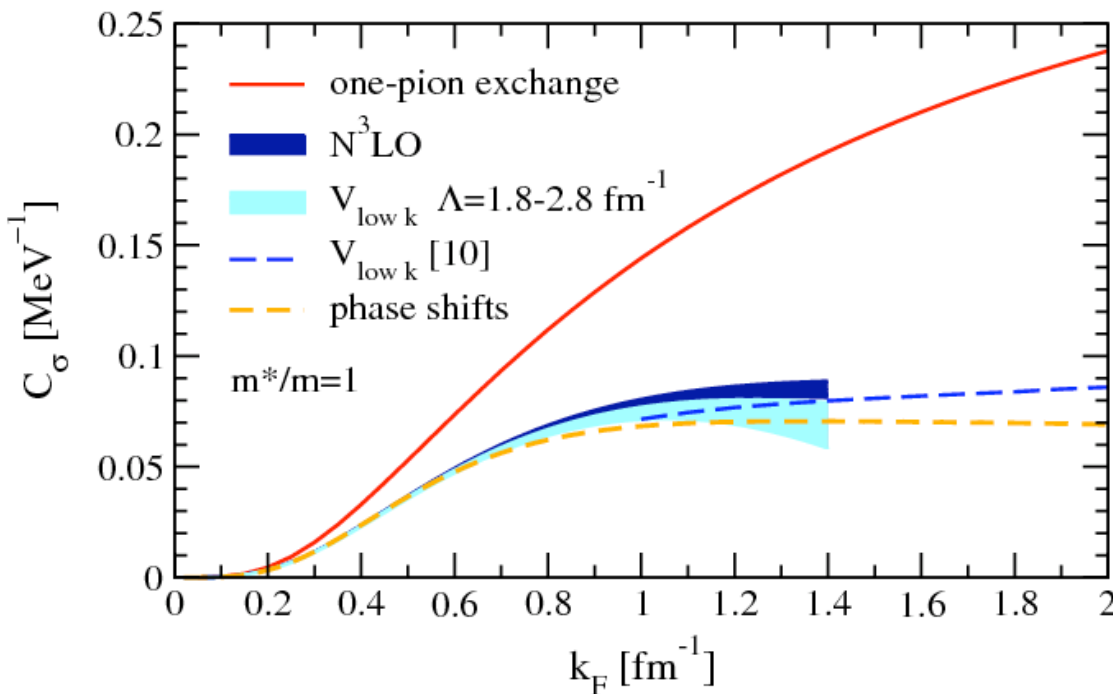
error bands from cutoff variation

convergence with successively higher orders,  
OPE significantly overestimates  $C_\sigma$  for all relevant densities

at NLO: leading two-pion exchange and noncentral contact interactions,  
constrained by NN scattering data

at  $N^3\text{LO}$  (accurately reproduces NN scattering): interaction independent  
first model-independent results at subnuclear densities

## Comparison to rates based on NN phase shifts



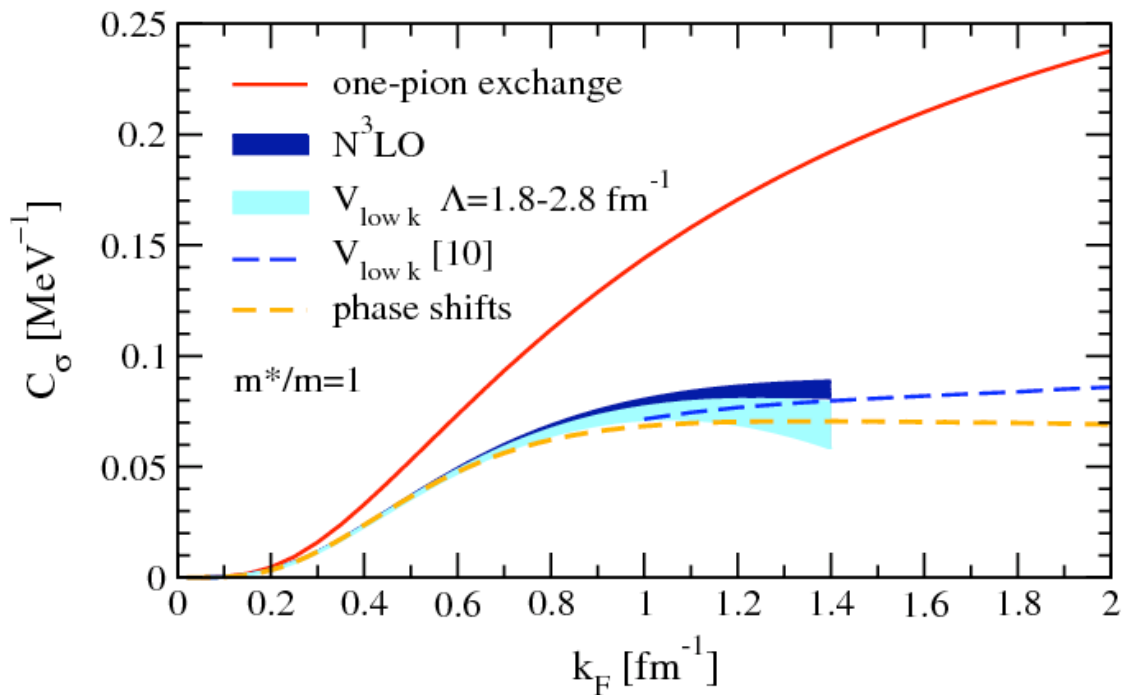
extended cutoff variation and estimate of uncertainty using RG-evolved low-momentum interactions  $V_{\text{low } k}$

low densities: two-nucleon collisions dominate, model-independent result based on NN phase shifts from NN partial wave analysis (nn-online.org)  
see also Hanhart, Phillips, Reddy (2001)

rates from chiral  $N^3\text{LO}$  interactions in Born approximation close to rates from phase shifts

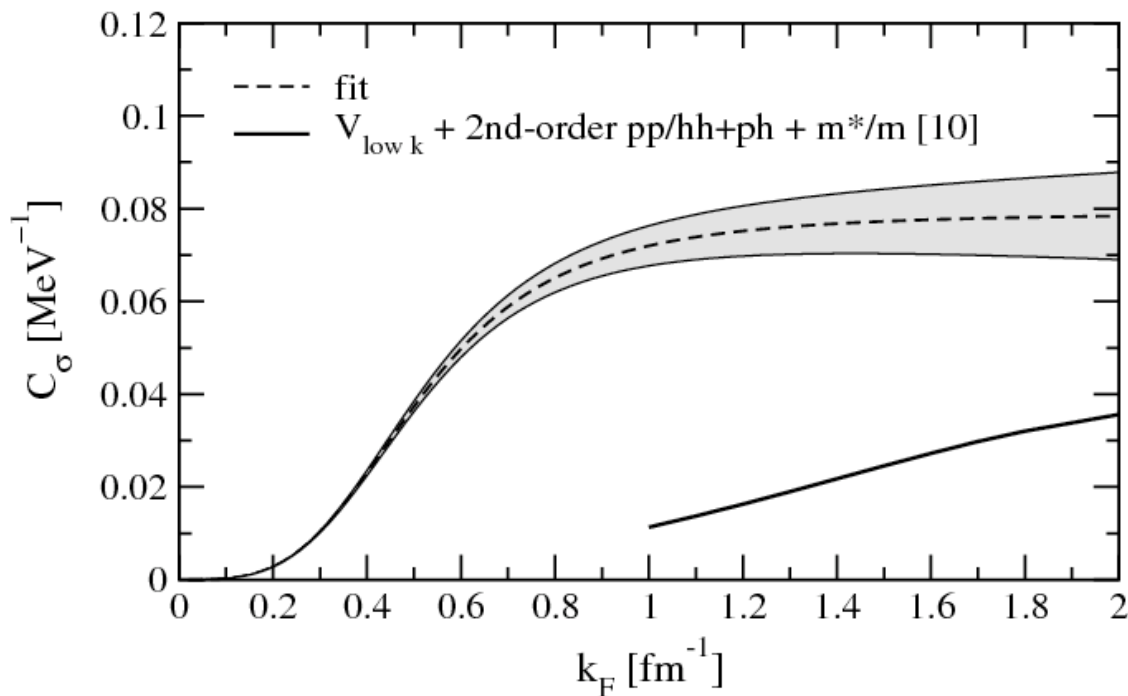
noncentral part of the strong neutron-neutron amplitude is perturbative, rates based on phase shifts would otherwise be unreliable

## Fit and many-body contributions



at subnuclear densities:  
 $\rho < 10^{14} \text{ g cm}^{-3}$  ( $k_F < 1.2 \text{ fm}^{-1}$ )  
the spin response is well constrained  
all realistic results lie within a band

## Fit and many-body contributions



at subnuclear densities:  
 $\rho < 10^{14} \text{ g cm}^{-3}$  ( $k_F < 1.2 \text{ fm}^{-1}$ )

the spin response is well constrained

all realistic results lie within a band

simple fit function representing our results:  $\frac{C_\sigma}{\text{MeV}} = \frac{0.86 (k_F/\text{fm}^{-1})^{3.6}}{1 + 10.9 (k_F/\text{fm}^{-1})^{3.6}}$

further reduction from particle-hole and  $(m^*/m)^3$  effects  
(particle-hole mixing of tensor with strong central interactions)

sensitivity tests with  $C_\sigma$  times suppression over different density ranges  
→ where to put many-body calculational effort

## Mean-free paths and energy transfer

thermally-averaged inverse mf path due to neutrino-pair absorption

long-wavelength approximation  $\langle \lambda^{-1} \rangle = \frac{C_A^2 G_F^2}{20\pi} \frac{n}{T^3} \int_0^\infty d\omega \omega^5 e^{-\omega/T} S_\sigma(\omega)$

Hannestad, Raffelt (1998)

$G_0$		0	0.8	0	0.8
$k_F$ [fm $^{-1}$ ]	$T$ [MeV]	$C_\sigma$ from OPE		$V_{\text{low } k}$	
1.0	5	0.0770	0.0697	0.0397	0.0386
	10	1.08	0.798	0.612	0.554
1.7	5	0.119	0.107	0.0476	0.0468
	10	1.66	1.21	0.744	0.700

in km $^{-1}$

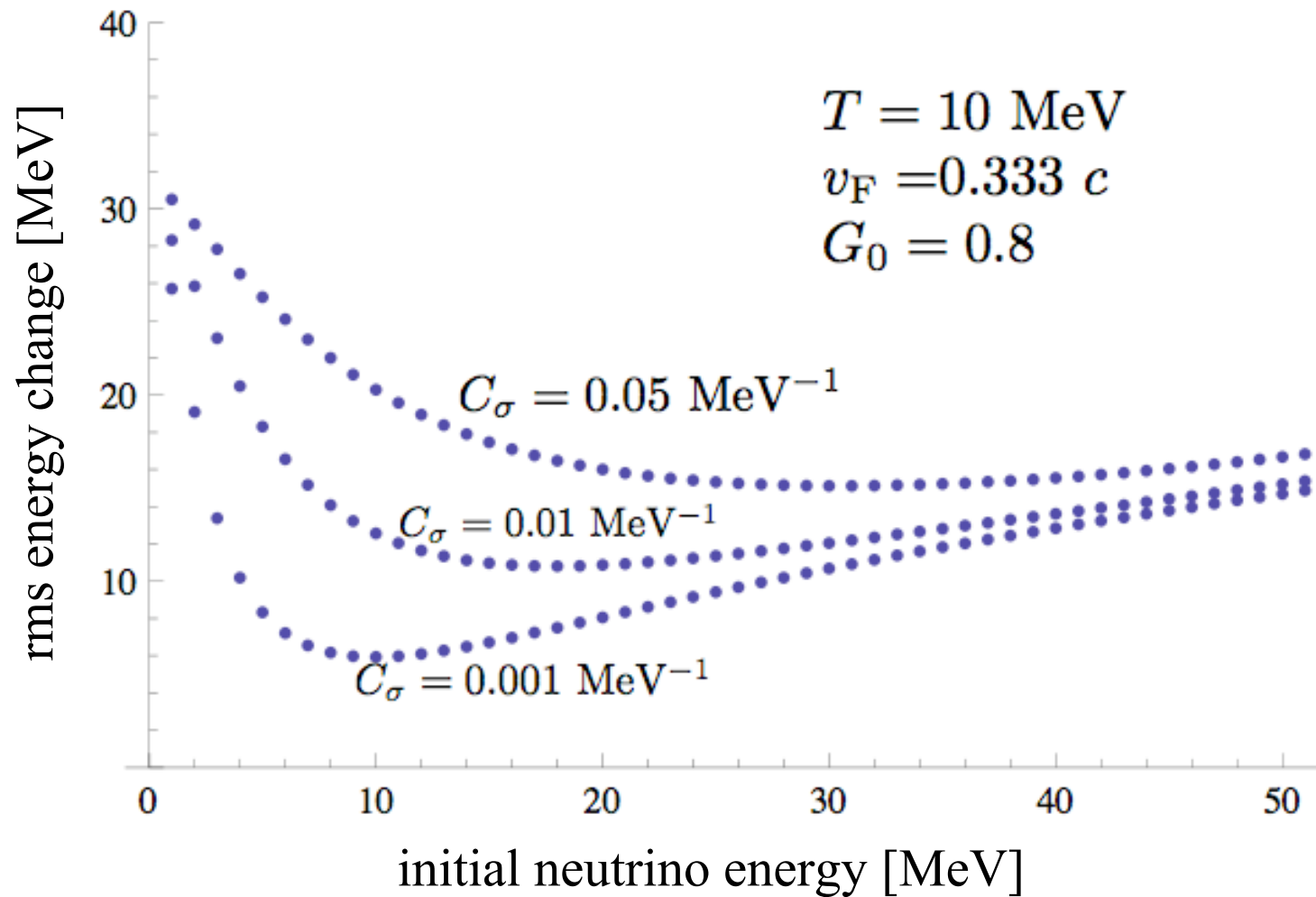
note: OPE based on solution to qp transport equation (not OPE in SN)

significantly longer mf paths compared to OPE,  
consequently weaker mean-field effects ( $G_0=0.8$  vs.  $G_0=0$ )

similar changes for energy loss due to neutrino-pair emission and  
energy transfer (inelastic scattering  $\nu nn \leftrightarrow \nu nn$  important)

## Energy transfer in neutrino scattering

rms energy change in neutrino scattering including recoil effects



significant dependence on spin relaxation rate

## Summary and outlook

unified approach to neutrino processes based on Landau Fermi liquid theory, includes one- and two-quasiparticle-quasihole pair states

derived dynamical structure factors from qp transport equation in a relaxation time approximation

first neutrino rates for supernovae based on chiral EFT, to  $N^3LO$ , over wide density range and including theoretical uncertainties

two-pion exchange interactions and shorter-range noncentral forces reduce neutrino rates significantly

spin response is well constrained for densities  $\rho < 10^{14} \text{ g cm}^{-3}$

Future: neutron-proton mixtures, extend to less degenerate conditions, two-body contributions to weak currents, charged current interactions, extension to superfluid phases,...

## Summary

Exciting era with advances on many fronts

For the first time, approaches from light to heavy nuclei  
and for astrophysics based on the same interactions

Three-nucleon interactions are a frontier

Exciting intersections with problems in many related areas

Major investments in new facilities and institutes worldwide

Thank you for listening, for your interest,  
your warm hospitality and a terrific time!!

